INFORMATION TO USERS

This manuscript has been reproduced from the microfilm master. UMI films the text directly from the original or copy submitted. Thus, some thesis and dissertation copies are in typewriter face, while others may be from any type of computer printer.

The quality of this reproduction is dependent upon the quality of the copy submitted. Broken or indistinct print, colored or poor quality illustrations and photographs, print bleedthrough, substandard margins, and improper alignment can adversely affect reproduction.

In the unlikely event that the author did not send UMI a complete manuscript and there are missing pages, these will be noted. Also, if unauthorized copyright material had to be removed, a note will indicate the deletion.

Oversize materials (e.g., maps, drawings, charts) are reproduced by sectioning the original, beginning at the upper left-hand corner and continuing from left to right in equal sections with small overlaps.

Photographs included in the original manuscript have been reproduced xerographically in this copy. Higher quality 6" x 9" black and white photographic prints are available for any photographs or illustrations appearing in this copy for an additional charge. Contact UMI directly to order.

Bell & Howell Information and Learning
300 North Zeeb Road, Ann Arbor, MI 48106-1346 USA
800-521-0600

UMI®

Université d'Ottawa · University of Ottawa

MECHANISMS OF ISCHEMIC TOLERANCE IN THE RAT BRAIN PRECONDITIONED WITH CORTICAL SPREADING DEPRESSION

By

Fuhu Wang

A thesis submitted to the School of Graduate Studies of the University of Ottawa in partial fulfillment of the requirements for the degree of Doctor of Philosophy in the Anatomy and Neurobiology Program, Department of Cellular and Molecular Medicine, Faculty of Medicine.

To my family.

ABSTRACT

Cortical spreading depression (CSD) imparts delayed neuroprotection against cerebral ischemia. We hypothesized that prior CSD preconditioning attenuates ischemic excitotoxicity by reducing glutamate synaptic responses. We assessed this hypothesis by measuring cerebral blood flow (CBF), tissue depolarization and N-methyl-d-aspartate (NMDA) receptor activation during subsequent ischemic insult. We also measured cerebral glucose utilization and quantified excitatory amino acid transporters (EAAT) at various time intervals after CSD. The methodology included autoradiography and immunoblotting. CSD preconditioning reduced neocortical infarct volume from 43.3 ± 21.9 mm^3 (n=18) to 22.2 ± 25.3 mm^3 (n=12) ($p<0.01$). We found [^{3}H]dizocilpine (MK-801) in vivo distribution increased significantly in the outer neocortex during recurrent CSD, suggesting increases in extracellular glutamate. During focal insult on day 3 after CSD, regional CBF outside the ischemic core was higher at 147 ± 27 mL $100g^{-1}$ min^{-1} (n=6) in CSD preconditioned cortex compared with 73 ± 41 mL $100g^{-1}$ min^{-1} (n=6) in sham studies ($p<0.005$). The ratio of [^{3}H]nimodipine ipsilateral/contralateral volume of distribution (uptake ratio), indicating membrane depolarization, was attenuated in the ischemic core from 1.91 ± 0.26 (n = 7) in sham studies to 1.30 ± 0.27 (n = 9) in CSD preconditioned studies ($p<0.02$). [^{3}H]Dizocilpine in vivo distribution, used to map NMDA receptor activation, showed restricted distribution of [^{3}H]dizocilpine in the ischemic core. The ipsilateral/contralateral ratio of regional cerebral glucose utilization, measured with [^{14}C]deoxyglucose in the neocortex, was reduced 10% in CSD preconditioned studies on day 3 ($p<0.05$) and day 7 ($p<0.001$) after CSD. Astrocytic, but not neuronal EAAT, were downregulated in plasma membranes. Semi-quantitative immunoprotein analysis indicated that the ratio of ipsilateral/contralateral band intensities was reduced up to 80% for EAAT2 ($p<0.0001$) and 45% for EAAT1 ($p<0.001$) on day 3 after CSD. We draw three conclusions from our data: (1) CSD preconditioning improves cerebral blood flow in the periinfarct region and attenuates ischemic tissue depolarization in the ischemic core; (2) CSD preconditioning induces a reduction in regional cerebral glucose utilization; (3) CSD preconditioning downregulates astrocytic glutamate transporters, leading to attenuated glutamate exposure during subsequent ischemic insult. CSD preconditioning may therefore include improvement of blood flow and attenuation of glutamate excitotoxicity.

ACKNOWLEDGMENTS

I am grateful to Dr. M. J. Hogan for providing me the opportunity to work in his laboratory from August 1995 to June 1999 and his supervision during my Ph.D. program. I owe my thanks to Dr. A. M. Buchan for bringing me to Ottawa and for the opportunity to work in his laboratories for nearly two years from September 1993 to June 1995. I feel greatly in debt to Dr. A. M. Hakim for his help through some of the most difficult periods in the last six years.

I thank Drs. P. A. Fortier, J. N. Fryer, M. T. Hincke, L. Maler, K. C. Marshall, P. Morley, G. S. Robertson, Wm. A. Staines and B. S. Tuana for their involvement in my course work and in my committee supervision.

I thank Dr. A. Douen for his encouragement and collaborative work. His contribution to the design and initiation of excitatory amino acid transporter project is appreciated. Credits are due to Ms. Li Dong for the immunoblots she carefully produced. I appreciate the technical assistance from Ms. Georgette Roy for sectioning [^{3}H]nimodipine labeled brains and cresyl violet staining of the brain sections. I feel lucky to know so many kind individuals in the Neuroscience Research Institute and the Department of Anatomy and Neurobiology.

TABLE OF CONTENTS

LIST OF ABBREVIATIONS

AMPA	- α-amino-3-hydroxy-5-methyl-4-isoxazole propionic acid
ATP	- adenosine triphosphate
ADP-ribosyl	- adenosine diphosphate-ribosyl
BDNF	- brain-derived neurotrophic factor
cAMP	- cyclic adenosine monophosphate
CBF	- cerebral blood flow
cGMP	- cyclic guanosine monophosphate
CGU	- cerebral glucose utilization
CSD	- cortical spreading depression
DC	- direct current
EAAT	- excitatory amino acid transporter
GTP	- guanosine triphosphate
IAP	- iodoantipyrine
iGluR	- ionotropic glutamate receptor
MCA	- middle cerebral artery
mGluR	- metabotropic glutamate receptor
NO	- nitric oxide
NOS	- nitric oxide synthase
NMDA	- *N*-methyl-D-aspartate
PMSF	- phenylmethanesulfonyl fluoride
ROI	- region of interest
SD	- standard deviation
SDS	- sodium dodecyl sulfate
V_d	- volume of distribution
VOI	- volume of interest
VSCC	- voltage sensitive calcium channel

LIST OF TABLES

LIST OF FIGURES

CHAPTER 1. INTRODUCTION

A fundamental issue in neurobiology concerns the adaptive modification of the central nervous system with experience. For instance, the cerebral cortex may be preconditioned with cortical depolarization to better tolerate a future ischemic insult. Brief periods of transient sublethal global ischemia (ischemic preconditioning) induce a delayed protection against subsequent lethal global (Kato et al., 1991; Kirino et al., 1991) or focal (Matsushima and Hakim, 1995; Simon et al., 1993) cerebral ischemia. More recently cortical spreading depression (CSD) has been reported to impart a delayed protection against global (Kawahara et al., 1995; Kobayashi et al., 1995; Taga et al., 1997) or focal ischemia (Matsushima et al., 1996; Matsushima et al., 1998; Yanamoto et al., 1998) (CSD preconditioning).

Both the duration of ischemic preconditioning and the interval between preconditioning and subsequent lethal ischemia determine the degree of protection (Kato et al., 1991; Kirino et al., 1991). Global ischemic preconditioning for a period of 2 minutes induces ischemic preconditioning in gerbils, whereas 3 minutes of ischemia results in neuronal injury (Kato et al., 1991) and 1 minute of ischemia does not induce ischemic tolerance (Kato et al., 1991; Kirino et al., 1991). Neuroprotection can be demonstrated between day 1 and 7 after preconditioning, and may last up to day 21 (Kato et al., 1991). Ischemic tolerance can be induced repeatedly (Chen et al., 1994) and prevented by hypothermia during the preconditioning ischemia (Wada et al., 1997). It is

uncertain if the protection is permanent. Preconditioning with 1.5 minutes of global ischemia produced incomplete behavioural protection within the first 10 days and failed to halt the progressive loss of CA1 neurons over 1 month after a 5 minute ischemic insult (Corbett and Crooks, 1997). CSD is also a depolarization event (Munoz-Martinez, 1970; Osuga et al., 1997) that produces ischemic tolerance from day 1 to 7 after preconditioning, but not on day 21 (Kobayashi et al., 1995; Matsushima et al., 1996; Yanamoto et al., 1998).

There is evidence to support that increases in extracellular glutamate and glutamate receptor activation are important events during preconditioning. It has been demonstrated that ischemic preconditioning can be prevented by blockade of NMDA receptor channel with dizocilpine (MK-801), a non-competitive NMDA receptor blocker, during preconditioning (Kato et al., 1992c). Similarly, if KCl-induced cortical depolarization is blocked by ketamine, an NMDA antagonist, CSD-induced ischemic tolerance cannot be established (Taga et al., 1997). Increased extracellular glutamate during preconditioning may signal the cerebral tissue to enter an ischemic tolerant state. The delayed onset and eventual disappearance of induced ischemic tolerance support the notion that intracellular signaling is involved (Kato et al., 1991; Yanamoto et al., 1998). Following CSD preconditioning, levels of message and protein for growth factors are upregulated in both neurons and astrocytes (Kariko et al., 1998; Kawahara et al., 1997; Kokaia et al., 1993; Matsushima et al., 1998). Both ischemic (Belayev et al., 1996) and CSD (Herdegen et al., 1993; Herrera et al., 1993) preconditioning upregulate the

transcription and translation of immediate early genes. The finding that ischemic preconditioning requires de novo protein synthesis provides further evidence (Barone et al., 1998). Improved [^{14}C]leucine incorporation recovery indicates increased protein synthesis in ischemia (Nakagomi et al., 1993) or CSD (Kawahara et al., 1994a; b) preconditioned rats.

Preconditioning appears to increase tolerance against excitotoxicity. Evidence indicates that ischemic preconditioning reduces mRNA editing at the R/G site, resulting in a decrease in the steady-state currents of AMPA receptors (Lomeli et al., 1994; Seeburg, 1996; Yamaguchi et al., 1999). This reduction occurs on day 3 and returns to normal level on day 14 (Yamaguchi et al., 1999). Ischemic preconditioning increases release of synaptic adenosine and activates ATP-sensitive K^+ channel through adenosine A2 receptor (Heurteaux et al., 1995; Reshef et al., 2000). Consistent with the notion of increased tolerance, total glutamate exposure in focal ischemic neocortex, defined as the integrated extracellular glutamate concentration over time, was found to be reduced by CSD preconditioning (Douen et al., 2000). However, glutamate release from the presynaptic terminal during ischemia fails to account for all the increases in glutamate in the extracellular milieu (Coorssen et al., 1998; Sudhof, 1995). The bulk of the increases has been demonstrated to result from the leakage from the astrocytes through excitatory amino acid transporters (EAAT) (Kimelberg et al., 1995; Obrenovitch, 1996; Rutledge and Kimelberg, 1996; Seki et al., 1999). Astrocytic functional transformation occurs after both ischemic (Kato et al., 1994;

Westenbroek et al., 1998) and CSD (Belayev et al., 1996; Bonthius and Steward, 1993) preconditioning, accompanied by upregulation of glial fibrillary acidic protein (GFAP) message and protein throughout the treated neocortex. CSD-induced astrocytic activation can be blocked by dizocilpine (Bonthius and Steward, 1993; Herrera and Cuello, 1992; Herrera and Robertson, 1990).

The changes in membrane channels and transporters may be mediated by second messenger signaling. CSD preconditioning increased activation of phospholipase A_2 through NMDA receptor activation, resulting in increased cyclooxygenase-2 in the neocortex (Caggiano et al, 1996; Miettinen et al., 1997). There is evidence that the ability of the mitochondria to modulate cytoplasmic Ca^{2+} is improved in the ischemic preconditioned gerbil brain (Ohta et al., 1996), in addition to attenuated cytoplasmic Ca^{2+} responses (Shimazaki et al., 1998). In hippocampus, 2 minutes of ischemic preconditioning prevented the loss of membrane receptors and channel proteins, which would otherwise be reduced on day 7 after ischemia (Kato et al., 1992b). Downregulation of adenylate cyclase, cAMP-dependent kinase, phosphodiesterase by 3 minutes global ischemia on day 7 can be prevented by preconditioning with 2 minutes ischemia (Kato et al., 1992b).

The role of regional cerebral blood flow (CBF) in ischemic tolerance has been controversial. Measured with the H_2 clearance method, regional CBF was reported to increase in a region outside the ischemic core during subsequent severe focal ischemia (Matsushima and Hakim, 1995). Contrary to this report, regional CBF, measured with the [^{14}C]iodoantipyrine (IAP)

method, was reported unaltered on day 3 after three episodes (10 minutes each) of middle cerebral artery occlusion (Chen et al., 1996). After CSD preconditioning, regional CBF was found unaltered with the H_2 clearance method and the laser-Doppler method (Matsushima et al., 1996; Yanamoto et al., 1998). Yet, CSD-induced astrocytic transformation also coincides with increases in the translation of neuronal nitric oxide synthase (NOS) in astrocytes 6 hours and 72 hours after the preconditioning (Caggiano and Kraig, 1998). Increased NOS expression can potentially lead to increases in regional CBF caused by increased NO synthesis upon activation of NMDA glutamate receptor and Ca^{2+} influx (Zhang and Snyder, 1995).

The level of energy consumption directly correlates with the ability of cerebral tissue to withstand ischemic insult (Folbergrova et al., 1992; Sokoloff, 1981). Ischemic preconditioned tissue uses less energy as indicated by slower oxygen depletion in global cerebral ischemic tissue (Li et al., 1997). Secondary adenosine triphosphate (ATP) depletion on day 3 and day 7 after lethal ischemic insult is slowed (Katayama et al., 1991). However, the available reports on the regional energy metabolism remain inadequate (Kawahara et al., 1994a; b).

In summary, induced ischemic tolerance represents the ability of the central nervous system to modify its response to subsequent lethal ischemia. Though the mechanisms are poorly understood, many of the molecular changes coincide with glutamate signaling during the preconditioning events and with reduced glutamate excitotoxicity during the subsequent ischemic

insult. Closer association may be found by examining the key components in synaptic transmission and in ischemic tissue injury. Thus, background information will be reviewed in the following areas: (1) Key components of synaptic transmission; (2) Roles of glutamate in energy metabolism and CBF coupling; (3) Cortical spreading depression; and (4) Ischemic injury and the excitotoxicity theory.

Key components of synaptic transmission

Both ionotropic and metabotropic glutamate receptors are used for neural transmission in the central nervous system. Ionotropic glutamate receptors (iGluR) are heterogeneous or homogenous pentamers of their genetically diversified subunits (Bettler and Mulle, 1995; McBain and Mayer, 1994). Three classes of iGluR have been identified and cloned: AMPA, kainate and NMDA receptors (Bettler and Mulle, 1995; McBain and Mayer, 1994). AMPA receptors are permeable primarily to Na^+ influx and K^+ efflux. Receptors containing the iGluR2 subunit are also permeable to Ca^{2+}, depending on the extent of the glutamine/arginine substitution among the receptor subunits (iGluR2 Q/R switch) (Carriedo et al., 1998; Seeburg, 1996). Similarly, kainate receptors are permeable predominantly to Na^+ influx and K^+ efflux, and the glycine/arginine switch in kainate iGluR5 and iGluR6 (iGluR5 and iGluR6 Q/R switch) permits Ca^{2+} influx (Chittajallu et al., 1999). AMPA receptors (iGluR2, 3 and 4, but not iGluR1) may also be subject to the arginine/glycine substitution (iGluR R/G switch) (Lomeli et al., 1994; Seeburg, 1996). The increased editing at the R/G site renders the AMPA receptor more

permeable (Lomeli et al., 1994). These receptors mediate fast membrane depolarization and desensitize quickly. In contrast, NMDA receptors require strong membrane depolarization to remove the Mg^{2+} block and show high Ca^{2+} permeability in addition to Na^{+} influx and K^{+} efflux. NMDA receptor activation requires the presence glycine as a modulator (McBain and Mayer, 1994). NMDA receptors are also identified on the presynaptic membrane and modulate Ca^{2+} influx through presynaptic VSCC (Cochilla and Alford, 1999; Schwartz and Alford, 1998).

In addition, a family of metabotropic glutamate receptors (mGluR) linked to G-proteins has been identified and cloned (Conn and Pin, 1997; Nakanishi, 1994). These metabotropic receptors belong to a superfamily of G-protein linked membrane receptors with seven transmembrane domains, located on presynaptic, postsynaptic as well as astrocytic membranes (Ikeda, 1996; Miller, 1998). There are eight cloned metabotropic glutamate receptors, classified into three groups according to the homology of their amino acid sequence (Conn and Pin, 1997). Group I mGluR are positively coupled with G_q proteins to activate phospholipase C. Group II and III receptors are negatively coupled with G_o/G_i proteins to inhibit adenylate cyclase (Conn and Pin, 1997). In addition to their effects mediated through the dissociated G-protein α subunit, mGluR can also mediate membrane delimited effects through G-protein β/γ subunits (Conn and Pin, 1997).

Clearance of synaptic glutamate depends on the fast kinetic binding with high affinity EAAT located on the neuronal and astrocytic membranes (Rothstein et al., 1994). At least five different high affinity transporters have been identified in the mammalian central nervous system, designated EAAT1-5 (Conti et al., 1998). These transporters share up to 50% sequence homology and are differentially distributed throughout the central nervous system (Conti et al., 1998). EAAT1 and EAAT2, also known as GLAST and GLT-1 respectively, are primarily astrocytic. EAAT3 and EAAT4 are predominantly present on neurons of the cerebral and cerebellar cortex, respectively (Conti et al., 1998; Furuta et al., 1997; Rothstein et al., 1996; Shashidharan et al., 1997). EAAT5 is exclusively located in the retina (Conti et al., 1998). EAAT mediate high affinity, electrogenic uptake of extracellular glutamate. Glutamate is first bound with the EAAT in milliseconds (Bergles et al., 1997), and then transported with 3 Na^+ (or 2 Na^+ and 1 H^+) ions intracellularly, in exchange for 1 K^+ and 1 Cl^- (or 1 HCO_3^-) ion in the opposite direction (Bouvier et al., 1992; Zhang et al., 1998). A complete cycle of glutamate uptake takes 50 - 100 milliseconds (Bergles et al., 1997). The uptake is modulated by increased extracellular K^+ (Kimelberg et al., 1995; Rutledge and Kimelberg, 1996). At slightly increased extracellular K^+, glutamate uptake is stimulated (Judd et al., 1996). At higher K^+, however, the uptake is inhibited or even reversed (Billups and Attwell, 1996; Higashida et al., 1974; Rutledge and Kimelberg, 1996), leaking glutamate into the extracellular space. Raised intracellular H^+ inhibits both forward and reversed glutamate

transport (Billups and Attwell, 1996; Kimelberg et al., 1995). The reversal is not an electroneutral process indicating other ions are transported at the same time (Billups and Attwell, 1996).

Knockout studies have shown that the astrocytic transporters EAAT1 and EAAT2, but not the neuronal EAAT3, are responsible for the bulk of glutamate clearance (Rothstein et al., 1996). Pharmacological studies demonstrated that blocking EAAT2 exacerbated the increases in glutamate in the ischemic striatum (Seki et al., 1999). Notably, EAAT1 and EAAT2, but not EAAT3, appear to be regulated proteins (Ginsberg et al., 1995; Rothstein, 1996). Downregulation of both EAAT1 and EAAT2 has been observed in a membrane fraction isolated from the rat cerebral cortex following controlled impact cortical injury (Raghavendra Rao et al., 1998). Chronic downregulation of the EAAT2 has been linked to neuronal cell death in other neural degenerative diseases (Robinson and Dowd, 1997).

Glutamate synaptic transmission is regulated by VSCC. According to their sensitivity to membrane voltage changes, VSCC are classified into high voltage-activated, including L-type, N-type, P-type and Q-type, and low voltage-activated, including R-type and T-type (Dolphin, 1995; Williams et al., 1999). Functional VSCC are heteromultimers that contain four subunits, named $\alpha 1$, β, γ and $\alpha 2/\delta$ (Dunlap et al., 1995). The $\alpha 1$ subunit not only constitutes the Ca^{2+}-selective core but also contains the voltage sensor (Snutch and Reiner, 1992). Four conserved glutamate residues within the pore form Ca^{2+} selector that facilitates fast selective single-file passage through the pore

(Yang and Tsien, 1993). N-type VSCC contains α1B isomer whereas P-type VSCC contains α1A isomer. N-type VSCC is specifically antagonized by ω-conotopeptide GVIA (Witcher et al., 1993) whereas P-type VSCC by ω-agatoxin IVA (Dolphin, 1995). Q-type VSCC also contains α1A isomer with a similar single channel conductance with N-type VSCC, but it is insensitive to ω-conotopeptide GVIA (Wheeler et al., 1994). These VSCC are not exclusively localized in the synaptic terminal. Immunocytochemical studies indicated that α1A isomer can be detected in the neuronal soma (Craig et al., 1998). L-type VSCC α1 is composed of either α1C or α1D isomers (Dunlap et al., 1995). Immunocytochemical studies indicated that α1D is located in neuronal cell bodies and proximal dendritic membranes in clusters while α1C is located in more distal dendrites on the surface membrane (Hell et al., 1993).

VSCC functional diversity is further generated by other subunits with which α1 subunit is associated (Jones et al., 1998). The functions of β subunit are to direct the VSCC complex to the plasma membrane and to regulate its channel properties (De Waard et al., 1994; Jones et al., 1998; Vance et al., 1998). It is known that β subunit interacts with α1 subunit through a conserved section in I-II cytoplasmic linker (Garcia et al., 1998; Pragnell et al., 1994). By contrast, the α2/δ subunits convert the channels into molecules responding more rapidly to voltage (Qin et al., 1998), and increase current density by

facilitating the translation and the maturation of the channels (Jones et al., 1998).

The VSCC is subject to G-protein mediated modulation. Presynaptic VSCC are modulated by G-protein coupled receptors specific to metabotropic glutamate receptors (Ikeda, 1996) and adenosine receptors (Yawo and Chuhma, 1993). Activated G-protein β/γ subunits can inhibit N-type, P-type and Q-type VSCC activation through VSCC $\alpha 1$ subunit I-II linker, which also contains the amino acid residues interacting with the β subunit of VSCC (De Waard et al., 1997). The G-protein α subunit modulates VSCC through the second messenger systems. Protein kinase C upregulates channel activity through a serine residue on VSCC $\alpha 1$ subunit I-II linker (Zamponi et al., 1997) and other sites in the amino terminus (Page et al., 1998). There is cross talk between the protein kinase C and β/γ G-protein. Protein kinase C phosphorylates one of the β/γ subunit interaction sites to antagonize β/γ subunit induced inhibition through the I - II linker (Zamponi et al., 1997).

The role of N-type, P-type and Q-type VSCC in synaptic transmitter release has been firmly established. Ca^{2+} influx through N-type, P-type and Q-type VSCC is predominantly localized in the presynaptic terminal, particularly in the presynaptic active zone (Dolphin, 1995; Dunlap et al., 1995; Elliott et al., 1995; Luebke et al., 1993). These VSCC subtypes may modulate diverse characteristics of vesicle release with different activation pattern (Reid

et al., 1998; Sheng et al., 1998). An influx of Ca^{2+} through presynaptic VSCC is both necessary and sufficient to trigger fusion of the preconditioned vesicle with presynaptic membrane (Coorssen et al., 1998; Sudhof, 1995). L-type VSCC allow localized Ca^{2+} entry (Gallin and Greenberg, 1995). The localization of L-type VSCC on the neuronal cell membrane suggests that they participate in the integration of neuronal membrane activities (Hell et al., 1993). Ca^{2+} influxes mainly through L-type VSCC in the neuronal dendrites (α1C), the soma and the base of the neurites (α1D) (Hell et al., 1993) and, to a lesser degree, through P-type and Q-type VSCC in the neuronal soma (Craig et al., 1998).

Ca^{2+} can be released into the cytoplasm from internal stores. Activation of group I mGluR and trk receptors activate phospholipase C, which in turn catalyzes the turnover of membrane lipids and produce 2 active derivatives, diacylglycerol and inositol triphosphate (Conn and Pin, 1997; Lewin and Barde, 1996). Diacylglycerol binds and activates protein kinase C which functions to modify membrane proteins. Inositol triphosphate releases Ca^{2+} from the internal stores by activating inositol triphosphate receptors located on the endoplasmic reticulum (Ramos-Franco et al., 1998). Glutamate also induces Ca^{2+} release from the endoplasmic reticulum through nitric oxide (NO). Increased cytoplasmic Ca^{2+} activates calmodulin, which tightly binds with NOS and increases the synthesis of NO (Moncada, 1992; Zhang and Snyder, 1995). NO then diffuses freely into adjacent cells and binds the iron in the heme moiety in guanylate cyclase to convert guanosine triphosphate

(GTP) to cyclic guanosine monophosphate (cGMP). In neurons and astrocytes, increased cGMP activates adenosine diphosphate-ribosyl (ADP-ribosyl) cyclase, which converts oxidated nicotinamide adenine dinucleotide (NAD^+) into cyclic ADP ribose. Cyclic ADP ribose has long been hypothesized to be the natural ligand of ryanodine receptors located on the endoplasmic reticulum (Berridge, 1993; Simpson et al., 1998). In blood vessels, increased cGMP activates cGMP-dependent kinase to mediate smooth muscle relaxation. Three nitric oxide synthase (NOS) isoenzymes have been characterized and cloned, including neuronal NOS, epithelial NOS and inducible NOS (Moncada, 1992). NO synthesis is induced by NMDA receptor mainly in neurons (Zhang and Snyder, 1995), and by mGluR in astrocytes (Agullo and Garcia, 1992).

Glutamate in energy metabolism and cerebral blood flow coupling

More than a century has passed since Sherrington first established the concept of cerebral energy metabolism and functional activity coupling (Roy and Sherrington, 1890). Regional CBF is normally distributed among the cerebral structures in almost exact proportion to their rates of energy consumption and fluctuates in synchronization with regional energy consumption in response to changes in functional activity (Akgoren et al., 1994; Sokoloff, 1981). The link between the synaptic activity and the local rate of energy metabolism has been hypothesized to be EAAT, more likely EAAT1 (Pellerin and Magistretti, 1994; Pellerin and Magistretti, 1997). However, uncoupling between CBF and the rate of cerebral energy metabolism does

occur under physiological (Cruz et al., 1999; Fox and Raichle, 1986) and ischemic conditions (Baron et al., 1984), indicating uncoupling may be a compensatory mechanism.

Both neurons and astrocytes use glucose directly as their source of energy at basal levels (Pellerin and Magistretti, 1994; Schurr et al., 1999). However, under conditions of increased synaptic activity, coupling between cerebral activity and energy metabolism hinges on the molecular function of EAAT and Na^+,K^+-ATPase (Magistretti et al., 1999). Glucose is first transported across the cerebral endothelium by the glucose transporter (Pardridge, 1991). Astrocytic capillary end-feet, concentrated in glucose transporter, cover virtually all capillary walls in the brain whereas their neuronal end-feet, concentrated in EAAT, are located in close proximity of the synaptic terminals. Glutamate released from the synaptic terminal is quickly bound by high affinity EAAT and ferried across the astrocytic membrane (Bergles and Jahr, 1997). Glucose first undergoes glycolysis to produce 2 ATP in astrocytes. One ATP is used by the Na^+,K^+-ATPase for the extrusion of 3 Na^+ ions from astrocytes; the other ATP is used for the synthesis of glutamine from glutamate (Pellerin and Magistretti, 1994; Pellerin et al., 1997). Nuclear magnetic resonance studies with ^{13}C have provided evidence of this molecular coupling in the functioning cortex and have established the stoichiometry of glucose consumption and glutamate/glutamine cycling. The rate of glutamate to glutamine conversion, indicating synaptic activity, is

almost the same as the rate of tricarboxylic acid cycle in the neuron with small corrections (Sibson et al., 1998b).

The fate of astrocytic glucose is determined by the constitution of lactate dehydrogenase. Subtypes of lactate dehydrogenase that favor the formation of lactate or pyruvate are located in astrocytes, whereas only the subtype that favors the formation of pyruvate is located in neurons (Bittar et al., 1996). Thus, neurons utilize glucose as well as lactate as their sources of energy (Bittar et al., 1996; Kauppinen and Nicholls, 1986). Uptake of glutamate is powered by cross membrane Na^+ and K^+ concentration gradient, maintained by activation of the Na^+,K^+-ATPase (Robinson and Dowd, 1997). Independent of any other signaling mechanism, increases in intracellular Na^+ generated by glutamate uptake activates Na^+,K^+-ATPase, which restores the intracellular ionic homeostasis of astrocytes (Pellerin and Magistretti, 1994). Retrieved glutamate is converted into glutamine by astrocytic glutamine synthase (Robinson and Dowd, 1997). Glutamine subsequently diffuses to the presynaptic terminal and gets reconverted into glutamate which is actively taken up by recycling glutamate vesicles (Betz and Angleson, 1998; Sudhof, 1995).

The coupling mechanism between blood flow and cerebral activity seems diverse. Both NO and adenosine modulate CBF (Dirnagl et al., 1994; Iadecola and Xu, 1994; Iadecola and Zhang, 1994; Stamler et al., 1997). Studies of regional (Faraci and Heistad, 1992) and systemic (Tanaka et al., 1991) administration of NOS inhibitors have shown that NOS is constantly active

at low levels, suggesting that NO participates in the maintenance of cerebral vasculature tone (Iadecola et al., 1994). Whether NO mediates increases in CBF elicited by functional activation appears controversial (Iadecola et al., 1994). Morphological studies have shown that the acetylcholine and vasoactive intestinal peptide (VIP) nerve terminals, originating from distinct neuronal populations, are localized in closer proximity of astrocytes than of microvessels (Chedotal et al., 1994). This observation led to the suggestion of a neuronal/glial/vascular pathway in the neurogenic control of the intracortical microcirculation (Chedotal et al., 1994). Extrinsic perivascular nerves originating from cranial autonomic ganglia give rise to a perivascular plexus and innervate cerebral arteries and veins up to vessels 50 - 100 μm in diameter. Intrinsic pathways originating from neurons located within the central nervous system and their activation can modify CBF substantially (Branston, 1995; Iadecola et al., 1994). Stimulation of these fibers elicits vasodilatation independent of the endothelium (Branston, 1995). Cerebral vasculature is also subject to the effect of trigeminovascular neurons located outside of the cranium (Markowitz and Moskowitz, 1986; Moskowitz, 1984).

Cortical spreading depression and astrocytes

CSD is a negative direct current (DC) potential shift accompanied by the flattening of the electroencephalogram recording (Leao, 1944; Leao, 1986). All components of the cerebral tissue are affected by CSD, including the neurons, the glia and the vasculature. Simultaneous recording of the extracellular and intracellular potentials from a single glial cell has shown that the change in

extracellular DC potential is of opposite polarity to the glial intracellular potential (Sugaya et al., 1975). Neuronal depolarization has an early rapid depolarization phase with burst discharges and a later gradual phase with no spike (Higashida et al., 1974; Munoz-Martinez, 1970; Sugaya et al., 1975). Both changes in DC shift and neuronal firing are more pronounced in the outer cortical layers but much attenuated in the deeper layers (Munoz-Martinez, 1970). The influx of Na^+, Cl^-, Ca^{2+} and H_2O causes swelling resulting in shrinkage of the extracellular space (Hansen and Olsen, 1980). Reduction in the extracellular space in turn increases the tissue opacity and impedance, which is more significant in the outer cortex than in the inner cortex (Hoffman et al., 1973). Predominantly due to the ionic exchange across the astrocytic plasma membrane (Na^+, Cl^- and Ca^{2+} influx in exchange for K^+ and H^+), neuronal cytoplasm and interstitial fluid become acidotic, whereas glial cytoplasm becomes alkaline (Cruz et al., 1999; Somjen et al., 1992). The response of the cortex to recurrent CSD is not static; CSD wave forms as well as the extracellular K^+ profile undergo gradual alterations in magnitude and duration over time (Richter and Lehmenkuhler, 1993).

It has been postulated that influx of extracellular K^+ underlies the DC potential shift (Grafstein, 1956). Consistent with this hypothesis self-sustaining waves of increased extracellular K^+ can be recorded to pass through the cortical glial cells and the extracellular space (Gardner-Medwin and Nicholson, 1983; Obrenovitch et al., 1996; Reid et al., 1987). The propagation

of CSD has also been reported to require gap junction conductance accompanied by increases in intracellular Ca^{2+} (Nedergaard et al., 1995).

During CSD there are large increases in extracellular glutamate (Marrannes et al., 1988; Nedergaard et al., 1995), which result from both increased vesicle release and reduced uptake by the glial cells and the neurons (Kimelberg et al., 1995; Rutledge and Kimelberg, 1996). Although increased extracellular K^+ initiates CSD and increased extracellular glutamate seems secondary (Obrenovitch and Zilkha, 1995; Obrenovitch et al., 1996), their roles are still very much intertwined. For instance, CSD can be attenuated with non-competitive or competitive NMDA antagonists (Lauritzen and Hansen, 1992; McLachlan, 1992; Nellgard and Wieloch, 1992; Willette et al., 1994), but not AMPA antagonists (Nellgard and Wieloch, 1992). Although it was noted that intracellular Ca^{2+} oscillations, spreading through the glial syncytium during CSD, bear similarities with CSD waves (Giaume and Venance, 1998), they are not necessary for the initiation of CSD (Basarsky et al., 1998).

There is a marked increase in glucose utilization during and shortly after CSD (Cruz et al., 1999; Gjedde et al., 1981; Shinohara et al., 1979), far in excess of the increase in O_2 consumption (Mayevsky and Weiss, 1991; Rosenthal and Somjen, 1973). The marked increase of local cerebral glucose utilization (CGU) in the neocortex shows no obvious difference among the cortical layers during CSD (Shinohara et al., 1979) and contributes little to the acidosis during CSD for the regional increases in lactate is quickly transferred into the blood stream (Cruz et al., 1999; Somjen et al., 1992). The increase in

oxidative metabolism is proportional with the increases in DC potential and extracellular K^+ (Rosenthal and Somjen, 1973). Intracellular ATP is decreased (Mies and Paschen, 1984), suggesting increased consumption of intracellular high phosphate energy. There is a slow-down in protein synthesis, as indicated by [^{14}C]leucine incorporation (Krivanek, 1970; Mies, 1993).

CSD associated CBF changes can be divided into three phases, a brief hypoperfusion preceding the DC potential shift, a marked hyperperfusion that out-lasts the DC potential shift, followed by a prolonged hypoperfusion (Fabricius et al., 1995). Autoregulation is only transiently affected in the brief hypoperfusion phase (Florence et al., 1994). The prolonged hypoperfusion lasts up to 3 hours (Duckrow, 1991; Lauritzen et al., 1982), but the CBF increase in response to CO_2 is impaired for up to 10 hours (Piper et al., 1991). The initial brief hypoperfusion is mediated by the autonomic nerve supply (Fabricius et al., 1995; Markowitz and Moskowitz, 1986; Moskowitz, 1984). The mediation of the hyperperfusion may involve increases in production of NO (Colonna et al., 1994; Colonna et al., 1997) and autonomic nerve controls (Fabricius et al., 1995; Goadsby et al., 1992; Zhang et al., 1994). Interestingly, the prolonged hypoperfusion seems to be mediated by both autonomic innervation and, to a lesser degree, by NO synthesis (Fabricius et al., 1995; Gault et al., 1994). The CBF increase as visualized with [^{14}C]IAP distribution revealed a relatively homogenous band that ran across the thickness of the cortex (Hansen and Olsen, 1980; Mies and Paschen, 1984). However CBF measured with laser-Doppler flowometry demonstrated that CBF in the outer

cortical layer up to 500 μm is less elevated than that in the inner layer (Fabricius et al., 1997).

Although not universally confirmed, there is evidence to indicate that about 40% of CSD elicited from the neocortex penetrate through the entorhinal cortex and amygdala into the striatum. The majority of these waves return to the neocortex (Vinogradova et al., 1991). On the contrary [^{3}H]nimodipine mapping of tissue depolarization during CSD was consistent with the idea that CSD is limited to the ipsilateral cortex (Osuga et al., 1997). It has been reported that subcortical structures may also be affected in terms of regional CBF and CGU 90 minutes after CSD (Mraovitch et al., 1992). CSD triggers antidromic burst activity of locus coeruleus neurons, which has been hypothesized to release noradrenaline in the extensive terminal field of locus coeruleus resulting in functional changes (Arakawa et al., 1997).

Periinfarct depolarizations have been observed during cerebral ischemia. The characteristics of the small depolarizations seem to be similar to typical CSD in amplitude and duration (K^+ buffering, Ca^{2+} signaling) (Dietrich et al., 1994; Nedergaard and Hansen, 1993), but the large depolarizations of both higher amplitude and longer duration also exist (Wolf et al., 1997). These periinfarct depolarizations may result from ischemic injury. They increase energy consumption in the stressed tissue and exacerbate the ischemic tissue injury (Back et al., 1994; Els et al., 1997; Hossmann, 1996; Mies et al., 1993a). Blocking the periinfarct CSD with

dizocilpine has been reported to reduce focal ischemic injury (Andine et al., 1992).

There is accumulating evidence to indicate that astrocytes provide protective and compensatory mechanisms during physiological and pathological conditions. Astrocytic resting membrane potential is predominantly mediated by inward rectifying K^+ current (Barres, 1991; Sontheimer et al., 1996). This potential is sensitive to increases in extracellular K^+ (Mennerick and Zorumski, 1994; Sontheimer et al., 1996), since it is more negative than the neuronal resting potential under physiological conditions (Higashida et al., 1974). Astrocytes are also equipped with other voltage-gated K^+, Na^+, Cl^- and Ca^{2+} channels found on the neuronal membranes, although the density of Na^+ and Ca^{2+} channels are much lower and more localized (Mennerick and Zorumski, 1994; Ritchie, 1992). Astrocytes may modulate local K^+ by spatial buffering and local sequestering (Barres, 1991). Consistent with this understanding it has been demonstrated that CSD becomes lethal when glial function fails under normal perfusion (Largo et al., 1996).

Excitotoxicity theories and ischemic injury

It is widely accepted that excitotoxicity mediated by increased extracellular glutamate is an important mechanism leading to ischemic tissue injury. The extracellular glutamate is clearly higher in ischemic cerebral tissue (Baker et al., 1991) and glutamate neurotoxicity seems to have two distinct but overlapping components (Olney, 1986). The first component,

characterized by acute neuronal swelling and necrosis, depends on extracellular Na^+ and Cl^- and can be mimicked by other depolarizing agents (Choi, 1987; Rothman, 1985). Opening of membrane channels and energy failure leads to a Na^+ influx, membrane depolarization, a secondary influx of Cl^- and H_2O and excitotoxic cell swelling. The second component, characterized by delayed neuronal degeneration, depends on extracellular Ca^{2+} and may thus be mediated by the toxic effects of excessive cytoplasmic Ca^{2+} triggered by glutamate toxicity (Choi et al., 1988).

Of the three classes of ionotropic glutamate receptors, AMPA receptors are of greater significance in the mediation of excitotoxicity. If rapid desensitization of the AMPA receptor is blocked, both AMPA and NMDA antagonists are required to reduce the neurotoxicity of glutamate (Choi et al., 1988; Michaels and Rothman, 1990). Abolishing rapid desensitization of AMPA renders it the properties of NMDA receptor since AMPA receptor and kainate receptor are often permeable to Ca^{2+} (Chittajallu et al., 1999; Paschen et al., 1996; Seeburg, 1996). It has even been argued that the opening of Ca^{2+} permeable AMPA and kainate receptors is more significant than increases in Ca^{2+} permeability through potentiated NMDA receptor channels in delayed tissue injury (Paschen, 1996). Not only are AMPA receptors permeable to Ca^{2+} but AMPA receptor activation is required to abolish the Mg^{2+} block of the ionic channel of the NMDA receptor (McBain et al., 1994). These characteristics of glutamate ionotropic receptors explains why NMDA antagonists enjoyed only limited success in reducing in vivo ischemic injury

(Buchan et al., 1991a; Buchan and Pulsinelli, 1990; Rothman and Olney, 1995). AMPA antagonism may be more useful (Buchan et al., 1991c; Li and Buchan, 1993).

The cycling of synaptic vesicles is energy-dependent. Energy reserve in the synaptic terminal can only sustain a short period of synaptic release. In addition, not all vesicles in the synaptic terminal are capable of being released. Only those vesicles docked at the active zone of the presynaptic membrane and fully primed for exocytosis are capable of energy-independent release (Coorssen et al., 1998; Sudhof, 1995). Therefore, during acute ischemic insult, increases in extracellular glutamate do not result from unlimited synaptic release. A brief early increase of extracellular glutamate, recorded with microdialysis probably corresponds to the release of these vesicles (Asai et al., 1996). However, increased extracellular K^+ can trigger instant reversal of the EAAT, leading to leakage of glutamate from astrocytes (Kimelberg et al., 1995; Obrenovitch, 1996; Rutledge and Kimelberg, 1996; Seki et al., 1999). The leakage is limited by eventual high H^+ in the extracellular space (Billups and Attwell, 1996). Conversion of glutamate to glutamine in the astrocytes is also an energy-dependent process. The glutamine synthesis, as part of the synaptic vesicle regeneration cycle, is interrupted by restricted glucose supply during ischemia (Pellerin and Magistretti, 1994; Szatkowski and Attwell, 1994). The adjacency of the end-feet of astrocyte to the synapses enables synaptic glutamate in the synaptic cleft to increase instantaneously (Chaudhry et al., 1995).

It is uncertain if increases in glutamate are the direct culprit of delayed ischemic neuronal death (Obrenovitch, 1996; Szatkowski and Attwell, 1994). Except for acute injury caused by energy failure and increases in extracellular glutamate, ischemic cell injury typically undergoes a delayed process, associated with increased neuronal response to glutamate ionotropic receptor activation (Mitani et al., 1998). Early antagonism of glutamate receptors has been reported to be useful in reducing tissue injury (Buchan et al., 1993; Buchan et al., 1991b; Ozyurt et al., 1988). However, delayed antagonism of the glutamate ionotropic receptors has been reported more successful in reducing delayed neuronal loss (Buchan et al., 1991c; Li and Buchan, 1993; Zhang and Iadecola, 1994). Thus it has been hypothesized that during ischemia glutamate is mainly released by reversed operation of the EAAT, largely independent of presynaptic Ca^{2+} influx (Ikeda et al., 1989). Along with energy failure and loss of membrane depolarization, it mediates the acute injury by activating AMPA and NMDA receptors, leading to increases in the intracellular concentration of Na^{+}, Ca^{2+} and Cl^{-} and acute neuronal injury by necrosis. Through the activation of its phospholipase C coupled metabotropic (Group I mGluR) receptors this initial increase in synaptic glutamate greatly potentiates NMDA receptors (Alagarsamy et al., 1999; Salter, 1998), and possibly AMPA receptors, kainate receptors and membrane ionic channels. Subsequently, glutamate release by Ca^{2+}-dependent exocytosis activates an excessive influx of Ca^{2+} largely through potentiated postsynaptic NMDA receptor and, likely, through AMPA and kainate receptors (Mitani et al., 1998;

Szatkowski and Attwell, 1994). Delayed neuronal death by activating built-in cell death machinery results (Nicotera et al., 1999; Tenneti et al., 1998). By contrast, the activation of metabotropic glutamate receptors negatively coupled to adenylate cyclase (Group II, III mGluR) inhibit NMDA receptor activity and prevent neurotoxicity (Ambrosini et al., 1995; Battaglia et al., 1998; Birrell et al., 1993; Bruno et al., 1994; Koh et al., 1991).

Summary and Hypothesis

The previous sections have surveyed our current understanding of the induced ischemic tolerance, the major components of synaptic transmission, the coupling of CBF and cerebral metabolism with synaptic activities, and the glutamate excitotoxicity. As such, it has been clearly established that:

1. The induced ischemic tolerance is associated with events that induce tissue depolarization with a time delay for the ischemic tolerance to take effect. This preconditioning process is inevitably accompanied by a surge in extracellular glutamate and activation of glutamate receptors. During subsequent lethal ischemic insult, the extracellular glutamate may be reduced.

2. Glutamate is a key molecule in linking the synaptic transmission with cerebral energy metabolism through the activity of the EAAT and Na^+,K^+-ATPase, and with regional CBF through the activities of NOS. Both EAAT and NOS are tightly regulated proteins in neurons and astrocytes.

3. Energy failure, tissue depolarization and glutamate excitotoxicity form a vicious cycle at the onset of acute ischemic injury. After CSD

preconditioning, the components involved in the cycle are subject to modification of second messenger signaling mediated by ionotropic and metabotropic glutamate receptors and other signaling pathways.

Therefore, we hypothesized that prior CSD preconditioning attenuates ischemic excitotoxicity by reducing glutamate synaptic activity. We assessed this hypothesis by measuring cerebral blood flow (CBF), tissue depolarization and NMDA receptor activation during subsequent ischemic insult. We also measured cerebral glucose utilization and quantified excitatory amino acid transporters (EAAT) at various time intervals after CSD.

CHAPTER 2. RATIONALE AND APPROACHES

We hypothesized that prior CSD preconditioning attenuates ischemic excitotoxicity by reducing glutamate synaptic activity. We chose to test the hypothesis in an in vivo rat model of CSD preconditioning and subsequent focal ischemia, since this model has been well documented and validated. Data collected from these intact animal studies may potentially be extrapolated for human use in the investigation of therapies for patients at immediate risk of stroke. To confirm this model system, preliminary studies were performed to demonstrate CSD induced neuroprotection against subsequent ischemic insult. Regional increases in extracellular glutamate during recurrent CSD were also confirmed.

Regional CBF is so fundamental in the ischemic injury that small changes can influence excitotoxicity. Regardless of the underlying mechanisms, increased regional CBF provides neuroprotection. We therefore measured regional CBF during focal ischemia in CSD preconditioned and sham treated studies. We then investigated the effect of CSD preconditioning on excitotoxicity by examining the activation of L-type VSCC and the activation of NMDA receptors during focal ischemia. The binding capacity and affinity of L-type VSCC and NMDA receptors were studied, since changes in density of these postsynaptic Ca^{2+} channels could affect the susceptibility of the tissue to excitotoxicity.

The ability of the cerebral tissue to withstand ischemic insult depends on the level of its energy metabolism. Regional CGU was measured in CSD preconditioned animals at various time intervals after CSD treatment. Since extracellular glutamate is cleared from the synaptic cleft by the EAAT located on the cell membrane of astrocytes and neurons, we studied the subcellular distribution of the EAAT after CSD preconditioning.

Thus the goals of the thesis were:

(1) **To identify any changes in regional CBF after CSD preconditioning.** In a protection study, regional CBF must be assessed to test whether tissue perfusion is altered by the treatment. Regional CBF was measured during focal cerebral ischemia in CSD treated and sham treated rats on day 3 after CSD treatment;

(2) **To examine whether CSD preconditioning altered L-type VSCC activation during subsequent focal ischemia.** L-type VSCC activation results from membrane depolarization. [^{3}H]Nimodipine in vivo distribution can be used to indicate tissue depolarization and impending tissue injury. Thus L-type VSCC activation can be inferred from increased [^{3}H]nimodipine in vivo distribution. [^{3}H]Nimodipine in vitro binding measures the binding characteristics of VSCC. From the in vitro binding data, the total channel quantity and binding affinity can be estimated. Thus, [^{3}H]nimodipine in vivo distribution during focal cerebral ischemia in CSD treated and sham treated rats was measured on day 3 after CSD. [^{3}H]Nimodipine in vitro binding was performed on day 3 after CSD;

(3) **To examine whether CSD preconditioning altered NMDA receptor activation during subsequent focal ischemia.** Activation of NMDA receptors through increased extracellular space is the key mechanism of excitotoxicity. Dizocilpine binds to NMDA receptor in the presence of extracellular glutamate and membrane depolarization. Thus, [^{3}H]dizocilpine in vivo distribution identifies the presence of extracellular glutamate. [^{3}H]Dizocilpine in vitro binding measures the binding characteristics of the NMDA receptor. From the in vitro binding data, the total channel quantity and binding affinity can be estimated. Thus, [^{3}H]dizocilpine in vivo distribution during focal cerebral ischemia in CSD treated and sham treated rats was measured on day 3 after CSD. [^{3}H]Dizocilpine in vitro binding was performed on day 3 after CSD;

(4) **To test whether the level of tissue energy metabolism after CSD preconditioning was altered.** The level of energy metabolism of the cerebral tissue is directly proportional to its tolerance against cerebral ischemia. Lower regional CGU due to CSD preconditioning may provide a powerful mechanism of neuroprotection. Regional CGU in CSD treated and sham treated rats was measured on day 1, day 3 and day 7 after CSD;

(5) **To investigate whether CSD preconditioning altered the quantity of EAAT in subcellular structures.** Astrocytic and neuronal EAAT clear glutamate from the synaptic cleft. However, these glutamate transporters reverse their direction in increased extracellular K^+. During cerebral ischemia, membrane depolarization and membrane pump failure release K^+ into the extracellular space. Measuring EAAT protein quantity can provide

information on the degree of glutamate leakage during cerebral ischemia. Immunoprotein analysis of astrocytic EAAT1, EAAT2 and neuronal EAAT3 were performed on day 3 after CSD. The immunoprotein analysis of EAAT2 was studied on day 1, 3, 7 and 21 after CSD.

These experimental approaches are now described in more detail.

Validation of the experimental protocol of neuroprotection

The protective effect of CSD preconditioning against focal ischemia has been shown elsewhere (Matsushima et al., 1996; Matsushima et al., 1998). A similar experimental protocol was used with slight modification (Matsushima et al., 1998) to validate our laboratory. The rats received preconditioning with 2 hours of recurrent CSD or sham treatment 3 days prior to a focal ischemic insult. Ischemic infarct volumes were measured on day 3 after the focal insult.

In vivo [^{3}H]dizocilpine distribution during recurrent and single CSD

It has been observed that during CSD depolarization there are large increases in extracellular glutamate (Leao and Morison, 1945). Microdialysis has provided initial data on the degree and profile of glutamate increase (Obrenovitch, 1996). However, this approach can only study glutamate changes at a very limited number of locations and provide little anatomical correlation. A complete map of extracellular glutamate during recurrent CSD, such as its distribution across the cortex, its propagation into the paleocortex and subcortical structures, may provide better correlation between

the magnitude of glutamate receptor activation and the protective effect of CSD preconditioning.

Dizocilpine (MK-801) is a non-competitive NMDA receptor antagonist that binds within the open NMDA ionic channel pore (Watkins and Evans, 1981). High affinity binding of dizocilpine to NMDA receptor channel requires both glutamate and tissue depolarization (Foster and Wong, 1987; Watkins and Evans, 1981; Wong et al., 1986). Therefore, the characteristics of dizocilpine binding to the NMDA receptor channel was used to measure the degree and scope of glutamate release in vivo and in vitro in autoradiographic studies (Bowery et al., 1988; Schwartz and Wasterlain, 1993; Wallace et al., 1992). Since [^{3}H]dizocilpine in vivo distribution stabilizes at about 1 hour after injection, its distribution in the brain was used to map the increases in extracellular glutamate and the topography of the increases during 1 hour recurrent CSD. To explore whether the increased regional CBF during recurrent CSD contributes to the increased [^{3}H]dizocilpine distribution, [^{3}H]dizocilpine in vivo distribution was measured during a single CSD during a 16 minute period.

Measurement of regional CBF

Measurement of regional CBF provides direct information on the state of tissue perfusion. In ischemic studies, it is also the most direct parameter of ischemic tissue injury (Hakim, 1987). CBF response in CSD preconditioned brain has been investigated in the area surrounding the ischemic core and found unaltered (Matsushima et al., 1996). However, reactive gliosis

following CSD has been reported to include increased neuronal NOS in the astrocytes, suggesting that neuroprotective effects of CSD includes increased NO release during glutamate neurotoxicity (Caggiano and Kraig, 1998). Thus, Regional CBF was measured at 3 hours of focal ischemia to investigate the blood flow response in CSD or sham preconditioned brain.

Measurement of Ca^{2+} channel activation with [^{3}H]nimodipine and [^{3}H]dizocilpine in vivo distribution

[^{3}H]Nimodipine in vivo distribution has been used to measure ischemic tissue depolarization and impending ischemic injury, thus inferring VSCC activation (Hakim and Hogan, 1991; Hogan et al., 1991). Nimodipine is a 1,4-dihydropyridine that binds to a specific site on the α1C and α1D subunits of L-type VSCC with high affinity (Dunlap et al., 1995). This site has been localized to the extracellular III S5 transmembrane segment of the α1 subunit (He et al., 1997; Hockerman et al., 1997). The VSCC exists in three states, resting, open and inactivated (Triggle, 1994). The 1,4-dihydropyridine antagonists exhibit voltage-dependent binding consistent with their preferential interaction with inactivated states (Bean, 1984; Wei et al., 1989) and open states of the channel (Triggle, 1994), whereby binding affinity increases with increasing depolarization. The availability of the channels can be controlled through channel internalization and degradation. Thus reduced in vivo binding of the ligand marks attenuated membrane depolarization, or downregulation of channel protein, or both (Hakim and

Hogan, 1991; Hogan et al., 1991). Of the regulatory factors, depolarization is of particular importance because it is a physiological signal, but one that assumes a pathological role under conditions of ischemia when energy metabolism fails and extracellular glutamate accumulates (Triggle and Tabrizchi, 1993). [^{3}H]Nimodipine distribution has been employed to map regional depolarization in the central nervous system during CSD (Osuga et al., 1997) and cerebral ischemia (Hakim and Hogan, 1991; Hogan et al., 1991; Takizawa et al., 1994). The increased binding to ischemic brain is reversible with rapid restoration of CBF (Hogan and Hakim, 1992; Takizawa et al., 1994). The binding is so sensitive to tissue depolarization that it even precedes the rise in extracellular glutamate during focal ischemia (Osuga and Hakim, 1996), and persists as long the tissue remains depolarized (Hakim and Hogan, 1991). If CSD preconditioning attenuates ischemic excitotoxicity as hypothesized, [^{3}H]nimodipine in vivo distribution, as an early and sensitive indicator of cell membrane depolarization and impending ischemic injury (Osuga and Hakim, 1996; Takizawa et al., 1994), should be reduced.

[^{3}H]Dizocilpine in vivo distribution indicates increased NMDA activation and the opening of its Ca^{2+} channel as discussed in the previous section. During cerebral ischemia, energy failure results in neuronal depolarization and the Ca^{2+}-dependent glutamate release from the synaptic terminal. Increased ischemic membrane depolarization leads to an excessive increase in extracellular K^+ and reverses the functions EAAT, resulting in further increase in extracellular glutamate. If CSD preconditioning attenuates

ischemic excitotoxicity as hypothesized, [^{3}H]dizocilpine in vivo distribution, as an indicator of glutamate concentration and concurrent regional membrane depolarization (Schwartz and Wasterlain, 1993; Wallace et al., 1992), should also be reduced.

The ischemic tissue depolarization was measured using [^{3}H]nimodipine in vivo distribution, whereas increases in extracellular glutamate were measured using [^{3}H]dizocilpine in vivo distribution. Both measurements were carried out at 3 hours of focal cerebral ischemia in brains preconditioned with prior CSD or sham treatment. The characteristics of the distributions provide information about the tissue depolarization and the levels of glutamate release. These studies afford insights into physiological changes and corroboration of the CBF data with [^{3}H]nimodipine and [^{3}H]dizocilpine in vivo distribution should provide further information about the improved tolerance against excitotoxicity in CSD preconditioned cerebral tissue.

[^{3}H]Nimodipine and [^{3}H]dizocilpine in vitro binding

[^{3}H]Nimodipine in vivo distribution reflects the activation of L-type VSCC, but provides little information about the total quantity of the channels. [^{3}H]Nimodipine in vitro binding may be affected by L-type VSCC densities and binding affinities. Earlier studies of [^{3}H]nimodipine in vitro binding at 4 hours of focal ischemia detected no change in binding capacity or affinity (Hogan et al., 1995), indicating these parameters are quite stable. However, other reports suggested that L-type VSCC are regulated. [^{3}H]PN200-

110 (Isradipine, a 1,4-dihydropyridine VSCC antagonist) in vitro binding to the crude synaptosomal membranes of the cortex was shown to increase after 10 minutes of global ischemia and to return to near control levels after 2 hours of reperfusion (Hoehner et al., 1992). [^{3}H]PN200-110 in vitro binding to tissue sections also suggests that hypoperfusion, produced by ipsilateral occlusion of the common carotid for 1 hour in the rat, was sufficient to increase the binding capacity of [^{3}H]PN200-110 in the hippocampus but not in the cortex (Magnoni et al., 1988). The increase lasted up to 96 hours after the oligemic event. Delayed neuronal death is accompanied by the loss of [^{3}H]nimodipine binding sites (Araki et al., 1998). Recurrent CSD for 2 hours may modify the total availability and binding affinity of the VSCC.

Similarly, [^{3}H]dizocilpine in vivo distribution reflects the activation of NMDA receptor, but provides little information about the total quantity of the receptor. [^{3}H]dizocilpine in vitro binding may be affected by the NMDA receptor densities and binding affinities. [^{3}H]Dizocilpine in vitro binding has been reported to coincide with the NMDA receptor distribution in the brain (Bowery et al., 1988; Kato et al., 1992a) and is not changed by 1 hour of focal ischemia (Dewar et al., 1989; Wallace et al., 1992). Others have reported in a gerbil model of global ischemia that the binding is only lost in the CA1 region after cell death is apparent (Bowery et al., 1988; Kato et al., 1992a). It is unknown whether CSD preconditioning modifies the quantity and functionality of NMDA receptor channels. Recurrent CSD for 2 hours may modify the total availability and binding affinity of the NMDA receptor.

[^{3}H]Nimodipine and [^{3}H]dizocilpine in vitro binding studies were designed to estimate the densities and affinities of the VSCC and NMDA receptors after CSD treatment. [^{3}H]Nimodipine was used to identify L-type VSCC whereas [^{3}H]dizocilpine was used to identify the NMDA receptor. These studies were conducted without ischemia on day 3 after preconditioning with 2 hours of recurrent CSD or sham treatment. This information complements the data obtained from in vivo studies.

Regional cerebral glucose utilization at different time intervals after CSD preconditioning

Lower levels of energy consumption enable the cerebral tissue to better tolerate the energy failure associated with cerebral ischemia and excitotoxicity (Folbergrova et al., 1992). Reduced energy consumption should impart increased tolerance against substrate deprivation. Moreover, due to the tight coupling between extracellular glutamate and stimulated energy metabolism, the level of regional CGU should reflect the level of synaptic activity (Mason et al., 1995; Sibson et al., 1998a)

To investigate the temporal profile of cerebral energy metabolism after CSD treatment, regional CGU was measured in brains on day 1, 3 and 7 after preconditioning with CSD or sham treatment.

Immunoprotein analysis of high affinity glutamate transporters in the cortical tissue preconditioned with CSD

EAAT play a crucial role in the clearance of extracellular glutamate (Szatkowski and Attwell, 1994). However, it reverses the direction of glutamate transport in a milieu of high extracellular K^+ (Billups and Attwell, 1996; Kimelberg et al., 1995). Its abundance shifts with the functional state of the synapses (Ginsberg et al., 1995; Raghavendra Rao et al., 1998; Rothstein et al., 1996), suggesting that these membrane proteins may downregulate to reduce leakage of glutamate from astrocytes. Furthermore, the functional activity of EAAT forms the linkage between the synaptic activity and the energy supply of the synaptic terminal (Magistretti et al., 1999). Investigating the quantity of EAAT proteins may provide insights into the state of the energy metabolism in the preconditioned tissue. The results may also corroborate the direct measurement of tissue glucose utilization with [^{14}C]deoxyglucose.

The total availability of EAAT1, EAAT2 and EAAT3 protein present in the cerebral cytoplasmic membrane was analyzed in the cortex on day 0, 1, 3, 7 and 21 with immunoprotein blotting after preconditioning with CSD or sham treatment.

In summary, the neuroprotective effect of CSD preconditioning was first confirmed in our laboratory. The increased release of glutamate during recurrent CSD was mapped with [^{3}H]dizocilpine in vivo distribution. Our hypothesis was addressed by studying whether CSD preconditioning

attenuated subsequent excitotoxicity during focal ischemia. Regional CBF, [^{3}H]nimodipine and [^{3}H]dizocilpine in vivo distribution were measured during focal cerebral ischemia on day 3 after CSD. The effect of CSD preconditioning on VSCC and NMDA receptor binding kinetics was investigated with [^{3}H]nimodipine and [^{3}H]dizocilpine in vitro binding on day 3 after CSD without ischemia. The level of energy consumption in the CSD preconditioned tissue was measured with the [^{14}C]deoxyglucose method on day 1, 3 and 7 after CSD treatment without ischemia. The quantity of EAAT1, EAAT2 and EAAT3 in the cerebral plasma membrane was assessed on day 0, 1, 3, 7 and 21 after CSD without ischemia.

CHAPTER 3. CSD PRECONDITIONING REDUCED TISSUE LOSS CAUSED BY SUBSEQUENT FOCAL ISCHEMIA

The protective effect of CSD preconditioning against focal ischemia has been well documented (Matsushima et al., 1996; Matsushima et al., 1998; Yanamoto et al., 1998). The infarct volume measurement studies after CSD preconditioning, which was slightly modified from the published works, were designed to validate the focal ischemia protocol. In addition, in the published studies, the effect of tissue edema on infarct volume measurement has been reported to be adequately addressed by deriving the infarct volume from subtracting the remaining tissue volume in the ischemic hemisphere from that in the contralateral hemisphere (Matsushima and Hakim, 1995; Matsushima et al., 1998; Swanson et al., 1990). Current measurements attempted to understand this issue when the published approach failed to better correct the effect of cerebral edema on the infarct volume measurement.

Methods

Male Sprague-Dawley rats (Charles River, Montreal, Quebec, Canada) weighing 275 to 375 g were randomly assigned to study groups. All surgical manipulations and CSD were performed under inhalational anesthesia (Halothane 4% induction, 1% maintenance in 30% O_2 - 70% N_2O). Rats were allowed to breathe spontaneously during CSD preconditioning, but were

mechanically ventilated during focal ischemia. Body temperature (rectal) was maintained at 36.5 - 37.5°C in all studies.

Cortical spreading depression

CSD was induced in the left occipital cortex with 0.5 M KCl as described (Matsushima et al., 1998) with slight modification. A tail artery cannula was placed to monitor mean arterial blood pressure, arterial blood gases and blood glucose. The rats were placed in a stereotaxic frame (Stoelting, Oakwood Center, Illinois, USA). A platinum wire (0.13 mm diameter) was inserted through a 0.5 mm diameter burr hole into the left frontal cortex (Bregma 1.0 mm, lateral 5.0 mm, depth 2.0 mm) and connected to a DC amplifier with chart recorder (Servogor 430, Norma Goerz Instruments, Neudorf, Austria) to record CSD. In addition to the anterior platinum electrode, a second platinum wire was placed through an identical burr hole into cortex (Bregma -2.0 mm, lateral 5.5 mm, depth 2.0 mm) for measurement of CBF by the H_2 clearance method during subsequent MCA occlusion. The burr holes were then sealed with dental cement. A 2 mm diameter burr hole (Bregma -6.0 mm, lateral 5.6 mm) was made over the left occipital cortex leaving the dura intact. Recurrent CSD were induced in the CSD treatment group by placing small cotton pledgets soaked with 0.5 M KCl on the intact occipital dura. The pledgets were replaced every 15 minutes for 2 hours. Pledgets soaked in 0.5 M NaCl were used in the sham treatment group.

In three initial studies, the CSD signal recorded from the platinum electrode in the frontal cortex was compared with the signal obtained from the single-barreled Ag/AgCl glass microelectrode (20 MΩ resistance) placed alongside the platinum wire. The biphasic waves recorded with the platinum electrode corresponded to negative DC potential shifts of average amplitude 5.3 mV and duration 80 seconds, consistent with CSD depolarization (McLachlan, 1992; Somjen et al., 1992). All further studies used platinum electrodes to record CSD and periinfarct depolarization.

Middle cerebral artery occlusion

Focal cerebral ischemia was induced using intraluminal occlusion of the left MCA as described (Matsushima et al., 1998; Zea Longa et al., 1989). On day 3 after CSD or sham treatment, the rats were re-anesthetized following overnight fast. Femoral arterial and venous cannulae were placed for mean arterial blood pressure, arterial blood gas, blood glucose and blood radiotracer concentration measurements. Tympanic membrane temperature was continually monitored and maintained between 36.5 and 37.5°C. The anterior platinum electrode previous implanted was used to record periinfarct depolarizations during ischemia and the posterior electrode was connected to a customized amplifier to measure H_2 clearance as described (Farrar, 1987).

For MCA occlusion, the left common, external and internal carotid arteries were exposed. The proximal ends of the common carotid and the external carotid arteries were ligated. A 3-0 nylon monofilament thread with

a fire polished tip was inserted into the common carotid distal to the proximal ligation and was advanced 18.5 mm beyond the carotid bifurcation into the internal carotid artery. MCA occlusion was confirmed by measuring cortical blood flow using the H_2 clearance method following brief (1-3 minutes) inhalation of 10% H_2 gas in the anesthetic mixture (Appendix 1). At the end of the MCA occlusion, the incisions were sutured, anesthesia was discontinued and the rats were allowed free access to food and water.

Cortical DC potentials were monitored throughout the focal ischemia. Following MCA occlusion CBF was measured hourly and immediately after release of the MCA occlusion. During MCA occlusion, measurement of periinfarct depolarization was confounded by large DC potential shifts during inhalation of H_2 gas for measurement of CBF in the ipsilateral frontoparietal cortex. Thus transient DC potential shifts greater than 2 mV from baseline and lasting longer than 60 seconds were considered to be a periinfarct depolarization, and the calculated rate of occurrence of these events was corrected for the periods of time during H_2 inhalation when recording was not possible. Periinfarct integrated negativity (Back et al., 1994), defined as the area under the periinfarct depolarization wave, was also calculated.

Infarct volume measurement

The ischemic infarct volume was measured as described (Swanson et al., 1990). Briefly, on day 3 after MCA occlusion, the rats were decapitated under anesthesia, the brain was extracted and frozen. Brain sections, 20 μm in thickness and collected at every 840 μm interval, were stained with Cresyl

violet. To measure infarct volumes, the infarct areas in 15 coronal brain sections were measured on the Microcomputer Imaging Device (MCID) as described (Swanson et al., 1990). The ratio of the total ipsilateral volume over the total contralateral volume (edema ratio) was calculated in all studies (Hiramatsu et al., 1993), and the infarct volume was calculated as the difference between the contralateral regional volume and non-ischemic regional volume in the ipsilateral hemisphere / edema ratio (Appendix 2). A total of 12 CSD and 18 sham treated rats were studied.

Statistical analysis

All results are expressed as mean ± standard deviation (SD). The physiological data were analyzed using the two-sample t-test. The infarct volume measurement data were analyzed with analysis of covariance using average H_2 clearance CBF as covariate followed by Bonferroni adjustment for multiple comparisons (Systat, SPSS Inc., Chicago, Illinois, USA).

Results

Physiological variables

Physiological variables did not differ between the CSD and sham treated groups during the 2 hours preconditioning and the subsequent 3 hours of MCA occlusion. The data during MCA occlusion are summarized in Table 3-1. During treatment rectal temperature did not differ between the CSD (36.9 ± 0.2°C, n = 12) and sham (36.9 ± 0.2°C, n = 18) treated groups. Similarly, during MCA occlusion rectal temperature did not differ between

the CSD (36.9 ± 0.2°C, n = 12) and sham (36.8 ± 0.2°C; n = 18) treated groups. Tympanic membrane temperature was slightly higher in the CSD treated group (36.6 ± 0.3°C, n = 12) than in the sham treated group (36.5 ± 0.1°C, n =18) (p = 0.016), but this difference was insignificant physiologically.

Table 3-1. Physiological variables for infarct volume measurements

Parameters	CSD treated (n = 12)	Sham treated (n = 18)
MABP (mm Hg)	88 ± 4	87 ± 4
pH	7.44 ± 0.02	7.44 ± 0.02
P_aCO_2 (mm Hg)	43 ± 3	43 ± 3
P_aO_2 (mm Hg)	179 ± 35	167 ± 49
Blood glucose (mM)	6.46 ± 0.59	6.79 ± 1.04

Values are means ± SD. MCA occlusion, 3 hours. MABP, mean arterial blood pressure; MCA, middle cerebral artery; P_aCO_2, arterial partial pressure of carbon dioxide; P_aO_2, arterial partial pressure of oxygen; SD, standard deviation. Mechanical ventilation during focal ischemia.

Cortical spreading depression waves and periinfarct depolarization

In the CSD treated group CSD waves were recorded in the ipsilateral cortex as a transient negative or biphasic shift of DC potential (Matsushima et al., 1996) recorded from the anterior platinum electrode. The waves had an average amplitude of 8.0 ± 2.8 mV (n = 12) (Table 3-2) and a duration of 94.3 ± 26.0 seconds (n = 12), similar to previously reported characteristics of CSD recorded with platinum electrode (Matsushima et al., 1996). The rate of CSD

waves recorded was 6.3 ± 2.4 h^{-1} (n = 12) in the CSD treated group, whereas none was recorded in the sham treated group (Table 3-2).

Table 3-2. Rate of recurrent cortical and periinfarct depolarization waves during preconditioning and subsequent MCA occlusion

Parameters	CSD preconditioning (n = 12)	Sham (n = 18)
CSD wave forms (h^{-1})	6.3 ± 2.4	-
Ischemic periinfarct depolarization (h^{-1})	0.6 ± 0.8	0.9 ± 1.3
Ischemic periinfarct integrated negativity (mV min h^{-1})	4.7 ± 5.7	8.1 ± 10.8

Values are mean ± SD. Duration of recurrent CSD was 2 hours; duration of MCA occlusion was 3 hours. CSD, cortical spreading depression; MCA, middle cerebral artery; SD, standard deviation.

The rate of periinfarct depolarization events recorded during MCA occlusion was 0.6 ± 0.8 h^{-1} (n =12) in the CSD treated group and 0.9 ± 1.3 h^{-1} (n =18) in the sham treated group, without significant difference (Table 3-2). One rat in the sham treated group had a total of 11 periinfarct depolarization events in sequence during 3 hour of MCA occlusion. The appearance of the wave forms bore considerable resemblance with CSD reverberation (Shibata and Bures, 1974). The ischemic periinfarct integrated negativity was 4.7 ± 5.7 mV min h^{-1} (n =12) in the CSD treated group and 8.1 ± 10.8 mV min h^{-1} (n = 18) in the sham treated group with no significant difference between the two groups.

Regional CBF measured with H_2 clearance

At five time points (one immediately before MCA occlusion, hourly during MCA occlusion and one immediately after release of MCA occlusion) regional CBF was measured with the H_2 clearance method (Figure 3-1). No significant difference in flow or percent reduction from pre-occlusion levels was observed between the CSD and sham treated groups during MCA occlusion. Mean ipsilateral CBF in the somatosensory cortex was 27 ± 7 mL $100g^{-1}\,min^{-1}$ (n = 12) in the CSD treated group and 31 ± 9 mL $100g^{-1}\,min^{-1}$ (n = 18) in the sham treated group. These data represented 0.25 ± 0.13 (n =12) of the pre-ischemic measurement in the CSD treated group and 0.27 ± 0.08 (n =18) in the sham treated group. Immediately after release of MCA occlusion, mean regional CBF was 114 ± 35 mL $100g^{-1}\,min^{-1}$ (n = 12) in the CSD treated group and 123 ± 38 mL $100g^{-1}\,min^{-1}$ (n = 18) in the sham treated group. These data represented 1.02 ± 0.48 (n = 12) of the pre-ischemic measurement in the CSD treated group and 1.11 ± 0.36 (n = 18) in the sham treated group, with no significant difference between the two groups. There was no significant difference compared to pre-ischemic flow levels.

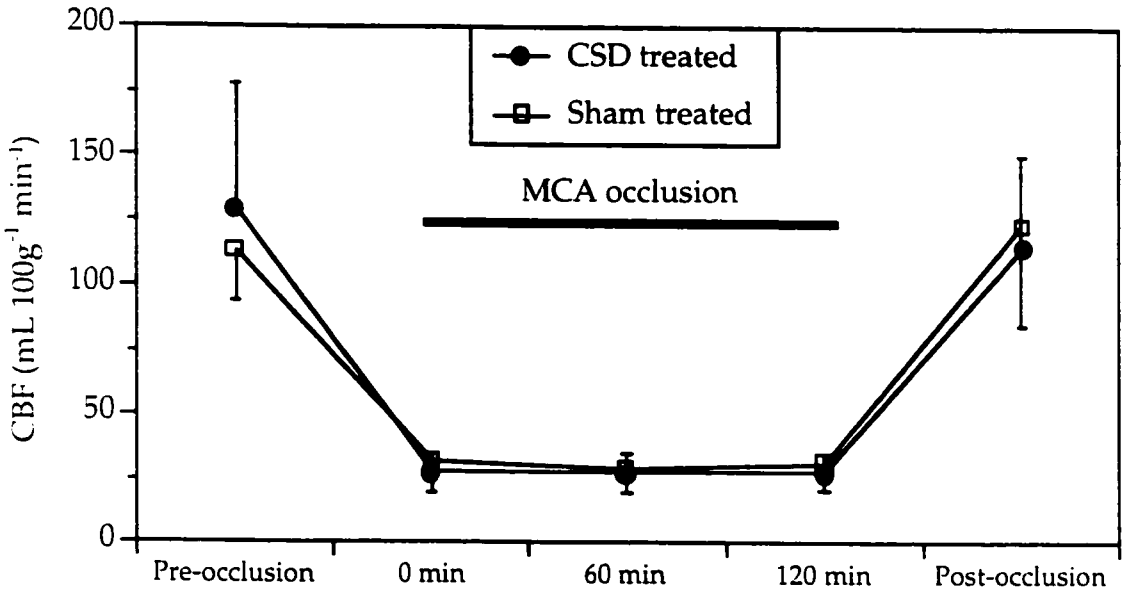

Figure 3-1. Time course of regional CBF during focal ischemia in the CSD treated group and sham treated group. Values are means ± SD. CSD, cortical spreading depression; SD, standard deviation.

Histological outcomes

In both groups, a zone of tissue necrosis, up to 1 mm deep was identified in the cortex under the dura where the cotton pledgets were placed regardless whether it was soaked with 0.5 M KCl or 0.5 M NaCl.

Infarction was noted in the cortex and the striatum in both groups. The infarct volume data were studied with analysis of variance using the regional CBF data obtained with H_2 clearance measurement as covariate. Initial examination of the data with a general linear model (Infarct volume = CONSTANT + group + CBF + group * CBF) indicated that the homogeneity of slopes assumption held ($p = 0.086$) (Figure 3-2). In the sham treated group

cortical infarction appeared to occur at higher regional CBF levels. The correlation between regional CBF and cortical volume of infarct was weak but significant ($r^2 = 0.4$, $F_{(1,16)} = 9.12$, $p = 0.008$). In the CSD treated group cortical infarct volumes seemed to have a more linear correlation with regional CBF ($r^2 = 0.7$, $F_{(1,10)} = 21.14$, $p = 0.001$). The difference in these correlations was highly significant ($r^2 = 0.53$, $F_{(1,27)} = 21.42$, $p < 0.001$ by one-way analysis of variance), indicating that CSD preconditioning resulted in reduced cortical infarct volumes over a range of regional CBF values (Figure 3-2). The correlation between the cortical infarct volume and the periinfarct integrated negativity was not significant ($r^2 = 0.09$, $F_{(1,27)} = 2.78$, $p = 0.11$).

Using regional CBF as covariate, the cortical infarct volumes in CSD preconditioned studies were significantly smaller than the sham treated studies ($p < 0.0001$). Total cortical infarct volume was 21.2 ± 25.3 mm^3 ($n = 18$) in the CSD treated group compared with 43.3 ± 21.9 mm^3 ($n = 12$) in the sham treated group ($p < 0.01$) (Table 3-3, Figure 3-2), indicating that CSD preconditioning significantly reduced cortical infarct volume. Infarct volume for the striatum was 9.3 ± 6.4 mm^3 ($n = 18$) in the CSD treated group and 7.7 ± 8.4 mm^3 ($n = 12$) in the sham treated group, with no significant difference. Figure 3-2 shows the relationship between infarct volume and regional CBF in individual rats. The edema ratio was 1.18 ± 0.08 ($n = 12$) in the CSD treated group and 1.18 ± 0.11 ($n = 18$) in the sham treated group, with no significant difference between the two groups.

Table 3-3. Infarct volume following 3 hours of focal cerebral ischemia in CSD and sham preconditioned rats

Parameters	CSD treated (n = 12)	Sham treated (n = 18)
Infarct volume (mm^3)		
Cortex	22.2 ± 25.3**	43.3 ± 21.9
Striatum	9.34 ± 6.42	7.70 ± 8.44
Edema ratio	1.18 ± 0.08	1.18 ± 0.11

CBF within ischemic cortex during middle cerebral artery occlusion did not differ between CSD (27.5 ± 6.8 mL 100 g^{-1} min^{-1}) and sham (30.8 ± 9.5 mL 100 g^{-1} min^{-1}) groups.

Values are means ± SD. Different from sham treated group: ** $p < 0.01$ analysis of covariance with Bonferroni adjustment. Edema ratio = Ipsilateral hemispheric volume / Contralateral hemispheric volume; Infarct volume = Integral (Contralateral tissue volume - Ipsilateral non-ischemic tissue volume / Edema Ratio). CBF, cerebral blood flow; CSD, cortical spreading depression; SD, standard deviation.

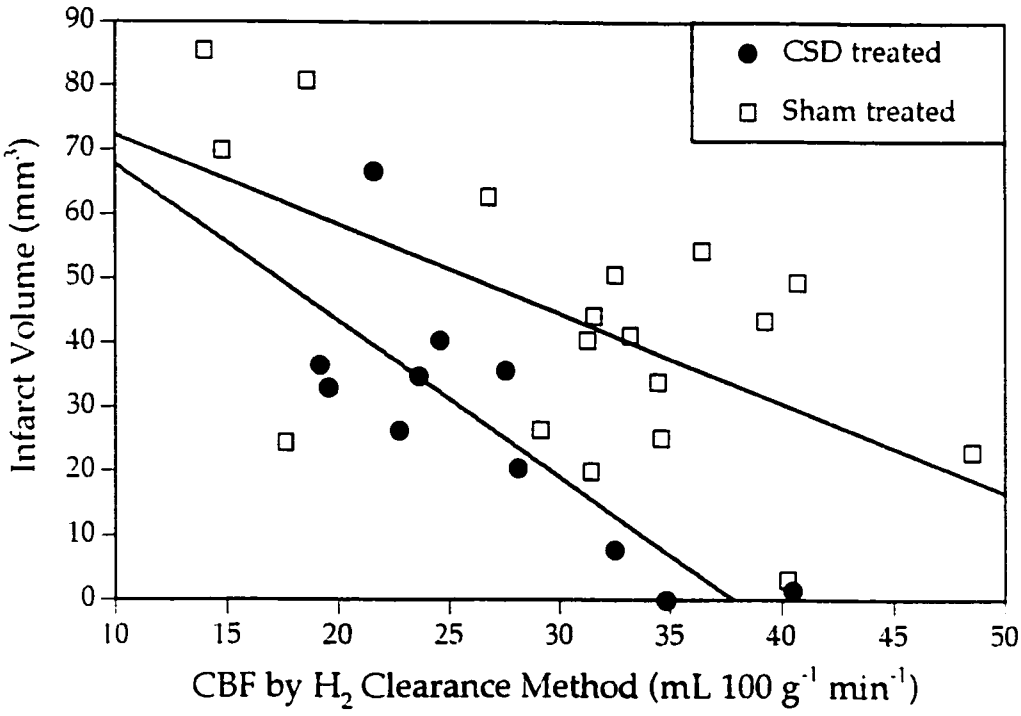

Figure 3-2. The relationship between mean regional CBF during ischemia and cortical infarct volume of each rat in CSD (n = 12) or sham (n = 18) treated groups. The equations for the linear regressions shown are: Infarct Volume (mm^3, CSD treated) = -2.44*[CBF] + 92.2; Infarct Volume (mm^3, sham treated) = -1.39*[CBF] + 86.3. The slope of the two linear regressions do not differ (p = 0.086). CBF, cerebral blood flow; CSD, cortical spreading depression; MCA, middle cerebral artery.

Discussion

Infarct volume was measured on day 3 after 3 hours of intraluminal MCA occlusion in the rat brain. The animals were subjected to 2 hours of recurrent CSD 72 hours prior to the focal ischemic event. The data indicated that the cortical infarct was reduced to about half the size found in the sham treated rats ($p < 0.001$) whereas the infarct in the striatum is not affected.

Cerebral edema, measured by the edema ratio derived from the ratio of ipsilateral forebrain volume over that of the contralateral side, was not different between the two groups. Regional CBF, measured with the H_2 clearance method through a platinum electrode implanted outside the ischemic core, was also not different between the CSD preconditioned and the sham group.

The protective effect of CSD has been reported in the same model elsewhere (Matsushima et al., 1996; Matsushima et al., 1998). The findings presented here confirmed the observation that CSD induces ischemic tolerance. Regional CBF in the somatosensory cortex, near the ischemic core, measured by the H_2 clearance method did not differ in the two study groups. CSD-induced ischemic protection supports the observation that the cortex can be preconditioned to better cope with a future ischemic insult.

Earlier reports excluded regional CBF as a mechanism in CSD-induced ischemic tolerance (Matsushima and Hakim, 1995; Matsushima et al., 1996). The H_2 clearance measurement employed here did not reveal a difference between CSD treated and sham treated groups either. However, the role of regional CBF could not be ruled out. Although the H_2 clearance method has the advantage to continuously monitor CBF, its use is limited to a small numbers of locations. The infarct volume measurement data support the published findings (Matsushima et al., 1996). The discrepancy between the infarct volume obtained here and the published data (Matsushima and Hakim, 1995; Matsushima et al., 1996) may be explained by the difference in

the experimental protocol. The previous report used H_2 clearance as an indicator of effective MCA occlusion and the cut-off of level of CBF was set at 25 mL min^{-1} g^{-1} (Matsushima and Hakim, 1995; Matsushima et al., 1996). The infarct volumes obtained with such a cut off were considerably larger.

The edema data indicated that the degree of the swelling is proportional to the damage sustained, consistent with other studies on ischemic edema (Hiramatsu et al., 1993). It is well known that post-ischemic edema exacerbates tissue injury in addition to complicating the infarct volume measurement (Belayev et al., 1996; Hiramatsu et al., 1993; Lin et al., 1993). Swanson et al recommend using the difference of the surviving tissue volume between two hemispheres to calculate the lost volume (Swanson et al., 1990). This approach assumes that the viable tissue surrounding the infarct does not undergo edematous reactions. This assumption may not hold in studies such as those presented here. Based on our data and those published by others (Hiramatsu et al., 1993), it seems that the normal tissue may react to the infarct and develop edematous responses. The use of edema ratio assumes that the viable tissue and damaged tissue have the same edematous response to the injury. Though the validity of this assumption may still be questioned, the current approach represents a better approximation. Ischemic edema, indicated by the edema ratio, did not seem to be affected by the preconditioning in the current measurement.

A platinum wire was used for DC potential measurement during CSD preconditioning and MCA occlusion. It was a convenient choice since the

electrodes had to be embedded long term. However as an electrode for DC recording and characterization, platinum is complex. In addition, to secure a good placement of the electrode, the electrode was inserted across the thickness of the cortex. This practice in effect integrates the DC signal across all layers of the cortex, which leads to the recording of distorted CSD and periinfarct waves. These deficiencies may explain why our CSD waves recorded with these electrodes are generally less pronounced than those recorded with Ag/AgCl electrode placed in a specific layer of the cortex (Leao and Morison, 1945; Munoz-Martinez, 1970; Ochs and Hunt, 1960), and why sometimes biphasic and predominantly positive waves were recorded. The same problem may also be responsible for the periinfarct waves recorded during subsequent MCA occlusion, which make comparison with reported studies less informative (Back et al., 1994). Nonetheless, for detecting a CSD event, platinum electrodes are sensitive and specific as indicated by the CSD data collected with an Ag/AgCl electrode placed alongside the platinum electrode.

In summary, CSD-induced ischemic tolerance was confirmed in the CSD-ischemia paradigm used in the studies. An edema ratio was introduced to correct the interference. CSD treatment did not seem have any effect on the edema ratio.

CHAPTER 4. IN VIVO [^{3}H]DIZOCILPINE (MK-801) MAPPING OF THE RAT BRAIN DURING CORTICAL SPREADING DEPRESSION

CSD preconditioning imparts neuroprotection against subsequent ischemic tissue injury (Kobayashi et al., 1995; Matsushima et al., 1996; Taga et al., 1997; Yanamoto et al., 1998). Microdialysis measurement has demonstrated that extracellular glutamate is increased during CSD (Obrenovitch, 1996). However, this approach can only study glutamate changes at a very limited number of locations and provide little anatomical correlation. A complete map of extracellular glutamate during recurrent CSD, such as its distribution across the cortex, its propagation into the paleocortex and subcortical structures, may provide better correlation between magnitude of glutamate receptor activation and the protective effect of CSD pretreatment.

Dizocilpine (MK-801) is a non-competitive NMDA receptor antagonist that binds within the open NMDA cation channel pore (Watkins and Evans, 1981; Wong et al., 1986). In vivo [^{3}H]dizocilpine autoradiographic imaging during acute focal ischemia has shown increased distribution in the ischemic cortical tissue (Wallace et al., 1992). This increase has been suggested to represent increased binding of [^{3}H]dizocilpine to the open NMDA receptor in response to increased extracellular glutamate, since opening of the NMDA gated cation channel requires both ligand binding to the NMDA receptor and concurrent cell membrane depolarization (McBain and Mayer, 1994).

[^{3}H]Dizocilpine binding to the NMDA receptor (McBain and Mayer, 1994; Wallace et al., 1992; Wong et al., 1986) was used to examine the degree and extent of NMDA receptor activation during CSD stimulation in the neocortex and other regions. It was found that in recurrent CSD during 1 hour period, there was an increase in [^{3}H]dizocilpine distribution in the outer layer of the neocortex. The results are consistent with the hypothesis that CSD elicits increases in extracellular glutamate to activate NMDA receptor. These findings provide visual evidence of the extent of NMDA receptor activation during CSD. There was also an increase in [^{3}H]dizocilpine distribution in the cortex that underwent a single CSD during a 16 minute period with a different pattern of [^{3}H]dizocilpine distribution.

Methods

Experimental animals and surgical anesthesia were identical to those employed in Chapter 3. Rats were allowed to breathe spontaneously during 1 hour of recurrent CSD. Body temperature (rectal) was maintained at 36.5 - 37.5°C during the experiments.

Cerebral [^{3}H]dizocilpine autoradiography

In recurrent CSD studies, CSD was induced from the left occipital cortex with 0.5 M KCl as described in Chapter 3 with slight modification. Only the anterior platinum electrode was inserted. Recurrent CSD were induced in the CSD treatment group by placing small cotton pledgets soaked with 0.5 M KCl on the intact occipital dura. The pledgets were replaced every 15 minutes for

60 minutes. Pledgets soaked in 0.5 M NaCl were used in the sham treatment group. [^{3}H]Dizocilpine autoradiography was carried out as previously described by Wallace et al (Wallace et al., 1992). Briefly, 50 µCi [^{3}H]dizocilpine (specific activity 23.9 Ci mmol^{-1}, Amersham International Plc, England) in 500 µl saline was injected intravenously immediately after the first cotton pledget containing 0.5 M KCl was applied. The radiotracer was allowed to circulate for 60 minutes during which time recurrent CSD were recorded. A 100 µl arterial blood sample was obtained immediately prior to decapitation. A total of 7 CSD treated and 7 sham treated rats were studied.

In single CSD studies, a second platinum electrode was inserted 3 m m posterior (bregma -2.0 mm, lateral 5.0 mm, depth 2.0 mm) of the anterior electrode to aid the timing of [^{3}H]dizocilpine injection. Briefly, 50 µCi [^{3}H]dizocilpine (specific activity 23.9 Ci mmol^{-1}, Amersham International Plc, England) in 500 µl saline was injected intravenously as soon as the typical upswing of the CSD wave was identified in the posterior electrode. The radiotracer was allowed to circulate for 16 minutes during which time only 1 CSD was elicited. A 100 µl arterial blood sample was taken 16 m in immediately prior to decapitation. A total of 6 CSD treated rats were studied.

At the end of the incubation period (60 minutes in recurrent CSD studies and 16 minutes in single CSD studies), the brain was rapidly removed, frozen and stored at -80°C. Plasma [3H]dizocilpine concentration was measured using liquid scintillation counting with appropriate quench correction obtained from internal standards. Coronal cryostat sections of the

rat brain at 20 µm thick were obtained in 140 µm interval at -20°C. Air dried sections were apposed to tritium sensitive film (Hyperfilm, Amersham, Oakville, ON, Canada) with 20 µm thick tissue paste [^{3}H] standards prepared from the forebrain homogenate for 60 days to allow calibration of the tissue ^{3}H content.

Image analysis

Autoradiographic images at 6 coronal levels in the brain were digitized using a microcomputer based imaging system (MCID, Imaging Research Inc., Brock University, St. Catharines, ON, Canada). The levels corresponded to coronal sections from Bregma in mm at 2.20 (level 0), 1.20 (level 1), 0.20 (level 2), -3.30 (level 3), -5.60 (level 4), -6.30 (level 5) (Paxinos and Watson, 1986). The resulting set of 6 images from each study were then spatially registered to a set of images from a selected [^{3}H]dizocilpine study, using multiple anatomically defined fiducial markers (35 -40) as implemented within MCID (Bookstein, 1990). A set of standardized anatomical regions of interest (ROI) template was used to sample regional ^{3}H radiotracer content (Figure 4-1, 4-6). To normalize the measurements of brain tissue [^{3}H]dizocilpine between studies, the volume of distribution (V_d) of [^{3}H]dizocilpine in each ROI was calculated as the ratio of [^{3}H]dizocilpine tissue content within the ROI over the plasma [^{3}H]dizocilpine concentration at study termination (Gjedde et al., 1981; Patlak et al., 1983).

To guide in the identification of groups of ROI with similar degrees of [^{3}H]dizocilpine distribution, a K-means cluster analysis (Systat, SPSS Inc.,

Chicago, Illinois, USA) was performed. For recurrent CSD studies, the variables for the cluster analysis were the average of the logarithm of the ratio of ipsilateral over contralateral [^{3}H]dizocilpine tissue content for all ROI on two conditions (CSD treated, sham treated). For single CSD studies, the variables for the cluster analysis are the average of the logarithm of the ratio of ipsilateral over contralateral [^{3}H]dizocilpine on one variable (CSD). The resulting ROI clusters were further subdivided to separate cortical and striatal regions into volume of interest (VOI). [^{3}H]Dizocilpine V_d measurements were weight-averaged over the resulting fixed set of VOI. The ratio of [^{3}H]Dizocilpine V_d between ipsilateral and contralateral hemispheric VOI was also calculated.

Statistical analysis

All results are expressed as mean ± SD. The physiological data were analyzed using the t-test. The V_d data were analyzed with one-way repeated measures analysis of variance (Systat, SPSS Inc., Chicago, Illinois, USA). Between-group difference was analyzed with adjusted degrees of freedom and mean square error followed by Bonferroni adjustment for multiple comparisons, whereas within–group difference was analyzed with Greenhouse-Geisser adjustment to the degree of freedom followed by post hoc comparison used Tukey's HSD test (Howell, 1992).

Results

Physiological variables

Physiological variables did not differ between CSD and sham groups. These variables were averaged over all studies in CSD and sham treated groups, and are summarized in Table 4-1. During the study period rectal temperature did not differ between the recurrent CSD studies (37.1 ± 0.3°C, n = 7) and sham studies (36.8 ± 0.2°C, n = 7). The average rectal temperature for single CSD studies was 36.7 ± 0.1 °C.

Table 4-1. Physiological variables for in vivo [^{3}H]dizocilpine binding

Parameters	Recurrent CSD (n = 7)	Sham (n = 7)	Single CSD* (n = 6)
MABP (mm Hg)	94 ± 10	92 ± 4	81 ± 3
pH	7.38 ± 0.02	7.38 ± 0.02	7.41 ± 0.02
P_aCO_2 (mm Hg)	50 ± 4	49 ± 2	49 ± 2
P_aO_2 (mm Hg)	248 ± 21	235 ± 32	250 ± 26
Blood glucose (mM)	5.67 ± 0.48	5.68 ± 0.47	6.71 ± 1.00

Values are means ± SD. MABP, mean arterial blood pressure; P_aCO_2, arterial partial pressure of carbon dioxide; P_aO_2, arterial partial pressure of oxygen. *Single CSD studies were performed separately from recurrent CSD studies.

Cortical spreading depression waves

Recurrent CSD waves during 1 hour of KCl application on the dura were recorded as transient negative or biphasic DC potential shifts. The amplitude of the CSD waves was 9.3 ± 2.5 mV (n = 7) with a duration of 77.4 ± 7.8 second (n = 7). The number of CSD waves in the CSD group during 1 hour was 5.5 ± 0.7 (n = 7). In the sham group, 1 CSD-like wave was recorded during [^{3}H]dizocilpine injection in one study. In the single CSD group, CSD waves were recorded as biphasic DC deflections of mean amplitude 10.6 ± 4.3 mV and mean duration 97.5 ± 18.9 seconds in the posterior electrode, and of mean amplitude of 10.6 ± 4.9 mV and mean duration 91.5 ± 21.3 seconds in the anterior electrode. The mean time delay between the posterior and anterior electrodes were 40.1 ± 21.0 seconds. The average propagation velocity was 4.59 ± 1.62 mm/min.

[^{3}H]Dizocilpine distribution

Recurrent CSD: K-means cluster analysis performed on ipsilateral / contralateral V_d values showed the within cluster sum of squares to decline most rapidly to three clusters in recurrent CSD studies (CSD, $F_{(2,40)} = 144.91$, $p << 0.001$; Sham, $F_{(2,40)} = 4.61$, $p < 0.02$) (Figure 4-1). The three initial ROI clusters were further divided on an anatomical basis to separate cortical and striatal regions, resulting in four final VOI (Figure 4-1). Cortex 1 covered the frontal cortex and outer cortical layers, whereas cortex 2 occupied mostly the posterior cortex and the inner cortical layers (Figure 4-1). Average [^{3}H]dizocilpine V_d image at 6 coronal levels from recurrent CSD studies are

shown in Figure 4-2. The difference image of average [^{3}H]dizocilpine V_d between recurrent CSD and sham studies are overlaid on spatially registered histological sections, shown in Figure 4-3. Increased [^{3}H]dizocilpine distribution was seen mainly in the anterior neocortex and the outer neocortex (Figure 4-2, Figure 4-3). However, the increased distribution became discontinuous at the occipital site where recurrent CSD were induced on the intact dura (Figure 4-2, Figure 4-3).

The V_d data in each ROI were weight-averaged within each VOI and are summarized in Figure 4-4. Comparing between the CSD and sham groups, [^{3}H]dizocilpine V_d in cortex 1 was 17.98 ± 3.56 mL g^{-1} in the CSD group, significantly higher than 12.29 ± 1.99 mL g^{-1} in the sham group ($p < 0.02$) (Figure 4-4). Within the CSD treatment group the ipsilateral cortex 1 (17.98 ± 3.56 mL g^{-1}) was significantly higher than contralateral cortex 1 (13.34 ± 3.74 mL g^{-1}) ($p < 0.01$) (Figure 4-4).

Single CSD: K-means cluster analysis performed on ipsilateral/ contralateral V_d values showed the within cluster sum of squared to decline most sharply to three clusters in the single CSD studies (CSD, $F_{(2,40)} = 108.24$, $p << 0.001$) (Figure 4-5). The three initial ROI clusters were further divided on an anatomical basis to separate cortical and striatal regions, resulting in four final VOI (Figure 4-5). For the single CSD studies, cortex 1 identified narrower outer cortical regions whereas cortex 2 included large areas (Figure 4-5). Average [^{3}H]dizocilpine V_d image at 6 coronal levels from recurrent CSD studies are shown in Figure 4-6. The ROI V_d data were averaged within each

VOI and are summarized in Figure 4-7. Compared with the corresponding contralateral VOI, [^{3}H]dizocilpine V_d in cortex 1 was 46.53 ± 7.34 mL g^{-1} compared with 37.06 ± 5.52 mL g^{-1} in the corresponding contralateral cortex 1 VOI in the single CSD group ($p<0.01$) (Figure 4-7).

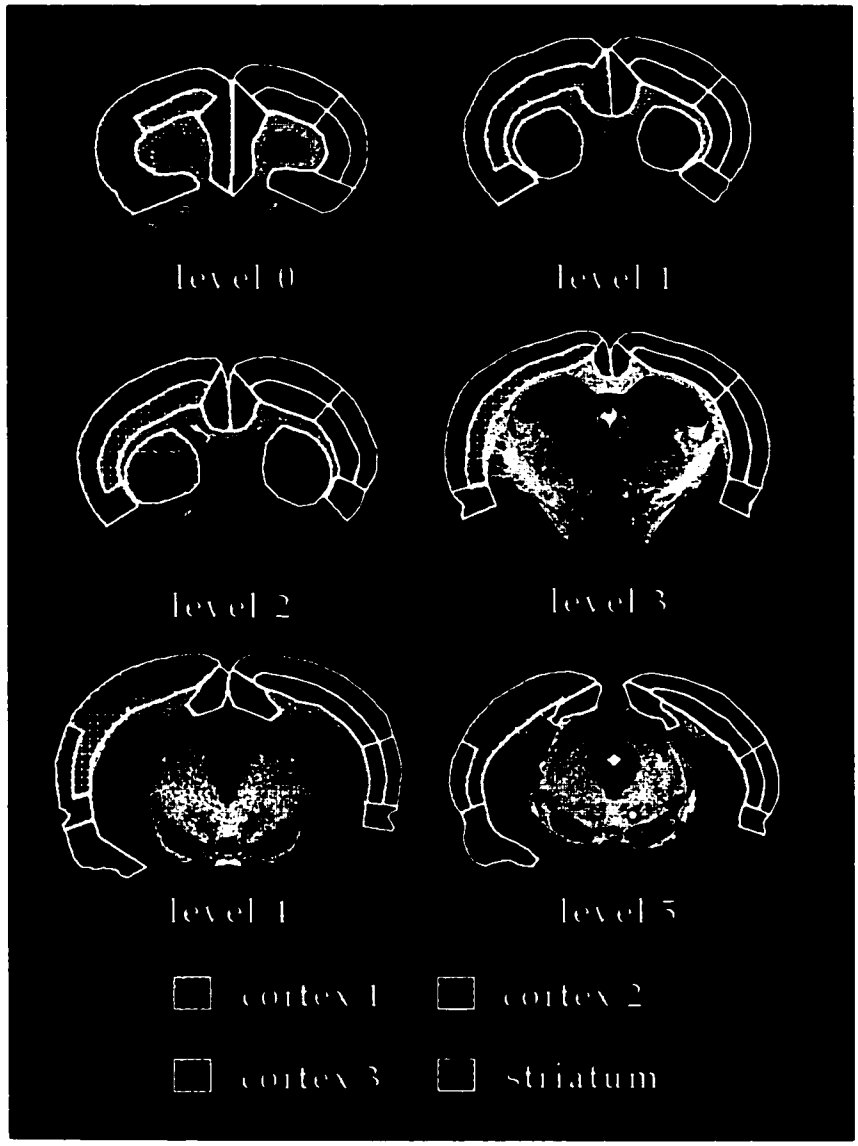

Figure 4-1. The region of interest (ROI) and volume of interest (VOI) template used to sample in vivo [^{3}H]dizocilpine distribution images during recurrent CSD. Six coronal levels in the rat brain are shown. These levels correspond to coronal sections from Bregma in mm at 2.20 (level 0), 1.20 (level 1), 0.20 (level 2), -3.30 (level 3), -5.60 (level 4), -6.30 (level 5). The ROI template is on the right side of the sections with lines to define ROI. The ROI groupings used to define the 4 VOI are on the left side of the sections and are labeled at the bottom of the figure.

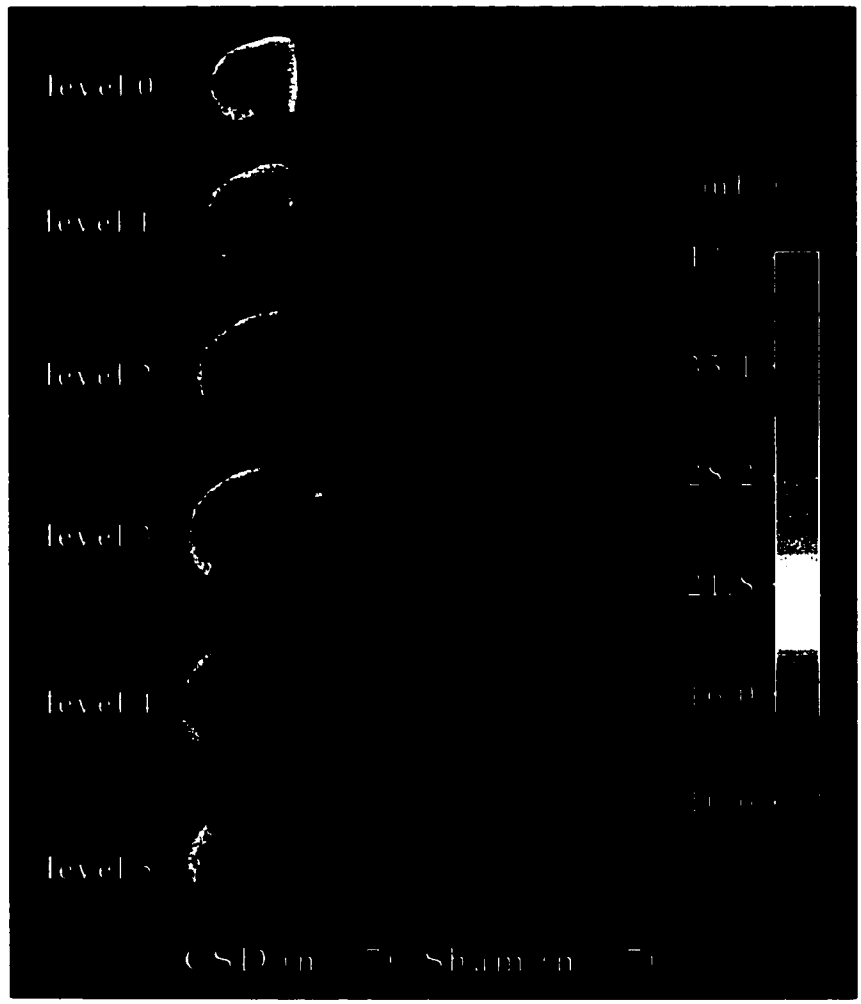

Figure 4-2. Autoradiographs of average [^{3}H]dizocilpine V_d images for CSD (n = 7) or sham (n = 7) treated groups. Autoradiographs from individual studies are spatially registered and averaged. The levels correspond to coronal sections from Bregma in mm at 2.20 (level 0), 1.20 (level 1), 0.20 (level 2), -3.30 (level 3), -5.60 (level 4), -6.30 (level 5). The treatment is on the left (ipsilateral) side of the sections. Calibrated colour scale is shown, as are the number of rats used to obtain each image. CSD, cortical spreading depression; V_d, volume of distribution.

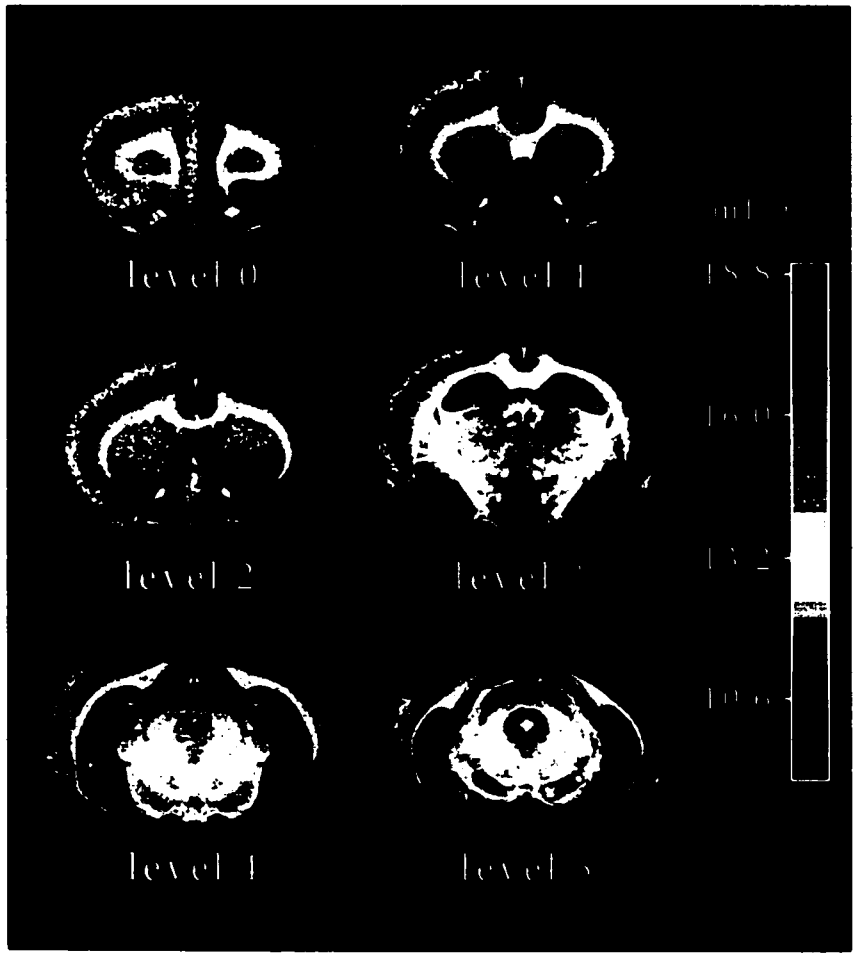

Figure 4-3. Histological correlation of increased [^{3}H]dizocilpine V_d. The averaged difference image between CSD (n = 7) and sham (n = 7) treated studies were coded with colour and overlaid on spatially registered gray levels histological images. The levels correspond to coronal sections from Bregma in mm at 2.20 (level 0), 1.20 (level 1), 0.20 (level 2), -3.30 (level 3), -5.60 (level 4), -6.30 (level 5). Calibrated colour scale indicates the intensity of [^{3}H]dizocilpine V_d. The treatment is on the left (ipsilateral) side of the sections. CSD, cortical spreading depression; V_d, volume of distribution.

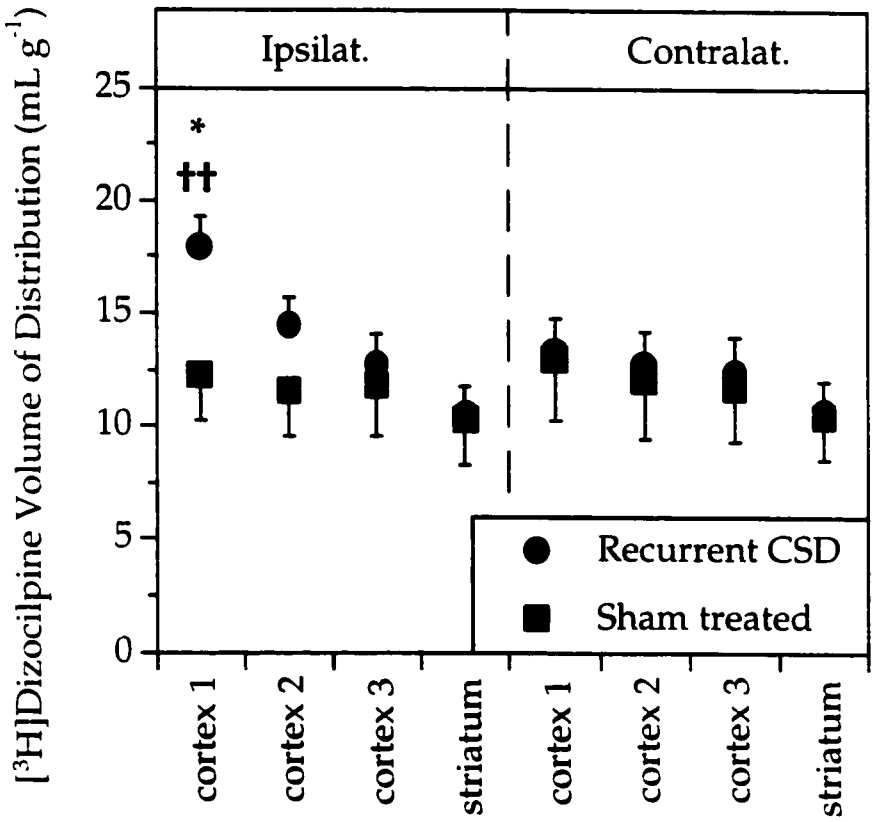

Figure 4-4. [^{3}H]Dizocilpine V_d data within VOI in the ipsilateral and contralateral hemispheres in CSD (n = 7) or sham (n = 7) treated groups. The VOI groupings are the same as the template in Figure 4-1. All values are mean ± SD. Different from the corresponding VOI in the contralateral hemisphere: †† $p < 0.01$. Different between the CSD and sham treated groups: *$p < 0.02$. CSD, cortical spreading depression; SD, standard deviation; VOI, volume of interest; V_d, volume of distribution.

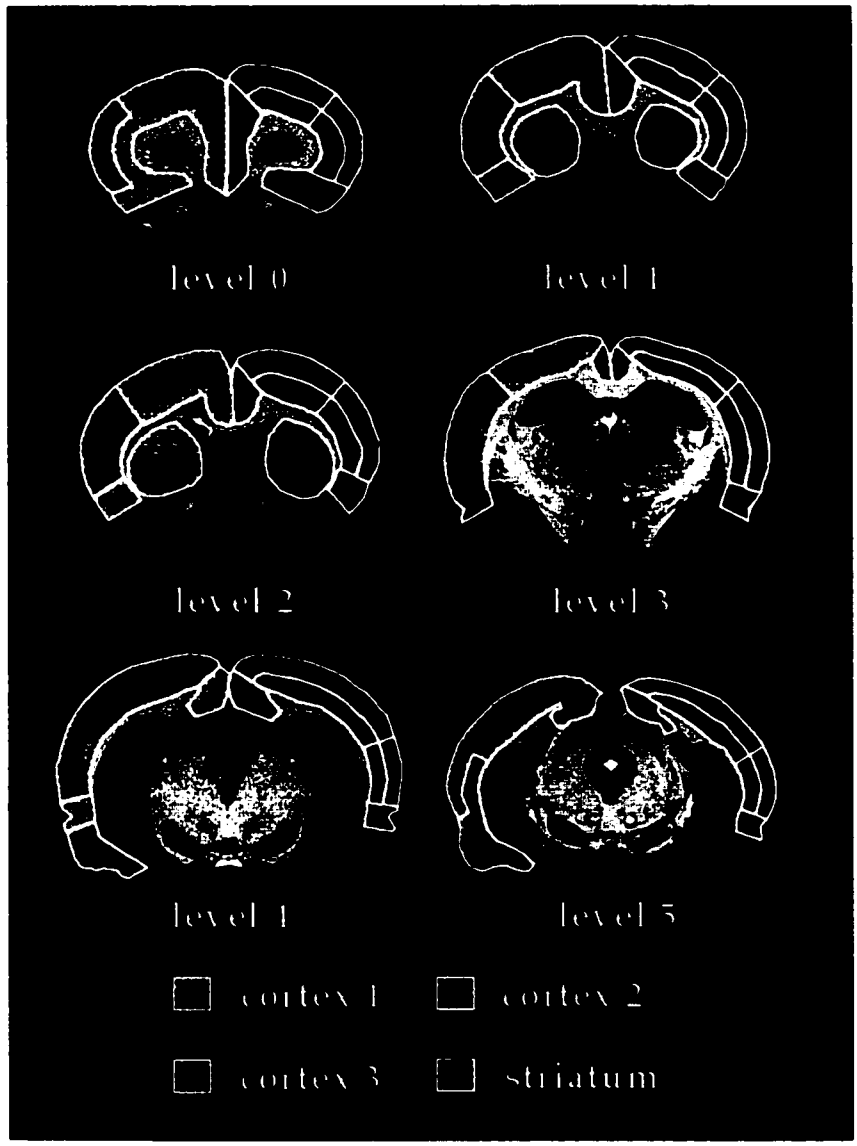

Figure 4-5. The region of interest (ROI) and volume of interest (VOI) template used to sample in vivo [^{3}H]dizocilpine distribution images in single CSD studies. Six coronal levels in the rat brain are shown. The levels correspond to coronal sections from Bregma in mm at 2.20 (level 0), 1.20 (level 1), 0.20 (level 2), -3.30 (level 3), -5.60 (level 4), -6.30 (level 5). The ROI template is on the right side of the sections with lines to define ROI. The ROI groupings used to define the 4 VOI are on the left side of the sections and are labeled at the bottom of the figure.

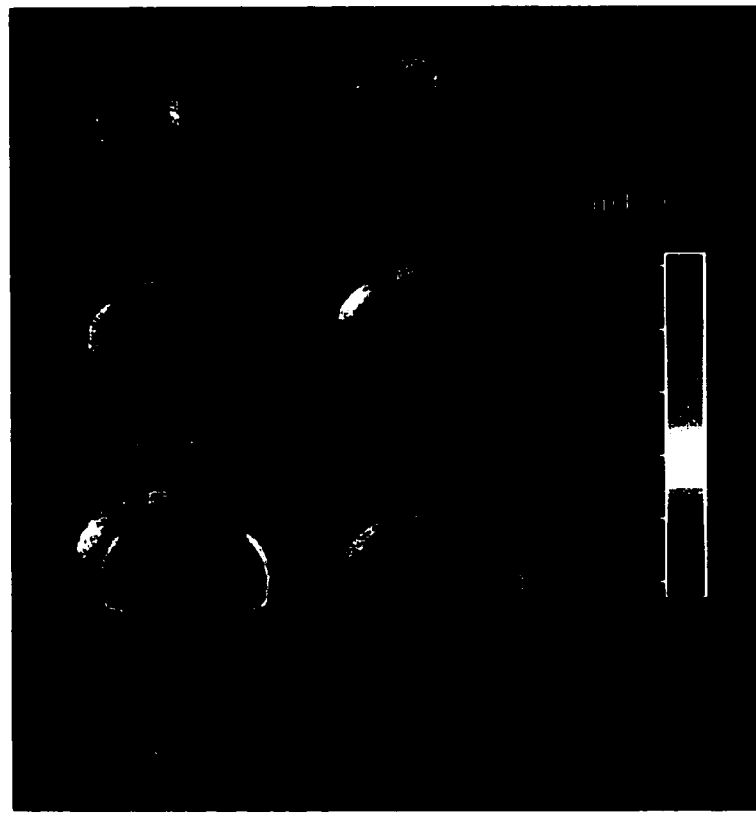

Figure 4-6. Autoradiographs of average [^{3}H]dizocilpine V_d images for single CSD (n = 6) studies. Autoradiographs from individual studies are spatially registered and averaged. The levels correspond to coronal sections from Bregma in mm at 2.20 (level 0), 1.20 (level 1), 0.20 (level 2), -3.30 (level 3), -5.60 (level 4), -6.30 (level 5). The treatment is on the left (ipsilateral) side of the sections. Calibrated colour scale is shown, as are the number of rats used to obtain each image. The coronal levels are the same as the template levels in Figure 4-1. CSD, cortical spreading depression; V_d, volume of distribution.

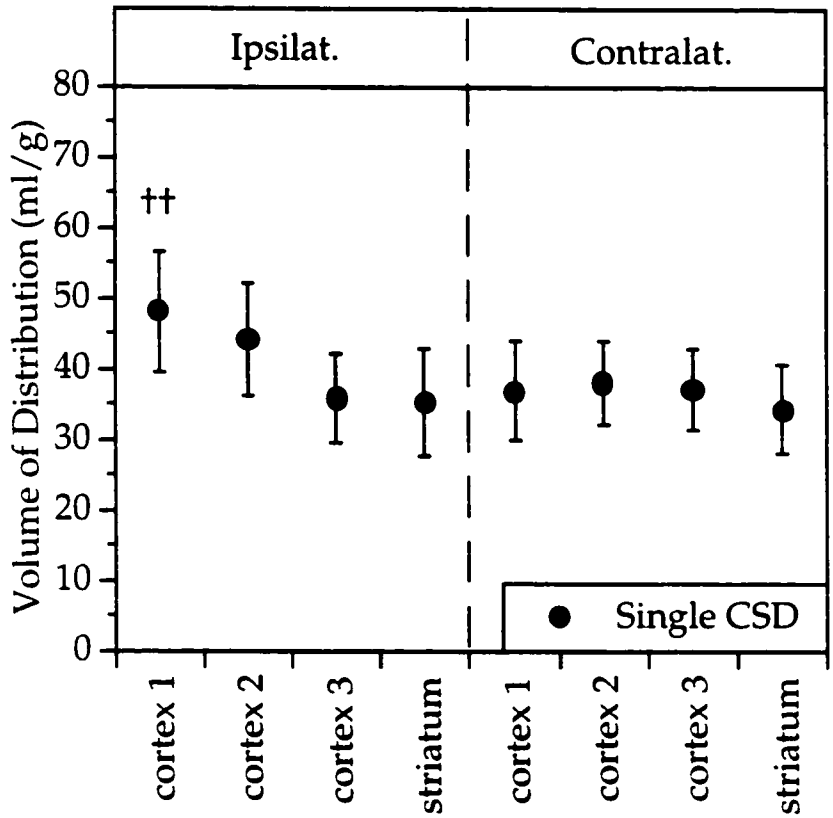

Figure 4-7. [^{3}H]Dizocilpine V_d data within VOI in the ipsilateral and contralateral hemispheres in single CSD (n = 6) studies. The VOI groupings are the same as the template in Figure 4-6. All values are mean ± SD. Different from the corresponding VOI in the contralateral hemisphere: †† $p < 0.05$. CSD, cortical spreading depression; SD, standard deviation; VOI, volume of interest; V_d, volume of distribution.

Discussion

[^{3}H]Dizocilpine in vivo distribution in the rat brain was mapped during 1 hour of recurrent CSD and sham treatment. Its distribution after a single CSD was also studied within a 16 minute period. It was observed that recurrent CSD treatment increased [^{3}H]dizocilpine distribution in the neocortex. A large cortical region, including the frontal cortex and outer cortical layers, showed pronounced increases in [^{3}H]dizocilpine distribution. The increased distribution was abruptly interrupted between the neocortex and paleocortex and absent at the site of CSD induction. No change was identified in the striatum. These findings are consistent with the current understanding that there is large increase in extracellular glutamate during CSD and activation of glutamate receptors. The layered appearance of [^{3}H]dizocilpine distribution reflects the observation that the tissue depolarization is more pronounced in the outer cortex, as indicated by the larger increase in extracellular K^+ in the outer cortex during CSD (Gardner-Medwin and Nicholson, 1983; Munoz-Martinez, 1970). In our hands, CSD induced with 0.5 M KCl at the occipital cortex does not seem to propagate beyond the ipsilateral neocortex, contrary to some previously published data (Vinogradova et al., 1991). [^{3}H]Dizocilpine distribution was increased in the cortex treated with a single CSD during a 16 minute period. The pattern of increase was different from that in the recurrent CSD studies, suggesting that [^{3}H]Dizocilpine distribution may not reach equilibrium at 16 minutes or

single CSD may have unique activation characteristics (Lehmenkuhler et al., 1976).

Although increased extracellular K^+ and astrocytic membrane depolarization are the main mechanisms of CSD initiation, both non-functional synaptic release and reduced astrocytic uptake result in extracellular glutamate increases (Kimelberg et al., 1995; Rutledge and Kimelberg, 1996). Due to the presence of increased extracellular glutamate and membrane depolarization during CSD, the increased [^{3}H]dizocilpine distribution in the cortex is best interpreted to represent the activation of NMDA receptors. It is well recognized that dizocilpine is a potent non-competitive NMDA antagonist (Watkins and Evans, 1981; Wong et al., 1986) that binds to the activated NMDA receptor (Bonhaus and McNamara, 1988; Foster and Wong, 1987; McBain and Mayer, 1994).

The pattern of increased [^{3}H]dizocilpine in vivo distribution provides further information about spatial distribution of increased glutamate during 1 hour of recurrent CSD. The increased [^{3}H]dizocilpine in vivo distribution in the outer cortex is consistent with the electrophysiological characteristics and the pattern of the [^{3}H]dizocilpine binding sites of CSD. Greater impedance (Hoffman et al., 1973) and longer and larger depolarizing currents in the outer cortical layer (Munoz-Martinez, 1970) substantiate the report that CSD propagates preferentially in the outer layers of the neocortex (Gardner-Medwin and Nicholson, 1983; Ochs and Hunt, 1960). Although immunocytochemistry studies indicate that the distribution of NMDA

receptor subunits is even in the neocortex (Petralia et al., 1994b), in vitro binding studies shows the outer cortex contains more [^{3}H]dizocilpine binding sites (Bowery et al., 1988; Wallace et al., 1992).

There are large fluctuations in both energy metabolism (Shinohara et al., 1979) and regional CBF (Fabricius et al., 1995) during CSD. During CSD regional CBF is largely coupled with energy metabolism so the pattern is similar between regional CGU and CBF changes (Fabricius et al., 1995; Shinohara et al., 1979). Regional CBF increases as visualized with [^{14}C]IAP distribution revealed a relatively homogenous band (Hansen and Olsen, 1980; Mies and Paschen, 1984), and the initial rise in regional CBF occurs at the decline phase of extracellular K^+ (Mies and Paschen, 1984). The regional CBF increase is brief and the following CBF depression is persistent even after a single CSD (Piper et al., 1991). The regional CBF fluctuation during CSD is a complicating factor in interpreting the in vivo [^{3}H]dizocilpine distribution data. The increase of regional CBF and subsequent prolonged hypoperfusion may lead to trapping of the radiolabled ligand. If this suspicion is correct the pattern of [^{3}H]dizocilpine distribution should correlate with the regional CBF mapping. Regional CBF measured with laser-Doppler flowometry demonstrated that CBF in the outer cortical layer is even lower than the inner layer up to 500 μm (Fabricius et al., 1997). This indicates that the regional CBF might be actually lower in the outer layers of the cortex, making the trapping of the radiolabeled ligand unlikely. Numerous reports have indicated that NO release is likely involved in the mediation of regional CBF response

during CSD (Fabricius et al., 1995; Gault et al., 1994). It is consistent with the observation that the CBF increase somewhat lags behind the tissue depolarization since increased NO release results from glutamate receptor activation (Colonna et al., 1997; Fabricius et al., 1995).

At 1 hour at least 90% of dizocilpine is unmetabolized (Schwartz and Wasterlain, 1991; Vezzani et al., 1989). The major derivatives of dizocilpine are in its hydroxylized forms, which become hydrophilic, so that they are no longer permeable through the blood brain barrier (Hucker et al., 1983). Thus, the increased [^{3}H]dizocilpine uptake into the brain tissue likely represents the accumulation of [^{3}H]dizocilpine which contains little of its metabolized derivatives (Hucker et al., 1983; Wallace et al., 1992).

Images obtained in this series clearly demarcate the border between the neocortex (6 cell layer) and paleocortex (3 cell layer) (Swanson and Petrovich, 1998) and the striatum and hippocampus are spared from the increases in [^{3}H]dizocilpine distribution. These observations are consistent with in vivo [^{3}H]nimodipine distribution during CSD (Osuga et al., 1997). There are significant increases in [^{3}H]nimodipine distribution in the neocortex but not in the striatum. Increased [^{3}H]nimodipine distribution in the hippocampus was thought to be a consequence of the direct stimulation of the microdialysis probe (Osuga et al., 1997). However, these observations are inconsistent with the claim that CSD induced with 0.5M KCl on the occipital cortex can establish ischemic tolerance in the hippocampus as effectively as CSD induced directly in the hippocampus (Kawahara et al., 1995). CSD induced directly in the

hippocampus has been reported equally protective (Kawahara et al., 1995). This observation is also contradictory to the report that CSD induced on the neocortex can propagate to the hippocampus and striatum via the entorhinal cortex (Vinogradova et al., 1991). [^{3}H]Dizocilpine distribution in single CSD during a 16 minutes period is increased in the CSD treated cortex. However, the pattern of increased [^{3}H]dizocilpine distribution bears no similarities with the observed increases in [^{3}H]dizocilpine distribution in the cortex in the recurrent CSD studies, suggesting that [^{3}H]dizocilpine distribution in the cortex may not be at equilibrium shortly after a single CSD. Alternatively, single CSD may have a different activation pattern compared to recurrent CSD.

The spreading extracellular K^+ waves and increases in extracellular glutamate have significant physiological consequences (Mayevsky and Weiss, 1991). Sokoloff and associates (Shinohara et al., 1979) reported a marked increase of local cerebral glucose phosphorylation in the neocortex without obvious differences among the cortical layers during CSD. A large portion of this increase in glucose uptake may be attributed to the increased EAAT activity resulting from the increased extracellular glutamate (Magistretti et al., 1999). The increase in the extracellular glutamate is a result of both release from synaptic terminals (Munoz-Martinez, 1970) and leakage from astrocytes (Billups and Attwell, 1996; Kimelberg et al., 1995; Seki et al., 1999). The spatial discrepancy in [^{3}H]dizocilpine distribution in this work and the reported increases in regional CGU is unclear. Perhaps increased glutamate release is

predominantly located in the dendritic layers (the outer cortex) but the effects are distributed through the whole glial syncytium and the neuronal cell body.

CSD not only causes metabolic disturbances but also initiates signaling events resulting from widespread membrane depolarization and increased glutamate receptor activation. During CSD there is a marked increase in cytoplasmic calcium that may originate from several sources. [^{3}H]Nimodipine in vivo uptake was increased during CSD indicating the activation of L-type VSCC, since the specific [^{3}H]nimodipine binding depends on the presence of the open and inactivated VSCC (Osuga et al., 1997). The finding of increased [^{3}H]dizocilpine distribution is consistent with the suggestion that the opening of NMDA receptor channel is also responsible for increases in intracellular calcium. It is therefore quite possible that the increased [^{3}H]dizocilpine uptake traces the waves of increased glutamate caused by recurrent CSD. These signaling events, including the activation of glutamate receptors and increases in intracellular Ca^{2+}, have lasting effects that change the cortical response to a subsequent ischemic insult.

The increased glutamate release during CSD may be responsible for a series of molecular changes identified so far. These changes include increases in neurotrophin transcription and translation (Levine and Black, 1997; Matsushima et al., 1998) in both neurons and astrocytes following CSD (Kariko et al., 1998; Kawahara et al., 1997; Kokaia et al., 1993). CSD also upregulates the transcription and translation of immediate early genes (Herdegen et al., 1993; Herrera et al., 1993). Moreover, CSD elicits functional

transformation of the astrocytes, indicated by the upregulation of glial fibrillary acidic protein throughout the treated cerebral cortex (Bonthius and Steward, 1993; Herrera and Cuello, 1992; Herrera et al., 1998; Herrera and Robertson, 1990). The functional transformation of astrocytes coincides with increases in BDNF mRNA transcription (Matsushima et al., 1998), neuronal NOS (Caggiano and Kraig, 1998) and immediate early genes (Herrera et al., 1998). Increased activation of phospholipase A_2 through NMDA receptor results in increased cyclooxygenase-2 in the neocortex (Caggiano et al, 1996; Miettinen et al., 1997).

In summary, there was a significant increase in [^{3}H]dizocilpine distribution in the outer cortical layer during recurrent CSD. The increased [^{3}H]dizocilpine in vivo distribution may represent the activation of NMDA receptors in the neocortex. These findings are consistent with the understanding that the CSD wave is essentially a wave of increased extracellular potassium which travels preferentially in the outer layers of the neocortex and that extracellular glutamate is considerably increased during CSD.

CHAPTER 5. REGIONAL BLOOD FLOW MEASUREMENT AND [^{3}H]NIMODIPINE DISTRIBUTION IN RATS PRECONDITIONED WITH CORTICAL SPREADING DEPRESSION

Cortical spreading depression (CSD) imparts protection against both global (Kawahara et al., 1995; Kobayashi et al., 1995) and focal ischemia (Matsushima et al., 1996; Yanamoto et al., 1998) (CSD preconditioning). However, the mechanisms leading to the ischemic tolerant state remain unclear. A critical issue is the role of CBF response in the ischemic tissue after preconditioning. Though earlier reports have indicated that changes in CBF during ischemic insult are unlikely to be a predominant mechanism (Matsushima and Hakim, 1995; Matsushima et al., 1996), immunochemistry studies (Caggiano and Kraig, 1998) have identified an upregulation of neuronal nitric oxide synthase in the astrocytes.

Mounting evidence has shown that CSD serves as a signaling event. CSD causes transient tissue depolarization (Osuga et al., 1997) with increased extracellular glutamate (Marrannes et al., 1988; Nedergaard et al., 1995). Administration of ketamine, an NMDA antagonist, during CSD was shown to abolish CSD-induced ischemic tolerance (Taga et al., 1997). It has been demonstrated that ischemic preconditioning includes release of adenosine and activation of adenosine A1 receptor mediated G-protein cascades, leading to the opening of sulfonylurea-sensitive ATP-sensitive K^+ channels (Heurteaux et al., 1995). CSD preconditioning increased activation of phospholipase A_2 through NMDA receptor activation, resulting in increased

cyclooxygenase-2 in the neocortex (Caggiano et al, 1996; Miettinen et al., 1997). Microdialysis studies in focal ischemic cortex demonstrated that tissue exposure to glutamate was attenuated in the CSD preconditioned cortex (Douen et al., 2000).

Astrocytic functional transformation occurs after CSD preconditioning (Belayev et al., 1996; Bonthius and Steward, 1993), accompanied by upregulation of glial fibrillary acidic protein (GFAP) message and protein throughout the treated neocortex. These events are likely mediated by an increase in extracellular glutamate (Levine and Black, 1997). CSD-induced astrocytic activation can be blocked by dizocilpine (Bonthius and Steward, 1993; Herrera and Cuello, 1992; Herrera and Robertson, 1990). Levels of message and protein of growth factors are upregulated in both neurons and astrocytes following CSD (Kariko et al., 1998; Kawahara et al., 1997; Kokaia et al., 1993; Matsushima et al., 1998). Both ischemic (Belayev et al., 1996) and CSD (Herdegen et al., 1993; Herrera et al., 1993) preconditioning upregulate the transcription and translation of immediate early genes.

To better understand the effects of CSD preconditioning on the tissue perfusion and the tissue depolarization during subsequent focal ischemia we measured CBF and tissue depolarization during focal cerebral ischemia on day 3 after preconditioning with 2 hours of recurrent CSD. The [^{14}C]Iodoantipyrine method was used to measure CBF (Sakurada et al., 1978). In parallel sets of studies, [^{3}H]nimodipine in vivo distribution was used to map cerebral depolarization during focal ischemia (Hakim and Hogan, 1991;

Hogan et al., 1991; Hogan and Hakim, 1992) whereas [^{3}H]dizocilpine in vivo distribution was used to estimate NMDA receptor activation (Bowery et al., 1988; Schwartz and Wasterlain, 1993; Wallace et al., 1992). Compared with sham treated controls, it was observed that prior treatment with CSD, under conditions confirmed to induce neuroprotection, improved regional CBF in the surrounding cortex outside the ischemic core; whereas it reduced in vivo [^{3}H]nimodipine distribution in ischemic core region, thus indicating decreased tissue depolarization. [^{3}H]Dizocilpine in vivo distribution data showed biphasic, but not significant, changes that may suggest increased tissue injury in the ischemic core and reduced tissue injury outside the ischemic core. Our data suggested that the improved tissue perfusion and reduced [^{3}H]nimodipine distribution are associated with an attenuated ischemic injury.

Methods

Experimental animals and surgical anesthesia were identical to those employed in Chapter 3. Rats were allowed to breathe spontaneously during CSD preconditioning and were mechanically ventilated during focal ischemia. Body temperature (rectal) was maintained at 36.5 - 37.5°C in all in vivo studies. In focal ischemic studies, brain temperature was monitored indirectly via a thermocouple probe placed in the ear canal (Tympanic).

Procedures of CSD or sham treatment were identical to those described in the infarct volume studies in Chapter 3. Regional CBF, [^{3}H]nimodipine

and [^{3}H]dizocilpine cerebral distribution were measured at 3 hours of focal ischemia introduced on day 3 after CSD or sham preconditioning.

Cerebral blood flow measurements

Regional CBF was measured using [^{14}C]IAP as described (Sakurada et al., 1978) (Appendix 1). One minute prior to the end of the 3 hours MCA occlusion, an intravenous ramp infusion of 32 μCi of [^{14}C]IAP (specific activity 57 mCi/mmol, Amersham International Plc, Little Chalfont, England, UK) in 2.0 mL normal saline was started. Arterial blood samples were collected at 5 second intervals and [^{14}C]IAP concentration measured using liquid scintillation counting with appropriate quench correction. The rats were decapitated after 1 minute of [^{14}C]IAP infusion and the brains were rapidly removed and frozen. A total of 6 CSD and 6 sham treated rats were studied.

Cerebral [^{3}H]nimodipine distribution

In vivo [^{3}H]nimodipine distribution within the brain was measured as previously described (Hakim and Hogan, 1991). Briefly, 200 μCi of [^{3}H]nimodipine (specific activity 127.7 Ci mmol^{-1}, NEN-Dupont, Boston, Massachusetts, USA) in 600 μl of carrier (96% ethanol - 200 g, polyethylene glycol 400 - 170 g, sodium citrate - 2 g and citric acid - 0.5 g) were infused intravenously 30 minutes before the end of the 3 hours MCA occlusion so that an equilibrium of distribution between plasma and brain was approached (Hogan et al., 1991). Plasma [^{3}H]nimodipine concentration was measured just prior to decapitation using liquid scintillation counting with appropriate

quench correction. Following decapitation the brains were rapidly removed and frozen. Previously determined metabolite correction factors in plasma and brain following intravenous administration were applied for [^{3}H]nimodipine studies (Hogan et al., 1991). A total of 9 CSD and 7 sham treated rats were studied. Five additional rats were studied on day 3 after CSD treatment without undergoing MCA occlusion.

Cerebral [^{3}H]dizocilpine distribution

In vivo [^{3}H]dizocilpine distribution within the brain was measured as previously described (Wallace et al., 1992). Briefly, 50 µCi [^{3}H]dizocilpine (specific activity 23.9 Ci/mmol, Amersham International Plc, England, UK) in 500 µl saline was injected intravenously 60 minutes before the end of the 3 hour MCA occlusion so that an equilibrium of distribution between plasma and brain was established (Schwartz and Wasterlain, 1991; Schwartz and Wasterlain, 1993). Plasma [^{3}H]dizocilpine concentration was measured just prior to decapitation using liquid scintillation counting with appropriate quench correction. Following decapitation the brains were rapidly removed and frozen. Previously published metabolite correction factors in plasma and brain following intravenous administration were applied for [^{3}H]dizocilpine studies (Schwartz and Wasterlain, 1991; Schwartz and Wasterlain, 1993). A total of 6 CSD and 6 sham treated rats were studied. Five additional rats were studied on day 3 after CSD treatment without undergoing MCA occlusion.

Autoradiography

The stored brains were warmed to -20°C and 20 µm cryostat sections were obtained every 140 µm. Sections from the [^{14}C]IAP studies were apposed to either Kodak SB-5 or BioMax Mr film (Picker International, Brampton, Ontario, Canada) for 7 to 10 days. Commercial ^{14}C microstandards (Amersham, Oakville, Ontario, Canada) were used to calibrate the autoradiographs of ^{14}C distribution. Sections from the [^{3}H]nimodipine and [^{3}H]dizocilpine studies were apposed to Hyperfilm (Kodak, Etobicoke, Ontario, Canada) for 60 - 120 days to obtain autoradiographs of ^{3}H distribution. These images were calibrated using 20 µm thick sections of brain paste standards containing known amounts of ^{3}H prepared from rat forebrain.

Image analysis

Autoradiographic images at five coronal levels in the brain were digitized using the MCID system. The levels corresponded to coronal sections from Bregma in mm at 1.20 (level 1), 0.20 (level 2), -3.30 (level 3), -5.60 (level 4), -6.30 (level 5) (Paxinos and Watson, 1986). Since ß-particles emitted from ^{14}C have sufficient energy to travel the full thickness of 20 µm brain sections, variation in section thickness may induce error in tissue ^{14}C measurement. However, ß-particles emitted from tritium decay have a maximum range of ~6 µm in brain sections and measurements of ^{3}H activity from 20 µm sections is insensitive to variation in section thickness. Therefore, at each coronal level ^{14}C activity was averaged over 3 aligned images while a single image

was used to measure ^{3}H activity. The resulting set of images at five coronal levels from each study were then spatially registered to a set of images from a selected [^{3}H]nimodipine study, using multiple anatomically defined fiducial markers (35 - 45) as implemented within MCID (Bookstein, 1990). All further calculations were carried out using these spatially registered images. In each [^{14}C]IAP study, CBF was calculated within each ROI using the measured tissue [^{14}C]IAP content and blood [^{14}C]IAP concentration profile as described (Sakurada et al., 1978). To normalize the measurements of brain tissue [^{3}H]nimodipine or [^{3}H]dizocilpine between studies, [^{3}H]nimodipine or [^{3}H]dizocilpine V_d was calculated as the ratio of the ^{3}H isotope tissue content over the plasma concentration at study termination (Gjedde et al., 1981; Patlak et al., 1983).

To identify regional effects resulting from CSD or sham treatment prior to focal ischemia, an approach using threshold templates was adopted (Hogan and Hakim, 1992). The threshold templates were derived from mean difference images between treatment conditions (CSD or sham); both density criteria (i.e. CBF or V_d) and a morphology criterion (size of the area identified) were used. For CBF studies, regional [^{14}C]IAP CBF images from the CSD treated (n = 6) or sham treated (n = 6) groups were averaged. A difference image (CBF_{CSD} - CBF_{sham}) was calculated. To reduce the heterogeneity of variance within the CBF images, the squareroot transformation was performed on the CBF images and a set of difference average images (Sqrt CBF_{CSD} - Sqrt CBF_{sham}) were calculated (Pulsinelli et al., 1982). The mean Sqrt

CBF value of all pixels and its SD were calculated in the contralateral forebrain gray matter of the transformed difference images. A threshold of 1 SD above the mean [(Sqrt CBF_{CSD} - Sqrt CBF_{sham}) + SD] and 1 SD below the mean [(Sqrt CBF_{CSD} - Sqrt CBF_{sham}) - SD] were used to identify potential regions of CBF changes caused by CSD. To minimize the effect of random fluctuations in the data only regions showing more than 50 contiguous image pixels (0.2 mm^2) with values outside the threshold were used to form the threshold template (Hogan and Hakim, 1992). The resulting templates were used to sample CBF in each [^{14}C]IAP study.

The [^{3}H]nimodipine V_d images were averaged for the CSD treated (n = 9) and sham treated (n = 7) groups and a set of difference images [V_d(sham) - V_d(CSD)] were calculated. A threshold of 1 SD above the mean [V_d(sham) - V_d(CSD)] + SD and 1 SD below the mean [V_d(sham) - V_d(CSD)] - SD volume of distribution values of the image pixels in the contralateral forebrain region of the difference image were used to identify changes in tissue [^{3}H]nimodipine distribution caused by CSD. The same size criterion was imposed. The resulting templates were then used to sample V_d images in each [^{3}H]nimodipine study and CBF images in each [^{14}C]IAP study.

The [^{3}H]dizocilpine V_d images were averaged for the CSD treated (n = 6) and sham treated (n = 6) groups and a set of difference images [V_d(sham) - V_d(CSD)] were calculated. A threshold of 1 SD above the mean [V_d(sham) - V_d(CSD)] + SD and 1 SD below the mean [V_d(sham) - V_d(CSD)] - SD volume of distribution values of the image pixels in the contralateral forebrain region of

the difference image were used to identify changes in tissue [^{3}H]dizocilpine distribution caused by CSD. The same size criterion was imposed. The resulting templates were then used to sample V_d images in each [^{3}H]dizocilpine study and CBF images in each [^{14}C]IAP study.

Statistical analysis

All results are expressed as mean ± SD. The physiological data were analyzed using the two-sample t-test. Data of regional CBF, [^{3}H]nimodipine and [^{3}H]dizocilpine in vivo distribution were analyzed with one-way repeated measures analysis of variance (Systat, SPSS Inc., Chicago, Illinois, USA). Between-group difference was analyzed with adjusted degrees of freedom and mean square error followed by Bonferroni adjustment for multiple comparisons (Howell, 1992).

Results

Physiological variables

Physiological variables did not differ between the CSD and sham treated groups during the 2 hours preconditioning period and the subsequent 3 hours of MCA occlusion in [^{14}C]IAP, [^{3}H]nimodipine and [^{3}H]dizocilpine studies. The physiological data are summarized in Table 5-1 for [^{14}C]IAP studies, Table 5-2 for [^{3}H]nimodipine studies and Table 5-3 for [^{3}H]dizocilpine studies. Rectal temperature was not significantly different between any CSD treated and sham treated groups during preconditioning or during MCA occlusion between CSD and sham treated groups. Rectal temperature was

maintained at 37.0 ± 0.2°C (n = 40) during preconditioning and 36.9 ± 0.2°C (n = 40) during MCA occlusion over all studies. Tympanic membrane temperature was maintained at 36.5 ± 0.2°C (n = 40) during MCA occlusion.

Table 5-1. Physiological variables for [^{14}C]IAP studies at 3 hours of MCA occlusion

Parameters	CSD treated (n = 6)	Sham treated (n = 6)
MABP (mm Hg)	85 ± 2	85 ± 3
pH	7.46 ± 0.06	7.44 ± 0.03
P_aCO_2 (mm Hg)	43 ± 3	42 ± 6
P_aO_2 (mm Hg)	191 ± 46	167 ± 30
Blood glucose (mM)	6.67 ± 1.57	6.89 ± 0.88

Values are means ± SD. MABP, mean arterial blood pressure; MCA, middle cerebral artery; P_aCO_2, arterial partial pressure of carbon dioxide; P_aO_2, arterial partial pressure of oxygen. The animals were mechanically ventilated during focal ischemia.

Table 5-2. Physiological variables for [^{3}H]nimodipine studies at 3 hours of MCA occlusion

Parameters	CSD treated (n = 9)	Sham treated (n = 7)
MABP (mm Hg)	94 ± 9	92 ± 9
pH	7.42 ± 0.02	7.42 ± 0.03
P_aCO_2 (mm Hg)	43 ± 3	40 ± 3
P_aO_2 (mm Hg)	139 ± 18	141 ± 23
Blood glucose (mM)	6.77 ± 0.92	6.03 ± 0.83

Values are means ± SD. MABP, mean arterial blood pressure; MCA, middle cerebral artery; P_aCO_2, arterial partial pressure of carbon dioxide; P_aO_2, arterial partial pressure of oxygen. The animals were mechanically ventilated during focal ischemia.

Table 5-3. Physiological variables for [^{3}H]dizocilpine studies at 3 hours of MCA occlusion

Parameters	CSD treated (n = 6)	Sham treated (n = 6)
MABP (mm Hg)	86 ± 4	85 ± 2
pH	7.43 ± 0.02	7.43 ± 0.04
P_aCO_2 (mm Hg)	45 ± 4	45 ± 3
P_aO_2 (mm Hg)	166 ± 22	164 ± 24
Blood glucose (mM)	6.86 ± 0.84	6.50 ± 1.22

Values are means ± SD. MABP, mean arterial blood pressure; MCA, middle cerebral artery; P_aCO_2, arterial partial pressure of carbon dioxide; P_aO_2, arterial partial pressure of oxygen. The animals were mechanically ventilated during focal ischemia.

Table 5-4. Physiological variables for in vivo [^{3}H]nimodipine and [^{3}H]dizocilpine studies during sham MCA occlusion

Parameters	MCA occlusion [^{3}H]nimodipine (n = 5)	MCA occlusion [^{3}H]dizocilpine (n = 5)
MABP (mm Hg)	88 ± 3	87 ± 3
pH	7.43 ± 0.02	7.44 ± 0.02
P_aCO_2 (mm Hg)	42 ± 1	45 ± 4
P_aO_2 (mm Hg)	187 ± 39	191 ± 41
Blood glucose (mM)	5.78 ± 1.03	5.88 ± 0.55

Values are means ± SD. MABP, mean arterial blood pressure; MCA, middle cerebral artery; P_aCO_2, arterial partial pressure of carbon dioxide; P_aO_2, arterial partial pressure of oxygen. Spontaneous ventilation during preconditioning, mechanical during focal ischemia.

[^{3}H]Nimodipine or [^{3}H]dizocilpine distribution were measured in two groups of rats that received sham MCA occlusion after CSD treatment. Physiological variables during the subsequent 3 hours of sham MCA occlusion were averaged in these two study groups and are summarized in Table 5-4. Rectal temperature was 36.9 ± 0.1°C (n = 10) during preconditioning and 36.7 ± 0.1°C (n = 10) during sham MCA occlusion. Tympanic temperature was 36.6 ± 0.1°C (n = 10) during sham MCA occlusion.

Cortical spreading depression waves and periinfarct depolarization

CSD waves were recorded from the anterior platinum electrode during preconditioning. For the animals that underwent subsequent MCA occlusions, the rate of CSD during 2 hour treatment is summarized in Table 5-5. Averaged over all CSD treated studies, the rate of CSD waves was 6.1 ± 1.6 h^{-1} (n = 21). Recurrent negative or biphasic waves of average amplitude 5.7 ± 2.4 mV (n = 21) and average duration 82.0 ± 10.3 seconds (n = 21) were recorded. No CSD were observed in the sham treatment groups.

For the animals that underwent subsequent sham MCA occlusions, the rate of CSD waves was 8.0 ± 1.2 h^{-1} (n = 5) with the average amplitude of 5.6 ± 2.4 mV (n = 5) and duration 83.8 ± 6.9 seconds (n = 5) in [^{3}H]nimodipine studies. In [^{3}H]dizocilpine studies, the rate of CSD waves was 6.4 ± 1.9 h^{-1} (n = 5) with the average amplitude of 6.6 ± 4.2 mV (n = 5) and duration 98.1 ± 16.3 seconds (n = 5).

Table 5-5. Rate of CSD and periinfarct depolarization waves during preconditioning and subsequent MCA occlusion

Parameters	CSD treated	Sham treated
[^{14}C]IAP studies	(n = 6)	(n = 6)
CSD wave forms (h^{-1})	6.1 ± 2.6	-
Ischemic periinfarct depolarization (h^{-1})	1.3 ± 1.1	1.3 ± 1.1
Ischemic periinfarct integrated negativity (mV min h^{-1})	14.4 ± 12.9	12.5 ± 17.5
[^{3}H]Nimodipine studies	(n = 9)	(n = 7)
CSD wave forms (h^{-1})	4.9 ± 0.9	-
Ischemic periinfarct depolarization (h^{-1})	0.7 ± 0.4	0.9 ± 0.6
Ischemic periinfarct integrated negativity (mV min h^{-1})	12.9 ± 10.9	16.1 ± 19.0
[^{3}H]Dizocilpine studies	(n = 6)	(n = 6)
CSD wave forms (h^{-1})	6.3 ± 1.0	-
Ischemic periinfarct depolarization (h^{-1})	1.3 ± 1.0	0.6 ± 0.4
Ischemic periinfarct integrated negativity (mV min h^{-1})	17.3 ± 21.4	5.9 ± 7.0

Values are mean ± SD. Recurrent CSD, 2 hours; IAP, iodoantipyrine; MCA occlusion, 3 hours. CSD, cortical spreading depression; MCA, middle cerebral artery; SD, standard deviation.

Periinfarct depolarization waves were recorded from the anterior platinum electrode during MCA occlusions. The number of depolarization events and the ischemic periinfarct integrated negativity were summarized in Table 5-5. The rate of periinfarct depolarization events and the periinfarct integrated negativity recorded during MCA occlusion were not significantly

different between any CSD treated and sham treated groups in the [^{14}C]IAP, [^{3}H]nimodipine and [^{3}H]dizocilpine studies. Overall, the periinfarct depolarization was 1.1 ± 0.9 h^{-1} (n = 21) in the CSD treated studies and 0.9 ± 0.8 h^{-1} (n =19) in the sham treated studies. The periinfarct integrated negativity was 14.6 ± 14.4 mV min h^{-1} (n = 21) in the CSD treated studies and 11.8 ± 15.4 mV min h^{-1} (n = 19) in the sham treated studies.

CBF measured with H_2 clearance

At 4 time points (one immediately before MCA occlusion and hourly during MCA occlusion) cortical blood flow was measured using H_2 clearance. No significant difference in flow or percent reduction from pre-ischemic levels was observed between any experimental and sham study groups in the [^{14}C]IAP, [^{3}H]nimodipine and [^{3}H]nimodipine studies. They were then averaged over all CSD treated or sham treated rats undergoing MCA occlusion. During MCA occlusion average cortical blood flow was 21 ± 4 mL $100g^{-1}$ min^{-1} (n = 21) in CSD treated rats and 21 ± 6 mL $100g^{-1}$ min^{-1} (n = 19) in sham treated rats.

CBF at three hours of MCA occlusion

Images of regional CBF calculated from brain [^{14}C]IAP content at the five coronal levels studied were averaged over all rats in each treatment group and are shown in Figure 5-1. The pixel ensemble defined by (Sqrt CBF_{CSD} – Sqrt CBF_{sham}) + SD, and meeting the minimum area criterion of 0.2 mm^2, is shown in blue in Figure 5-2. Within this region CBF was 147 ± 27 mL

$100g^{-1}\ min^{-1}$ in the CSD treated group (n = 6) and 73 ± 41 mL $100g^{-1}\ min^{-1}$ (n = 6) in the sham treated group ($p < 0.005$) (Figure 5-3).

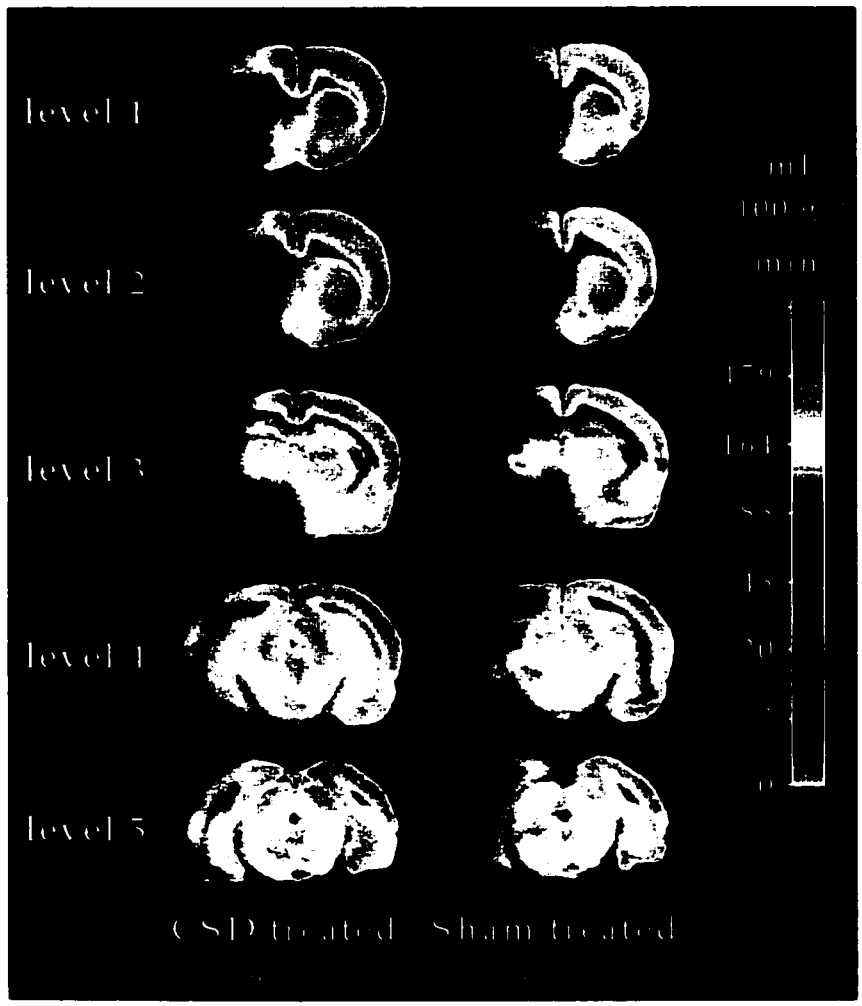

Figure 5-1. Averages of autoradiographic images of [^{14}C]IAP CBF measurements for CSD (n = 6) or sham (n = 6) treated groups. The levels correspond to coronal sections from Bregma in mm at 1.20 (level 1), 0.20 (level 2), -3.30 (level 3), -5.60 (level 4), -6.30 (level 5). The ischemic hemisphere is on the left side of the sections. Calibrated colour scale is shown, as are the number of rats used to obtain each image. CBF, cerebral blood flow; CSD, cortical spreading depression; IAP, iodoantipyrine.

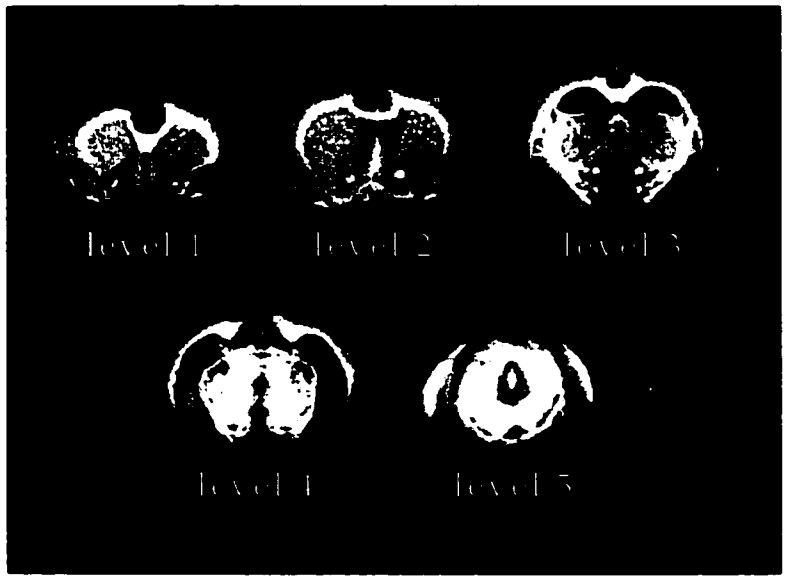

Figure 5-2. CBF threshold templates defined by (Sqrt CBF_{CSD} - Sqrt CBF_{sham}) + SD. The blue patches represent pixel assembles with a value 1 SD higher than the mean sampled from contralateral forebrain gray matter, and with a size larger than 0.2 mm^2 in the same template. The templates were overlaid on histological sections to indicate morphological correlation. The levels correspond to coronal sections from Bregma in mm at 1.20 (level 1), 0.20 (level 2), -3.30 (level 3), -5.60 (level 4), -6.30 (level 5). CBF, cerebral blood flow; CSD, cortical spreading depression; IAP, iodoantipyrine; SD, standard deviation.

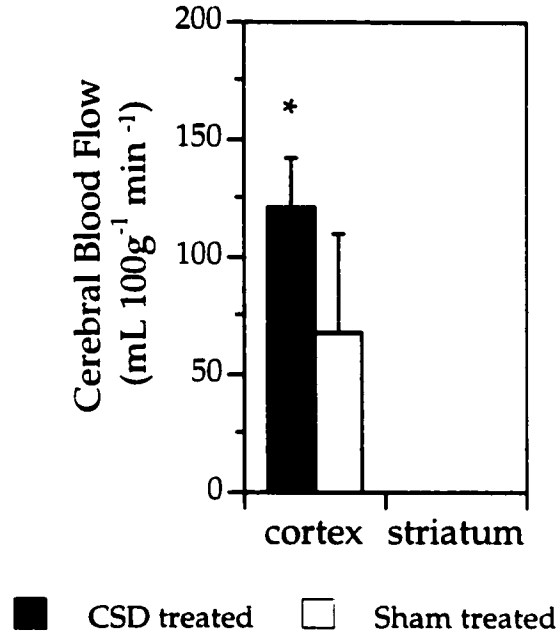

Figure 5-3. CBF data sampled with the (Sqrt CBF_{CSD} – Sqrt CBF_{sham}) + SD threshold templates. The data corresponds to the CSD and sham treated groups in regions identified with the pixel assembles defined by (Sqrt CBF_{CSD} – Sqrt CBF_{sham}) + SD shown in blue in Figure 5-2. All values are mean ± SD. CBF, cerebral blood flow; CSD, cortical spreading depression; Sqrt, squareroot; SD, standard deviation. Different from sham treated group: * $p < 0.05$.

[^{3}H]Nimodipine distribution

To visualize the average in vivo [^{3}H]nimodipine distribution in the CSD and sham treatment groups, [^{3}H]nimodipine V_d images were calculated from the autoradiographs of [^{3}H]nimodipine content. These images were averaged over all rats in the CSD and sham treated groups at the five coronal levels studied and are shown in Figure 5-4. In the contralateral forebrain, there were neither any regional differences nor any differences between the CSD and sham treated groups. Averaged over the cortical and striatal region in all rats [^{3}H]nimodipine V_d in this hemisphere were 1.04 ± 0.24 mL g^{-1} in the cortex, 1.07 ± 0.25 mL g^{-1} in the striatum.

The image pixel ensemble defined by the [^{3}H]nimodipine [V_d(sham) - V_d(CSD)] + SD templates, and meeting the minimum area criterion of 0.2 mm^2, is shown in red in Figure 5-5. The cortical ensemble of this template was 18% of the total cortical area scanned whereas the striatal ensemble was 10% of the total striatal area scanned. The image pixel ensemble defined by the [^{3}H]nimodipine [V_d(sham) - V_d(CSD)] - SD template, and meeting the minimum area criterion of 0.2 mm^2, is shown in blue in Figure 5-5. The cortical ensemble of the template corresponded to the lesion caused by KCl at the site of CSD induction and represented less than 1% of total cortical area scanned. The striatal ensemble was less than 2% total striatal area scanned.

[^{3}H]Nimodipine V_d was measured within the area identified by [^{3}H]nimodipine [V_d(sham) - V_d(CSD)] + SD. The ratio of [^{3}H]nimodipine V_d in

the cortical region, defined as the sampled values from the ipsilateral hemisphere divided by the forebrain average from the contralateral hemisphere, was 1.73 ± 0.49 (n = 7) in the sham treatment group compared with 1.13 ± 0.36 (n = 9) in the CSD treated group ($p < 0.01$) (Figure 5-5, 5-6A). Similarly, the ratio of [^{3}H]nimodipine V_d in the striatal region was 1.91 ± 0.26 (n = 7) in the sham treated group compared with 1.30 ± 0.27 (n = 9) in the CSD treated group (Figure 5-5, 5-6A). Within the cortical extent of the templates defined by [V_d(sham) - V_d(CSD)] + SD, [^{3}H]nimodipine V_d was 1.16 ± 0.43 mL g^{-1} (n = 9) in the CSD treated group and 1.89 ± 0.94 mL g^{-1} (n = 7) in the sham treated group. Within the striatal extent [^{3}H]nimodipine V_d was 2.10 ± 0.63 mL g^{-1} (n = 7) in the sham treated group and 1.39 ± 0.38 mL g^{-1} (n = 9) in the CSD treated group. Sampled with the identical templates, CBF was 23 ± 25 mL $100g^{-1}$ min^{-1} in the sham treated group compared with 56 ± 23 mL $100g^{-1}$ min^{-1} in the CSD treated group ($p < 0.05$) (Figure 5-6B). The difference in CBF within the striatal region was not significant.

In the CSD treated rats that did not undergo MCA occlusion (n = 5) on day 3 after CSD, [^{3}H]nimodipine V_d in the contralateral brain (no treatment) was 0.89 ± 0.19 mL g^{-1} in cortex and 0.95 ± 0.19 mL g^{-1} in striatum. [^{3}H]Nimodipine V_d in the area identified with both sets of the template was not different between the ipsilateral (CSD treated) and contralateral forebrain average (no treatment), indicating CSD preconditioning alone did not have any effect on [^{3}H]nimodipine regional distribution on day 3 after CSD.

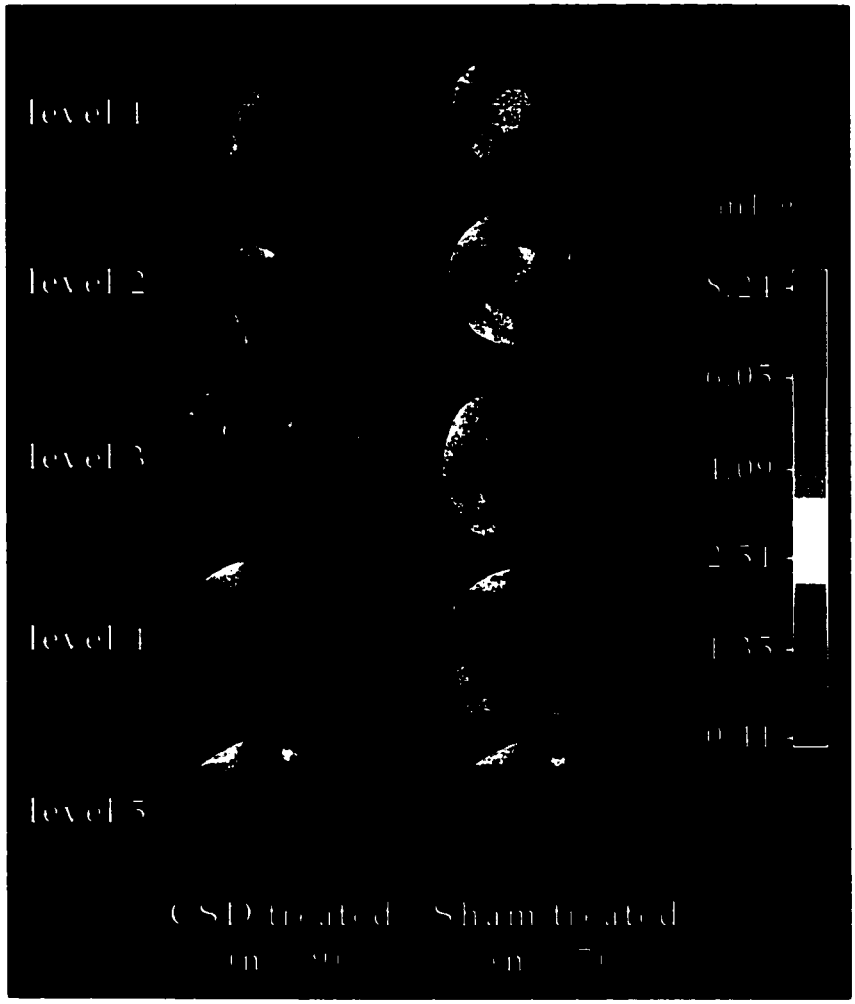

Figure 5-4. Averages of [^{3}H]nimodipine V_d images for CSD (n = 7) or sham (n = 9) treated groups. The levels correspond to coronal sections from Bregma in mm at 1.20 (level 1), 0.20 (level 2), -3.30 (level 3), -5.60 (level 4), -6.30 (level 5). The ischemic hemisphere is on the left side of the sections. Calibrated colour scale is shown, as are the number of rats used to obtain each image. CSD, cortical spreading depression; V_d, volume of distribution.

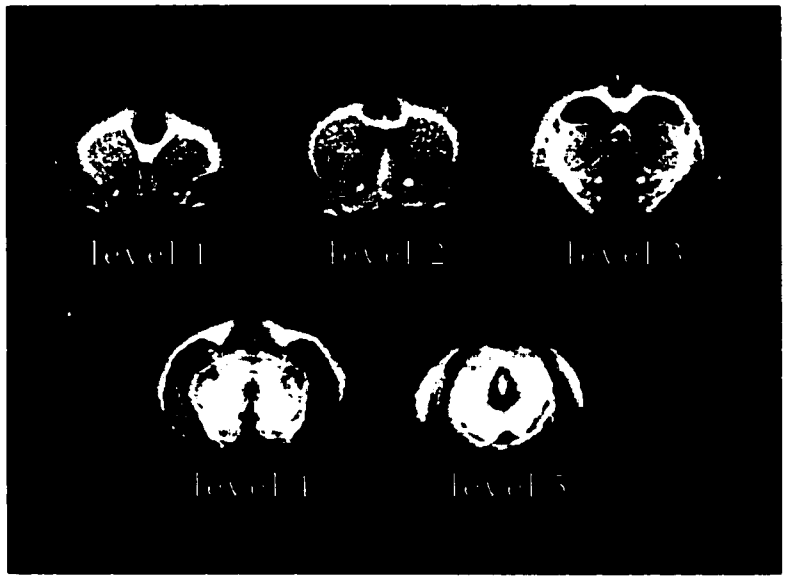

Figure 5-5. [^{3}H]Nimodipine V_d threshold templates used to sample [^{3}H]nimodipine and [^{14}C]IAP CBF images. The template are overlaid on registered histological sections. The levels correspond to coronal sections from Bregma in mm at 1.20 (level 1), 0.20 (level 2), -3.30 (level 3), -5.60 (level 4), -6.30 (level 5). The red patches represent the pixel assemble defined by [V_d(sham) - V_d(CSD)] + SD, with a size larger than 0.2 mm^2. The blue patches represent the pixel ensemble defined by [V_d(sham) - V_d(CSD)] - SD, with a size larger than 0.2 mm^2. IAP, iodoantipyrine; SD, standard deviation; V_d, volume of distribution.

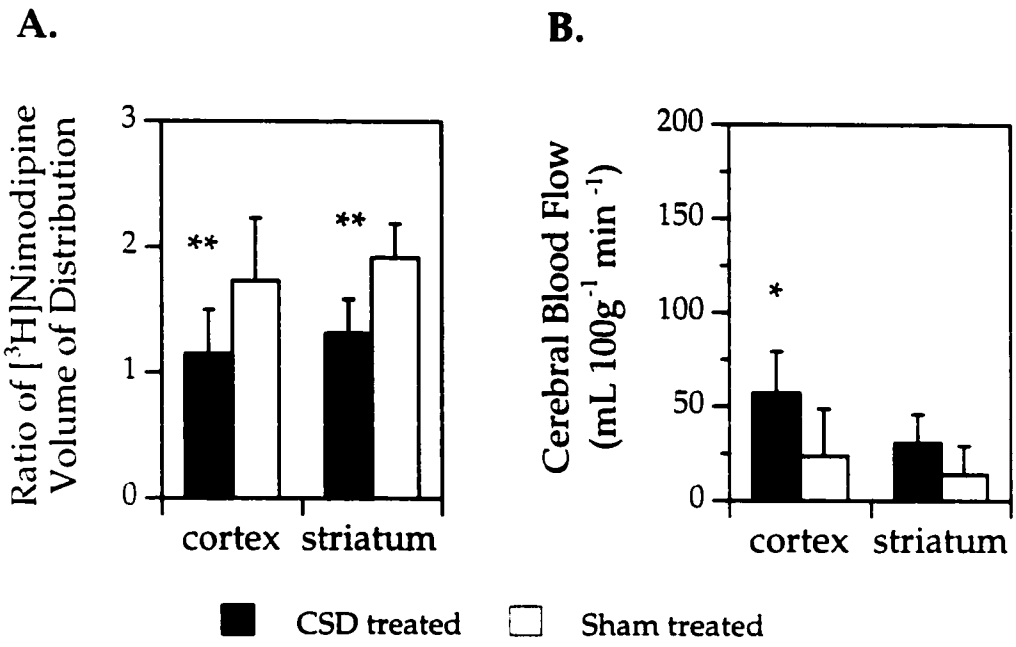

Figure 5-6. [^{3}H]Nimodipine V_d and CBF data sampled with threshold templates. **A)** The ratio of [^{3}H]nimodipine V_d for the CSD and sham treated groups obtained from the template defined by [V_d(sham) - V_d(CSD)] + SD, with a size larger than 0.2 mm^2 shown in red in Figure 5-5. **B)** CBF for the CSD and sham treated groups sampled with the same template as in A. All values are mean ± SD. CBF, cerebral blood flow; CSD, cortical spreading depression; SD, standard deviation; V_d, volume of distribution. Different from sham treated group: *$p < 0.05$, **$p < 0.01$.

[^{3}H]Dizocilpine distribution

To visualize the average in vivo [^{3}H]dizocilpine distribution in the CSD and sham treatment groups, [^{3}H]dizocilpine V_d images were calculated from the autoradiographs of [^{3}H]dizocilpine content. These images are averaged over all rats in the CSD and sham treated groups at the five coronal levels studied and are shown in Figure 5-7. Regional [^{3}H]dizocilpine V_d was calculated within the contralateral forebrain gray matter. There were neither any regional differences nor any differences between the CSD and sham treated groups. Averaged over the cortical and striatal region in all rats [^{3}H]dizocilpine V_d in this hemisphere were 26.11 ± 7.07 mL g^{-1} in the cortex, 22.26 ± 6.08 mL g^{-1} in the striatum. In the ipsilateral ischemic core region, [^{3}H]dizocilpine distribution was less than the contralateral non-ischemic tissues. At the site of CSD induction during preconditioning, [^{3}H]dizocilpine distribution was increased.

The image pixel ensemble defined by the [^{3}H]dizocilpine [V_d(sham) - V_d(CSD)] + SD template, and meeting the minimum area criterion of 0.2 mm^2, is shown in red in Figure 5-8. The cortical ensemble of this template was 8% of the total cortical area scanned whereas the striatal ensemble was 1% of the total striatal area scanned. The image pixel ensemble defined by the [^{3}H]dizocilpine [V_d(sham) - V_d(CSD)] - SD template, and meeting the minimum area criterion of 0.2 mm^2, is shown in blue in Figure 5-8. The

cortical ensemble of this template was 11% of the total cortical area scanned whereas the striatal ensemble was 32% of the total striatal area scanned.

Within the cortical extent defined by [^{3}H]dizocilpine [V_d(sham) - V_d(CSD)] + SD templates, [^{3}H]dizocilpine V_d was 27.53 ± 7.97 mL g^{-1} (n = 6) in the sham treated group and 19.39 ± 6.52 mL g^{-1} (n = 6) in the CSD treated group. Within the striatal extent [^{3}H]dizocilpine V_d was 27.12 ± 8.91 mL g^{-1} (n = 6) in the sham treated group and 19.28 ± 12.72 mL g^{-1} (n = 9) in the CSD treated group. The differences were not significant. Within the cortical extent of this template the ratio of [^{3}H]dizocilpine V_d was 1.03 ± 0.19 in the sham treatment group and 0.77 ± 0.15 in the CSD treatment group ($p = 0.08$, not significant) (Figure 5-9A). Within the striatal extent of this template the ratio of [^{3}H]dizocilpine V_d was 1.18 ± 0.17 in the sham treatment group and 0.85 ± 0.28 in the CSD treatment group ($p < 0.05$) (Figure 5-9A). CBF images were sampled with the identical template. Within the cortical extent CBF was 63 ± 41 mL $100g^{-1}$ min^{-1} in the sham treated group compared with 106 ± 25 mL $100g^{-1}$ min^{-1} in the CSD treated group ($p < 0.05$) (Figure 5-9B). Within the striatal extent CBF was 17 ± 21 mL $100g^{-1}$ min^{-1} in the sham treated group compared with 47 ± 28 mL $100g^{-1}$ min^{-1} in the CSD treated group (not significant) (Figure 5-9B).

Within the cortical extent of the templates defined by the [^{3}H]dizocilpine [V_d(sham) - V_d(CSD)] - SD, [^{3}H]dizocilpine V_d was 13.29 ± 7.04 mL g^{-1} (n = 6) in the sham treated group and 22.17 ± 9.40 mL g^{-1} (n = 6) in the CSD treated group. Within the striatal extent [^{3}H]dizocilpine V_d was 10.20 ±

7.49 mL g^{-1} (n = 6) in the sham treated group and 19.46 ± 14.17 mL g^{-1} (n = 6) in the CSD treated group. The differences were not significant. Within the cortical extent of this template the ratio of [^{3}H]dizocilpine V_d was 0.51 ± 0.26 in the sham treatment group and 0.86 ± 0.24 in the CSD treatment group (not significant) (Figure 5-9C). Within the striatal extent of this template the ratio of [^{3}H]dizocilpine V_d was 0.51 ± 0.43 in the sham treatment group and 0.86 ± 0.41 in the CSD treatment group (not significant) (Figure 5-9C). CBF images were sampled with the identical template. Within the cortical extent CBF was 23 ± 22 mL $100g^{-1}$ min^{-1} in the sham treated group compared with 47 ± 22 mL $100g^{-1}$ min^{-1} in the CSD treated group ($p < 0.05$) (Figure 5-9D). Within the striatal extent CBF was 3 ± 4 mL $100g^{-1}$ min^{-1} in the sham treated group compared with 17 ± 6 mL $100g^{-1}$ min^{-1} in the CSD treated group (not significant) (Figure 5-9D).

In the CSD treated rats that did not undergo subsequent MCA occlusion (n = 5) on day 3 after CSD, [^{3}H]dizocilpine V_d in the contralateral brain (no treatment) was 23.37 ± 3.79 mL g^{-1} in the cortex and 19.53 ± 2.83 mL g^{-1} in the striatum. [^{3}H]Dizocilpine V_d in the area identified with both sets of the template was not different between the ipsilateral (CSD treated) and contralateral forebrain average (no treatment), indicating CSD precondition alone did not have any effect on [^{3}H]dizocilpine regional distribution either.

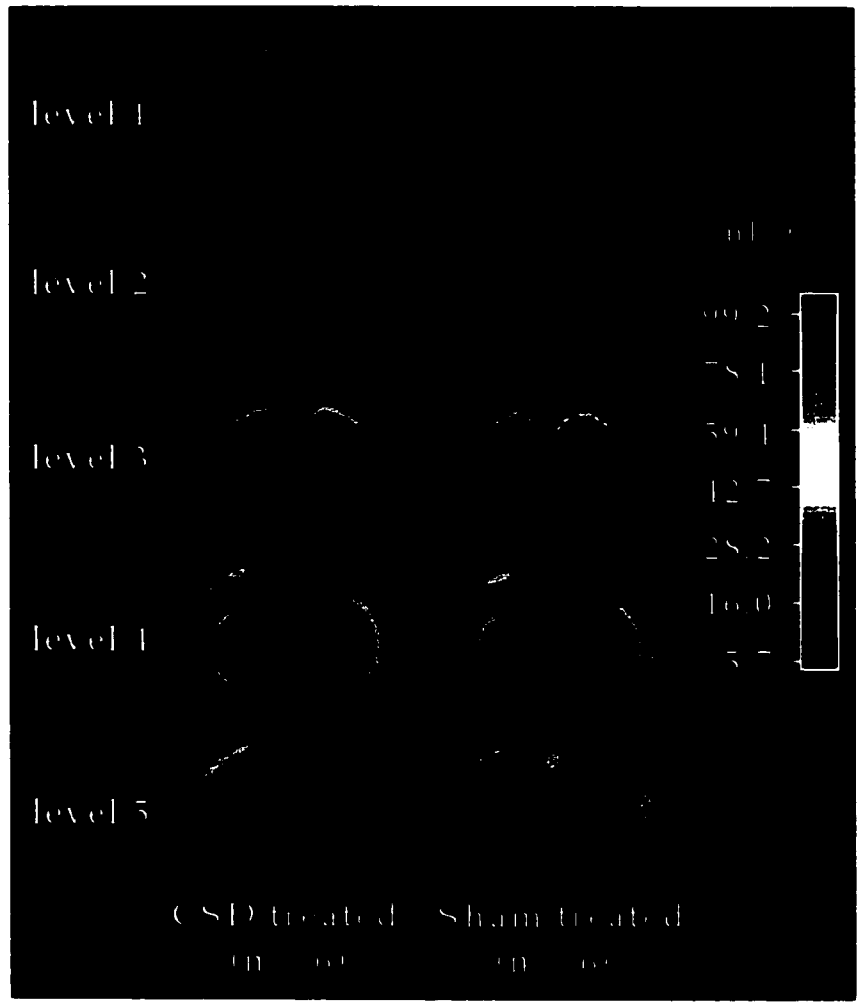

Figure 5-7. Averages of [^{3}H]dizocilpine V_d images for CSD (n = 6) or sham (n = 6) treated groups. The levels correspond to coronal sections from Bregma in mm at 1.20 (level 1), 0.20 (level 2), -3.30 (level 3), -5.60 (level 4), -6.30 (level 5). The ischemic hemisphere is on the left side of the sections. Calibrated colour scale is shown, as are the number of rats used to obtain each image. CSD, cortical spreading depression; V_d, volume of distribution.

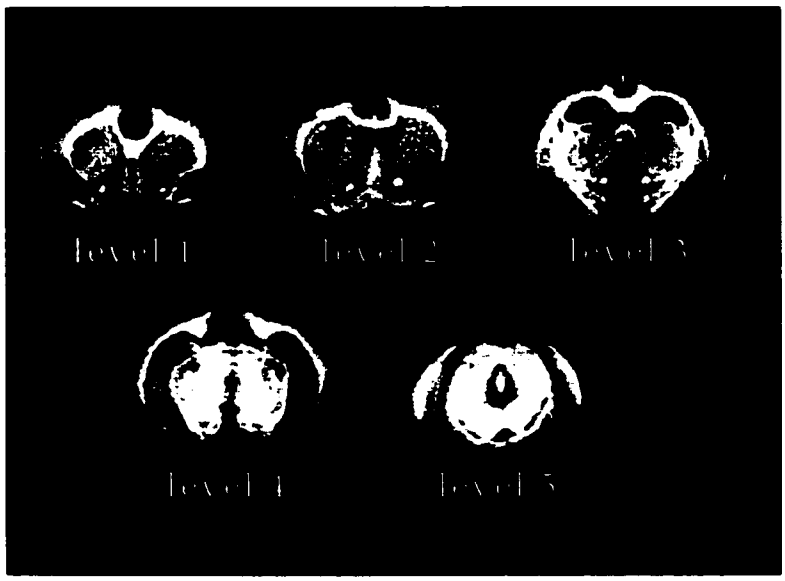

Figure 5-8. [^{3}H]Dizocilpine V_d threshold templates used to sample [^{3}H]dizocilpine and [^{14}C]IAP CBF images. The template are overlaid on registered histological sections. The levels correspond to coronal sections from Bregma in mm at 1.20 (level 1), 0.20 (level 2), -3.30 (level 3), -5.60 (level 4), -6.30 (level 5). The red patches represent the pixel assemble defined by [V_d(sham) - V_d(CSD)] + SD, with a size larger than 0.2 mm^2. The blue patches represent the pixel assemble defined by [V_d(sham) - V_d(CSD)] - SD, with a size larger than 0.2 mm^2. IAP, iodoantipyrine; SD, standard deviation; V_d, volume of distribution.

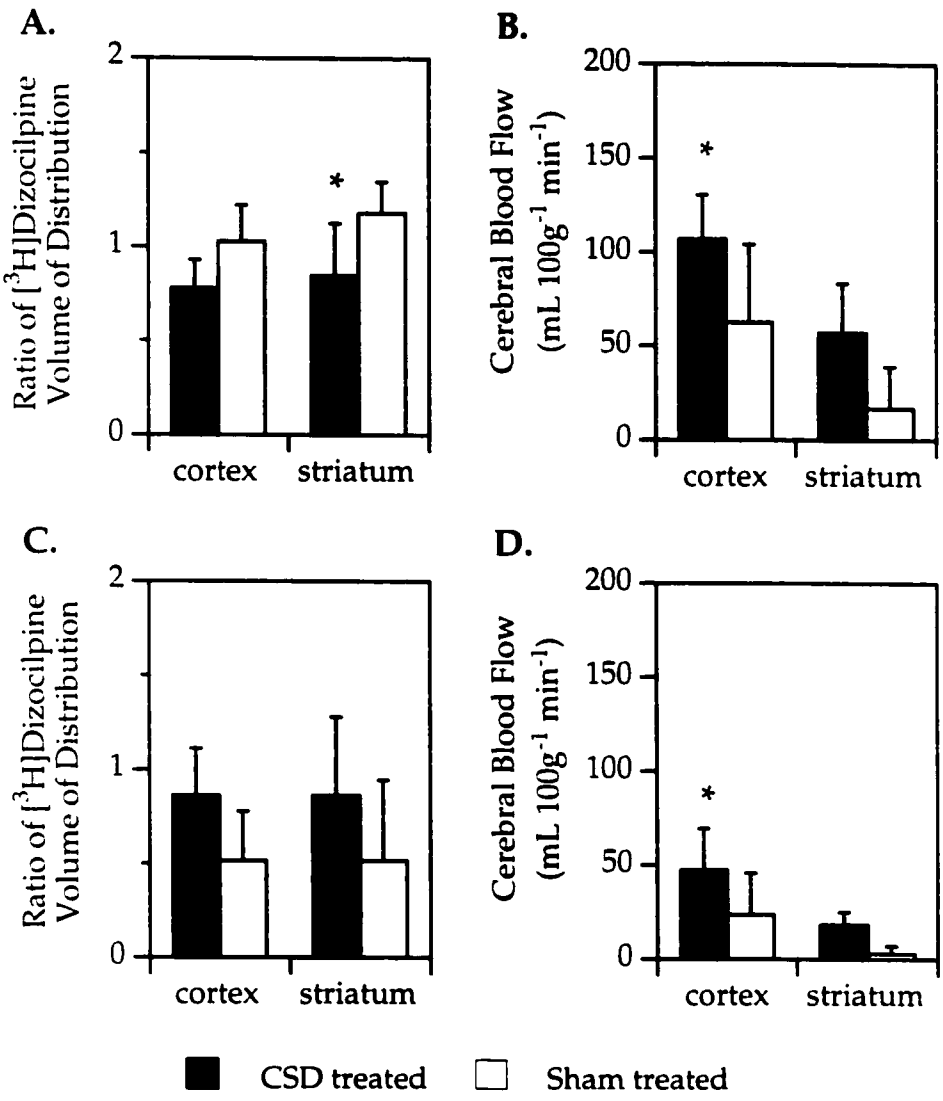

Figure 5-9. [^{3}H]Dizocilpine V_d and CBF data sampled with threshold templates. **A**) The ratio of [^{3}H]dizocilpine V_d for the CSD and sham treated groups obtained from [V_d(sham) - V_d(CSD)] + SD template as shown in red in Figure 5-8. **B**) CBF for the CSD and sham treated groups sampled with the same template as in A. **C**) The ratio of [^{3}H]dizocilpine V_d for the CSD and sham treated groups obtained from the [V_d(sham) - V_d(CSD)] - SD template as shown in blue in Figure 5-8. **D**) CBF for the CSD and sham treated groups sampled with the same template as in C. All values are mean ± SD. CBF, cerebral blood flow; CSD, cortical spreading depression; SD, standard deviation; V_d, volume of distribution. Different from sham treated group: * $p < 0.05$.

Discussion

Regional CBF was measured in separate studies from in vivo [^{3}H]nimodipine or [^{3}H]dizocilpine distribution at 3 hours of focal cerebral ischemia in CSD preconditioned or sham treated rats. Regional CBF was found to increase outside the ischemic core and adjacent non-ischemic medial cortex following CSD preconditioning. It was observed that CSD preconditioning attenuated the increased distribution of [^{3}H]nimodipine in focally ischemic cortex compared with the sham treated rats. In the same area in [^{14}C]IAP studies regional CBF was significantly higher in CSD preconditioned studies. Within a much smaller area of striatum both an increase and decrease of [^{3}H]nimodipine distribution was observed following CSD treatment compared with the sham treated group. Differences in [^{3}H]dizocilpine distribution data fails to reach statistical significance but some changes identified seem to agree with the regional CBF and [^{3}H]nimodipine in vivo distribution data. It is hypothesized that an increase in cortical regional CBF and an attenuation of ischemic depolarization during focal cerebral ischemia may reflect the increased ischemic tolerance following CSD preconditioning.

The studies included measurement of regional CBF during ischemia to determine if improved blood flow following CSD preconditioning contributes to the delay in ischemic depolarization. The result of the H_2 clearance measurements of CBF during focal cerebral ischemia was in agreement with previous measurements showing no effect of CSD or global ischemic

preconditioning on inter-ischemic blood flow (Matsushima and Hakim, 1995; Matsushima et al., 1996). However, the regional CBF measurements using the [^{14}C]IAP method demonstrated up to 70 mL min^{-1} g^{-1} less attenuation in regional CBF in an area outside the ischemic core and the non-ischemic parasagittal cortex outside the vascular territory of the occluded MCA between the CSD and sham treated groups. This finding appears to agree with an earlier report which demonstrated that sublethal focal ischemic preconditioning attenuated CBF in a region outside the focal ischemic core (Matsushima and Hakim, 1995). These discrepancies raise the question whether increased ischemic tolerance includes improvement of regional CBF in ischemic area, and if it does, what mechanism is involved.

CBF is subject to both NO modulation and autonomic nerve control (Branston, 1995; Iadecola et al., 1994). Whereas CBF modulation by NO is glutamate-dependent, the autonomic pathways are independent of the local synaptic activities. The finding that CSD preconditioning better preserves CBF perfusion during subsequent focal ischemia is consistent with the report that CSD pretreatment induced increased neuronal NOS translation in astrocytes (Caggiano and Kraig, 1998). Strong evidence has indicated that mice lacking neuronal NOS suffer less ischemic injury caused by focal insult (Huang et al., 1994), and that mice lacking epithelial NOS are more prone to ischemic injury (Huang et al., 1996). However, recent data determined that cellular localization for neuronal NOS activation in association with ischemic injury is critical (Eliasson et al., 1999). Whereas ischemia stimulates

more pronounced augmentation in NO production in the periinfarct than the infarct tissue, increased peroxynitrite formation are more restricted in the infarct tissue, but not present in the periinfarct tissue (Eliasson et al., 1999).

The present studies investigated the effect of CSD preconditioning on ischemic depolarization, an early metabolic consequence of cerebral ischemia (Hakim and Hogan, 1991). The studies measured [^{3}H]nimodipine in vivo distribution in ischemic brain to identify regional tissue depolarization. Previous studies have reported increased cortical [^{3}H]nimodipine in vivo binding to be an early and sensitive indicator of impending ischemic injury that even precedes increased extracellular glutamate increases (Hakim and Hogan, 1991; Osuga and Hakim, 1996). This increase in distribution is hypothesized to be the result of cell membrane depolarization with increased [^{3}H]nimodipine binding to open or inactivated L-type VSCC (Hogan et al., 1991). Studies measuring [^{3}H]nimodipine in vivo distribution in models of transient ischemia (Hogan and Hakim, 1992; Osuga et al., 1997; Takizawa et al., 1995) have confirmed the association of increased V_d measurements during depolarization and reversal of this increase following repolarization. Increased [^{3}H]nimodipine in vivo binding during ischemia cannot be attributed to changes in number of VSCC during ischemia for the density of L-type VSCC within the brain does not change during the first 4 hours of focal cerebral ischemia (Hogan et al., 1995). However, the possibility cannot be excluded that the attenuation of [^{3}H]nimodipine in vivo distribution in the

ischemic core is the result of the slight increase in regional CBF identified in the same in [^{14}C]IAP studies.

The regional [^{3}H]nimodipine V_d in brain after 3 hours of focal cerebral ischemia in the sham treated rats was comparable to values previously reported following 4 hours of focal ischemia (Hakim and Hogan, 1991) and increased distribution in ischemic brain was observed. However in the CSD treated rats the distribution of [^{3}H]nimodipine was significantly lower in ischemic cortex or striatum. Since the region CBF in the identical regional in the [^{14}C]IAP studies was higher in the CSD preconditioned cortex, the attenuation of [^{3}H]nimodipine in vivo distribution may result from the improved regional perfusion.

Other mechanisms may also account for the attenuation in [^{3}H]nimodipine in vivo distribution. Brain exposure to glutamate, defined as the integral of the extracellular glutamate profile, was reduced during ischemia in CSD preconditioned cortex (Douen et al., 2000). In the first 30 minutes of focal ischemia, increases in extracellular glutamate were comparable between CSD preconditioned and sham treated studies. The profile of extracellular glutamate started to diverge after 30 minutes between the two groups. Whereas extracellular glutamate kept on rising and peaked around 120 minutes in sham studies, it remained elevated, but stable, during the 200 minute study period in CSD preconditioned studies (Douen et al., 2000). An earlier microdialysis study in hippocampus during 3 minutes of global ischemia showed no difference in extracellular glutamate between

ischemia preconditioned and sham studies (Nakata et al., 1992). These observations were consistent with the notion that early increases in extracellular glutamate during cerebral ischemia reflect releases from the synaptic terminal whereas the reversed transportation of glutamate from the astrocytes to the extracellular space is a later event (Szatkowski and Attwell, 1994). Thus, decreased ischemic brain tissue depolarization observed at 3 hours of focal ischemia in the CSD preconditioned rats may represent the effect of less glutamate exposure in ischemic brain and slower progression to infarction.

There are several recent reports suggesting that the progression of ischemic injury may be slower following induction of ischemic tolerance. In a model of global cerebral ischemia tissue oxygen depletion occurred at a slower rate in ischemic tolerant gerbils (Li et al., 1997). Using similar image averaging methods, Matsushima et al. (1998) have mapped the region of cortex showing increased tolerance to ischemic injury in this model of CSD preconditioning and it coincides with the region of attenuated [^{3}H]nimodipine observed here. Following ischemic preconditioning delayed progression of infarction during subsequent focal ischemia has been observed up to 2 hours after MCA occlusion (Sorimachi et al., 1997).

Under the conditions in this study changes of [^{3}H]nimodipine in vivo distribution reflect binding affinity and do not directly measure the number of channels. A decrease of L-type VSCC density in preconditioned brain could potentially explain the attenuation. However, to reduce in vivo

[^{3}H]nimodipine distribution to levels comparable to those observed in the non-ischemic hemisphere, a large fraction of binding sites would be lost (Hogan et al., 1991). Although ischemic preconditioning was not observed to change nimodipine binding capacities (Kato et al., 1992a) (Chapter 6), ipsilateral occlusion of the common carotid for 1 hour only increased [^{3}H]PN200-110 binding in the rat hippocampus (Magnoni et al., 1988). Several other possibilities should be considered. A reduction in non-specific binding or an altered distribution of intracerebral [^{3}H]nimodipine metabolites in the preconditioned brain is unlikely since no suppression of [^{3}H]nimodipine distribution was observed in the hemisphere treated with CSD compared to the contralateral hemisphere in rats that did not undergo cerebral ischemia. Suppression of periinfarct depolarizations may lessen ischemic injury (Mies et al., 1993b) and would likely decrease [^{3}H]nimodipine distribution in ischemic brain (Osuga and Hakim, 1996). However, no differences in the rate of simple periinfarct depolarizations and integrated simple periinfarct depolarizations were observed between the CSD and sham treated groups. Potential changes in vascular volume (Shockley and LaManna, 1988) would be inconsistent with the pattern of the blood flow observation and would also be far too small to explain the large change in [^{3}H]nimodipine V_d observed in the ischemic core. Internalization of membrane bound L-type VSCC is observed in cell culture following prolonged depolarization (Liu et al., 1994). It is not known if this occurs in ischemic brain or if it can be modulated by prior CSD. However, nimodipine is lipophilic and readily crosses lipid

bilayers (Herbette et al., 1994) and should therefore have access to internalized binding sites. Following 4 hours of focal cerebral ischemia the maximal number of binding sites identified by in vivo binding of [^{3}H]nimodipine to ischemic cortex is comparable to that observed following in vitro binding (Hogan et al., 1991; Hogan et al., 1995) indicating that even if changes in L-type VSCC distribution occur during ischemia, the majority of binding sites can be identified by in vivo binding following ischemic depolarization. Since [^{3}H]nimodipine readily crosses the blood brain barrier (Van den Kerckhoff and Drewes, 1985) altered blood brain barrier permeability is also unlikely an explanation. [^{3}H]Nimodipine circulated for 30 minutes prior to study termination so that an equilibrium of distribution could be established between plasma and brain thus minimizing any effect of potential CBF changes on ligand distribution (Hogan et al., 1991). Therefore, we hypothesize that the attenuation of increased [^{3}H]nimodipine binding in the ischemic brain of the CSD preconditioned rats represents an attenuated cortical tissue depolarization resulting from less tissue injury.

CSD preconditioning does not confer ischemic tolerance to the striatum (Matsushima and Hakim, 1995; Taga et al., 1997). However within the ischemic striatum both attenuation and augmentation of increased [^{3}H]nimodipine distribution were observed. These regions were small (<2% of the total striatal area and total area of the attenuated [^{3}H]nimodipine signal) and their significance is uncertain. They do not correspond to protected brain regions (Matsushima et al., 1998). Within the striatum, regional CBF to the

small area of attenuated [^{3}H]nimodipine distribution in the sham studies (blue template in Figure 5-8) is 1 ± 3 mL/100g/min and equilibrium of distribution of [^{3}H]nimodipine to this severely ischemic brain will not be complete. The more medially located changes are adjacent to the edge of the recognized territory of infarction and may be a consequence of variability of injury inherent in this model of focal ischemia (Belayev et al., 1996). It is possible that the change in periinfarct CBF between CSD and sham treated groups may be contributing, however CBF did not differ in these striatal regions.

Data sampling used differences of average images obtained from each group to identify the effects of preconditioning on [^{3}H]nimodipine and [^{3}H]dizocilpine distribution. This method enabled the observer to identify differences in [^{3}H]nimodipine distribution between the two treatment groups that were not detected by the ROI template analysis. Partial volume effects in the template analysis will have contributed to this as the fixed templates extended through the full thickness of the cortex whereas the changes in [^{3}H]nimodipine distribution did not. Although statistical criteria were adopted to determine the threshold for the definition of templates on the difference images, the method remains only semi-quantitative. The template required at least 50 contiguous image pixels with values above 1 SD of the mean pixel values within normal brain regions to define a template region. This is consistent with the method used in a previous study to identify regions of increased [^{3}H]nimodipine distribution in ischemic brain (Hogan

and Hakim, 1992). However, the extent of changes in [^{3}H]nimodipine identified by this method may remain underestimated. To analyze the [^{14}C]IAP CBF data, the difference images were further processed using squareroot transformation to reduce the skew in the image data. Likewise, the method remains empirical even though the data transformation reduces the skew toward higher CBF values (Pulsinelli et al., 1982).

[^{3}H]Dizocilpine in vivo distribution during 3 hours of focal ischemia is puzzling. Dizocilpine has a higher V_d than that of nimodipine, as indicated by our work (Hogan et al., 1991) (Chapter 4, Chapter 5) and other's (Bowery et al., 1988; Wallace et al., 1992). Yet [^{3}H]dizocilpine in vivo distribution was severely restricted in the ischemic core region in spite of 1 hour of incubation period (Schwartz and Wasterlain, 1991; Schwartz and Wasterlain, 1993; Wallace et al., 1992), except in the site of CSD induction 3 days prior to the focal ischemia (Chapter 5, Figure 5-7). However, dizocilpine binding sites, i.e. NMDA receptor, are quite resistant to injury. It has been reported, by our laboratory using [^{3}H]CGS-19755 in vitro binding (Hogan et al., 1995) and Wallace et al using [^{3}H]dizocilpine (Wallace et al., 1992), that the NMDA receptor binding kinetics do not change in the brain regions sustained 3 to 4 hours of focal ischemia. In fact the binding was so robust that 12 hours of focal ischemia without reperfusion failed to alter [^{3}H]dizocilpine in vitro binding to the ischemic tissue and its sensitivity to glutamate (Dewar et al., 1989). Our own [^{3}H]dizocilpine in vitro binding data (Chapter 6) show that 2 hours of CSD preconditioning did not change the binding kinetics of

dizocilpine. Similar results were obtained by others after ischemic preconditioning (Kato et al., 1992a).

Severe focal ischemia complicated the interpretation of [^{3}H]dizocilpine in vivo distribution results. There have been questions as to whether [^{3}H]dizocilpine in vivo distribution in ischemic tissue is a short event that, by the time of 3 hours, the increases in [^{3}H]dizocilpine in vivo distribution have passed. However, increased [^{3}H]dizocilpine in vivo distribution in focal ischemic tissue has been reported by other authors (Bowery et al., 1988; Wallace et al., 1992). Published work done by our associates (Osuga and Hakim, 1996) has indicated that increases in extracellular glutamate, thought to be necessary for increased [^{3}H]dizocilpine in vivo distribution, occurred later than increased [^{3}H]nimodipine in vivo distribution.

It is of crucial importance to note that there was a lack of [^{3}H]dizocilpine distribution directly under the dura where recurrent CSD are induced (Figure 4-2, Figure 4-3). Histological damage was apparent. Such a trend even appeared after a single CSD during a 16 minute incubation period (Figure 4-6). However, at the same site on day 3 after CSD induction, [^{3}H]dizocilpine in vivo distribution was increased (Chapter 5, Figure 5-7). [^{3}H]Dizocilpine in vitro binding on day 3 after recurrent CSD saw no change in either [^{3}H]dizocilpine binding capacity or affinity, in other regions or at the site of CSD induction (Chapter 6, Figure 6-8), indicating [^{3}H]dizocilpine binding was intact.

[^{3}H]Dizocilpine data provided no clear information about the effect of CSD preconditioning on [^{3}H]dizocilpine in vivo distribution. Earlier studies elsewhere observed an obvious increase in the ischemic region at 1 hour of focal ischemia whereas at 15 minutes the distribution of [^{3}H]dizocilpine was inconsistent (Wallace et al., 1992). It is noteworthy that in [^{3}H]dizocilpine in vivo distribution studies the ischemic core had less [^{3}H]dizocilpine accumulation than in the non-ischemia area at 3 hours of focal ischemia. The lack of [^{3}H]dizocilpine distribution cannot be attributed to the ligand delivery for dizocilpine has a far greater cerebral clearance than nimodipine (personal communication, MJH). An extended period of ischemia does not seem to alter the in vitro binding of [^{3}H]dizocilpine in the brain or its response to exogenous glutamate (Dewar et al., 1989). [^{3}H]Dizocilpine in vitro binding studies (Bowery et al., 1988; Dewar et al., 1989; Kato et al., 1992a; Wallace et al., 1992) excluded the possibility that the binding capacity or affinity is altered. It is of interest that, at the site where CSD was induced on the intact dura 3 days prior to the focal ischemia, there is intense localized [^{3}H]dizocilpine accumulation. This is in sharp contrast to [^{3}H]dizocilpine in vivo distribution in the identical locale during recurrent CSD.

Nonetheless, using the template generated from the [V_d(sham)-V_d(CSD)] + SD difference images, an area of lower [^{3}H]dizocilpine was identified outside the ischemic core in the CSD treated studies. This attenuation appeared to correlate with improved regional CBF found in [^{14}C]IAP studies. There are several possibilities that may result in this

attenuation. Since the effect coincides with improved regional CBF, it may reflect ameliorated tissue injury due to improved tissue perfusion, consistent with the [^{14}C]IAP studies. This attenuation may also indicate reduced extracellular glutamate and tissue depolarization in the CSD preconditioned cortex. It has been reported that the increase in [^{3}H]dizocilpine in vivo distribution is relatively slower than that of the in vivo [^{3}H]nimodipine (Wallace et al., 1992), consistent with the suggestion that membrane depolarization precedes increases in extracellular glutamate (Osuga and Hakim, 1996).

Taken together it is clear that there was a lack of [^{3}H]dizocilpine in vivo distribution in the area of acute tissue injury with blood flow restriction ([^{3}H]dizocilpine in vivo distribution during focal ischemia) or without blood flow restriction ([^{3}H]dizocilpine in vivo distribution during 1 hour recurrent CSD). At the site of chronic injury [^{3}H]dizocilpine in vivo distribution was increased (Figure 5-7). It is very unlikely that [^{3}H]dizocilpine had restricted access to the injured areas caused by CSD treatment or severe focal ischemia, due to higher V_d of dizocilpine (Chapter 4 and Chapter 5). Immediate measurement of NMDA binding kinetics after severe ischemia found no alteration in the binding of [^{3}H]dizocilpine in the ischemic tissue (Wallace et al., 1992). Similarly, delayed measurement of [^{3}H]dizocilpine binding kinetics 12 hours after permanent MCA occlusion identified no alteration (Dewar et al., 1989). No alteration was found on day 3 after CSD treatment either

(Chapter 6). These analyses led to the hypothesis that the binding of dizocilpine with NMDA receptor is damaged during acute tissue injury.

In summary the studies have employed autoradiographic methods to identify regional changes of CBF, as well as [^{3}H]nimodipine and [^{3}H]nimodipine in vivo distribution, following CSD preconditioning. CSD preconditioning attenuated ischemia in the regions outside the ischemic core, consistent with the report that CSD treatment induces neuronal NOS in the astrocytes 3 days later. In vivo [^{3}H]nimodipine distribution was reduced in CSD preconditioned studies. Improved regional perfusion and attenuated VSCC activation may contribute to the reduction of [^{3}H]nimodipine in vivo distribution. It is concluded that increased ischemic tolerance induced by CSD preconditioning includes improvement of regional CBF and reduced ischemic depolarization.

CHAPTER 6. [^{3}H]NIMODIPINE AND [^{3}H]DIZOCILPINE IN VITRO BINDING TO RAT BRAIN THREE DAYS AFTER CSD PRECONDITIONING

Results from [^{3}H]nimodipine and [^{3}H]dizocilpine in vivo binding are not only affected by the level of L-type VSCC and NMDA receptor activation, but also reflect the receptor densities and affinities to their ligands. Since CSD has been reported to change protein synthesis and regional protein synthesis 72 hours after its induction (Krivanek, 1970; Mies, 1993), the protein level of the voltage-sensitive and NMDA calcium channel may be modified. Therefore, [^{3}H]nimodipine and [^{3}H]dizocilpine in vitro binding studies were designed to estimate the densities and affinities of the VSCC and NMDA receptors after CSD preconditioning. [^{3}H]Nimodipine was used to identify L-type VSCC whereas [^{3}H]dizocilpine was used to identify the NMDA receptor. [^{3}H]Nimodipine and [^{3}H]dizocilpine in vitro binding to brain were studied without ischemia on day 3 after preconditioning with 2 hours of recurrent CSD or sham treatment.

The binding capacity and affinity of VSCC and NMDA receptors have been previously studied with in vitro ligand binding using [^{3}H]nimodipine and [^{3}H]CGS-19755, a competitive NMDA antagonist. The data indicated that the in vitro binding at 4 hours of focal ischemia detected no change in binding capacity or affinity (Hogan et al., 1995). However, L-type VSCC may be affected by ischemic stimulation. [^{3}H]PN200-110 in vitro binding to the crude synaptosomal membranes of the cortex was shown to increase after 10

minutes of global ischemia and to return to near control levels after 2 hours of reperfusion (Hoehner et al., 1992). [^{3}H]PN200-110 in vitro binding to tissue sections also suggests that hypoperfusion, produced by ipsilateral occlusion of the common carotid for 1 hour in the rat, was sufficient to increase the binding capacity of [^{3}H]PN200-110 in the hippocampus but not in the cortex (Magnoni et al., 1988). The increase lasted up to 96 hours after the oligemic event. Delayed neuronal death is also accompanied by the loss of [^{3}H]nimodipine binding sites (Araki et al., 1998).

[^{3}H]Dizocilpine in vitro binding has been reported to correlate with the NMDA receptor distribution in the brain (Bowery et al., 1988; Kato et al., 1992a). However, [^{3}H]dizocilpine in vitro binding seems to be resistant to cerebral ischemia (Dewar et al., 1989; Wallace et al., 1992), only to be lost when cell death is prevalent after global ischemia in ischemic preconditioned gerbils (Kato et al., 1992a). It is unknown whether CSD-induced cerebral plasticity modifies the quantity and functionality of NMDA receptor channels. Changes in channel activation may or may not be accompanied by changes in overall channel protein level.

Methods

Experimental animals and surgical anesthesia were identical to those employed in Chapter 3. Rats were allowed to breathe spontaneously during CSD preconditioning. The animal body temperature (rectal) was maintained at 36.5 - 37.5°C in all in vivo studies. CSD was induced from the left occipital

cortex with 0.5 M KCl as described in Chapter 3. The posterior electrode was not used. [^{3}H]nimodipine and [^{3}H]dizocilpine in vitro binding to the brain sections were performed 3 days after CSD or sham preconditioning.

[^{3}H]Nimodipine binding

In vitro [^{3}H]nimodipine binding to brain sections was performed as described (Glossmann and Ferry, 1985) with slight modification. Sections were warmed to -20°C on the day before and to 23°C on the day of study. Sections were then preincubated in incubation buffer (170 mM Tris-HCl, 2.5 mM $CaCl_2$, 2.5 mM $MnCl_2$, pH 7.6). To determine total binding, the sections were incubated in the same buffer containing [^{3}H]nimodipine (specific activity 127.7 Ci $mmol^{-1}$, NEN-Dupont, Boston, Massachusetts, USA) with nominal concentrations ranging from 20 to 10,000 pM. Unlabeled nimodipine (Miles Pharmaceuticals, Etobicoke, Ontario, Canada) was added to [^{3}H]nimodipine to lower the specific activity for buffers containing more than 300 pM of nimodipine. Incubation was carried out for 60 minutes. Nonspecific binding was determined on adjacent sections in the same buffer containing 2 mM racemic PN200-110 (isradipine) (Sandoz, Dorval, Quebec, Canada). Following incubation, sections were washed with Tris buffer for 5 seconds at room temperature and then placed in ice-cold Tris buffer containing 0.25 g L^{-1} bovine serum albumin (Sigma Chemicals, St. Louis, Minnesota, USA) for 30 minutes. Finally sections were rinsed in ice-cold distilled water for 10 seconds and dried under a stream of cold air. A total of 6 CSD and 6 sham treated rats were studied.

[^{3}H]Dizocilpine binding

In vitro binding of [^{3}H]dizocilpine to tissue sections was performed as described (Bowery et al., 1988) with some modification. Sections were warmed to -20°C on the day before and to 23°C on the day of study. Sections were rinsed twice for 30 seconds in incubation buffer (50 mM Tris-HCl, pH 7.4). The sections were then preincubated in the incubation buffer containing 10 µM glutamate for 30 minutes and allowed to air dry. To determine total binding, 200 µL of incubation buffer containing [^{3}H]dizocilpine (specific activity 23.9 Ci mmol^{-1}, Amersham International Plc, England, UK) with nominal concentration ranging from 0.125 to 128 nM was applied over each section for 60 minutes at 23°C. Unlabeled dizocilpine (Research Biochemicals Inc., Natick, Massachusetts, USA) was added to [^{3}H]dizocilpine to lower the specific activity for buffers containing more than 4 nM of dizocilpine. Nonspecific binding was determined on adjacent sections by including 10 µM unlabeled dizocilpine in the incubation buffer. Following incubation, sections were washed with incubation buffer for 20 seconds twice. Sections were finally rinsed in ice-cold distilled water for 10 seconds and dried under a stream of cold air. A total of 6 CSD and 6 sham treated rats were studied.

Autoradiography

Following incubation, all sections were apposed to Hyperfilm for 7 to 120 days to obtain autoradiographs of regional [^{3}H]ligand distribution. Brain paste ^{3}H standards were exposed on the same film to allow calibration of the

autoradiographs. Autoradiographs of total and non-specific ligand binding were digitized on the MCID system. Autoradiographs from the same level were spatially registered to a set of images from a selected study, using multiple anatomically defined fiducial markers (35 - 45) as described above. The images were then averaged within the same group to form a mean image of radiotracer distribution at each individual incubation concentration. Regional tissue content of ^{3}H was determined at two coronal levels in both hemispheres using a standardized template (Figure 6-1).

Kinetic analysis

The known specific activity of ^{3}H-labeled ligands was used to convert all activity measurements to ligand concentrations. The concentration of free ligand was determined by taking aliquots of incubation medium at the end of the incubation period and measuring ^{3}H concentration by liquid scintillation counting with appropriate quench correction. Free ligand concentration obtained from incubations at the same nominal free ligand concentration (n = 6 for each group) were combined to obtain average free ligand concentration. Specific binding images were calculated by subtracting the mean non-specific image from the mean total image. Specific binding data were sampled from the specific binding images and were assumed to follow Michaelis-Menten kinetics. Models of one and two binding sites were studied and nonlinear regression analysis (Systat, SPSS Inc., Chicago, Illinois, USA) was used to estimate maximal binding and binding affinities (Appendix 3). Potential

difference between treatment conditions was identified with 95% and 99% confidence intervals.

Results

Physiological variables

Physiological variables did not differ between the CSD and sham treated groups during the 2 hours of preconditioning in [^{3}H]nimodipine and [^{3}H]dizocilpine in vitro binding studies. These variables are averaged over two treatment groups and summarized in Table 6-1. Rectal temperature was not significantly different between any experimental and sham groups during preconditioning. Rectal temperature was 36.9 ± 0.2°C (n = 24) during preconditioning over all studies. The average rate of CSD waves during precondition was 6.1 ± 1.5 h^{-1} (n = 24). No CSD wave was recorded in the sham treated groups.

Table 6-1. Physiological variables for in vitro ligand binding studies

Parameters	CSD treated (n = 12)	Sham treated (n = 12)
MABP (mm Hg)	86 ± 7	85 ± 7
pH	7.40 ± 0.03	7.40 ± 0.03
P_aCO_2 (mm Hg)	51 ± 5	53 ± 5
P_aO_2 (mm Hg)	212 ± 39	229 ± 41
Blood glucose (mM)	6.16 ± 0.57	6.15 ± 0.52

Values are means ± SD. MABP, mean arterial blood pressure; P_aCO_2, arterial partial pressure of carbon dioxide; P_aO_2, arterial partial pressure of oxygen.

Binding results

Figure 6-1 illustrates the ROI templates used to sample the concentration of regional radiotracer. The ROI templates were designed based on previously reported binding characteristics of [^{3}H]nimodipine and [^{3}H]CGS-19755 in vitro binding (Hogan et al., 1995) and preliminary data analysis. To avoid partial volume effects, the templates divided the neocortex into four quarters. They were dorsal medial outer cortex (DM outer), dorsal medial inner (DM inner), ventral lateral outer cortex (VL outer), ventral lateral inner cortex (VL inner) in both treated (CSD or sham) (ipsilateral) cortex and contralateral (no treatment) cortex. Striatum was sampled as an undivided structure. Data from the corresponding region at level 2 and 3, e.g., VL outer at level 2 and VL outer at level 3, were combined, forming a total of five VOI. All subsequent kinetic analysis was performed over the data sampled with these templates.

[^{3}H]Nimodipine binding

[^{3}H]Nimodipine binding was measured at 13 different free ligand concentrations ranging from 19.85 ± 0.30 to 8546.70 ± 565.33 pM. Non-specific binding to the tissue sections as a percentage of total binding was 42.0 ± 10.3% at a free ligand concentration of 9.73 pM and increased linearly to 99.3 ± 13.4% at a free ligand concentration of 8546.70 pM. Figure 6-2 shows average images of [^{3}H]nimodipine specific binding from the two studies groups at the average free ligand concentration of 238 ± 5 pM. Nonlinear regression using a model of one saturable binding site [Bound = B_{max} * Free/(K_d + Free)] was highly

significant for all regions ($F > 126$; $r^2 > 0.915$ $p < 0.00001$) (at 99% confidence interval). Addition of a second saturable binding site did not improve the fit in any of the VOI studied.

Figure 6-3 shows the estimates of B_{max} and K_d for one binding site model over 10 VOI (five ipsilateral, five contralateral) studied. The confidence interval at 99% of B_{max} and K_d are indicated with the horizontal scale. In the contralateral hemisphere (used as internal control), regional estimated B_{max} ranged from 8.2 ± 0.75 pmol g^{-1} (estimate ± standard error of estimate) to 29.6 ± 1.87 pmol g^{-1}, whereas K_d ranged from 114 ± 31 pM to 448 ± 52 pM, consistent with values previously reported (Hogan et al., 1995). In the CSD treated group, estimated B_{max} were symmetric between corresponding VOI in the ipsilateral and contralateral hemisphere. Estimated B_{max} and its 99% confidence interval in the ipsilateral outer ventrolateral cortex (VL outer) was 28.2 (23.6 - 32.8) pmol g^{-1} compared with 29.6 (23.5 - 35.7) pmol g^{-1} in the contralateral side. Estimated B_{max} and its 99% confidence interval in the ipsilateral inner ventrolateral cortex (VL inner) was 10.5 (6.7 - 14.3) pmol g^{-1} compared with 11.5 (8.3 - 14.7) pmol g^{-1}. However, similar symmetry did not exist in the sham treated group. Estimated B_{max} and its 99% confidence interval in the ipsilateral outer ventrolateral cortex (VL outer) was 40.1 (33.4 - 46.8) pmol g^{-1} compared with 24.1 (16.9 - 31.3) pmol g^{-1} in the contralateral side. Estimated B_{max} and its 99% confidence interval in the ipsilateral inner ventrolateral cortex (VL inner) was 17.8 (13.1 - 22.4) pmol g^{-1} compared with 8.3 (5.5 - 11.0) pmol g^{-1}. All 99% confidence intervals for the estimated K_d

between the treated hemisphere and contralateral hemisphere and between the CSD and sham treated groups overlapped. Figure 6-4 shows a Scatchard plot of specific [^{3}H]nimodipine binding in the ipsilateral ventrolateral outer cortex in the CSD, sham and control groups.

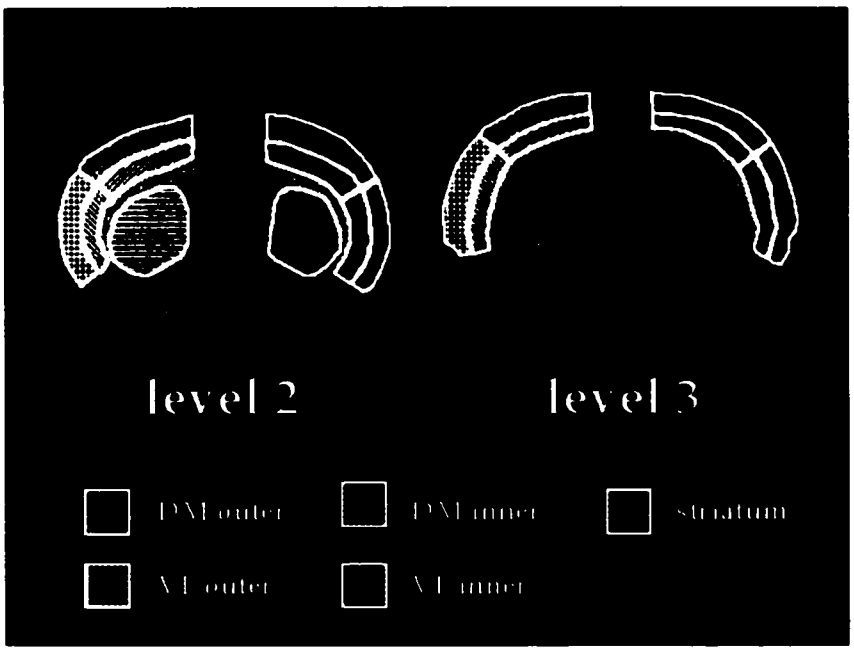

Figure 6-1. The region of interest (ROI) and volume of interest (VOI) templates used to sample [^{3}H]nimodipine and [^{3}H]dizocilpine in vitro binding images. The data were sampled at 2 coronal levels in the rat brain. The ROI templates are on the right side of the sections with lines to define ROI. The ROI groupings used to define the 5 VOI are on the left side of the sections and are labeled at the bottom of the figure. ROI, region of interest; VOI, volume of interest. DM outer, dorsal medial outer cortex; DM inner, dorsal medial inner cortex; VL outer, ventral lateral outer cortex; VL inner, ventral lateral inner cortex.

Figure 6-2. Average specific [^{3}H]nimodipine in vitro binding autoradiographs from 2 coronal levels studied. The CSD or sham preconditioned hemisphere is on the left side of the figures. Free ligand concentration was 238 ± 5 pM. Calibrated colour scale is shown, as are the number of rats used to obtain each image. CSD, cortical spreading depression.

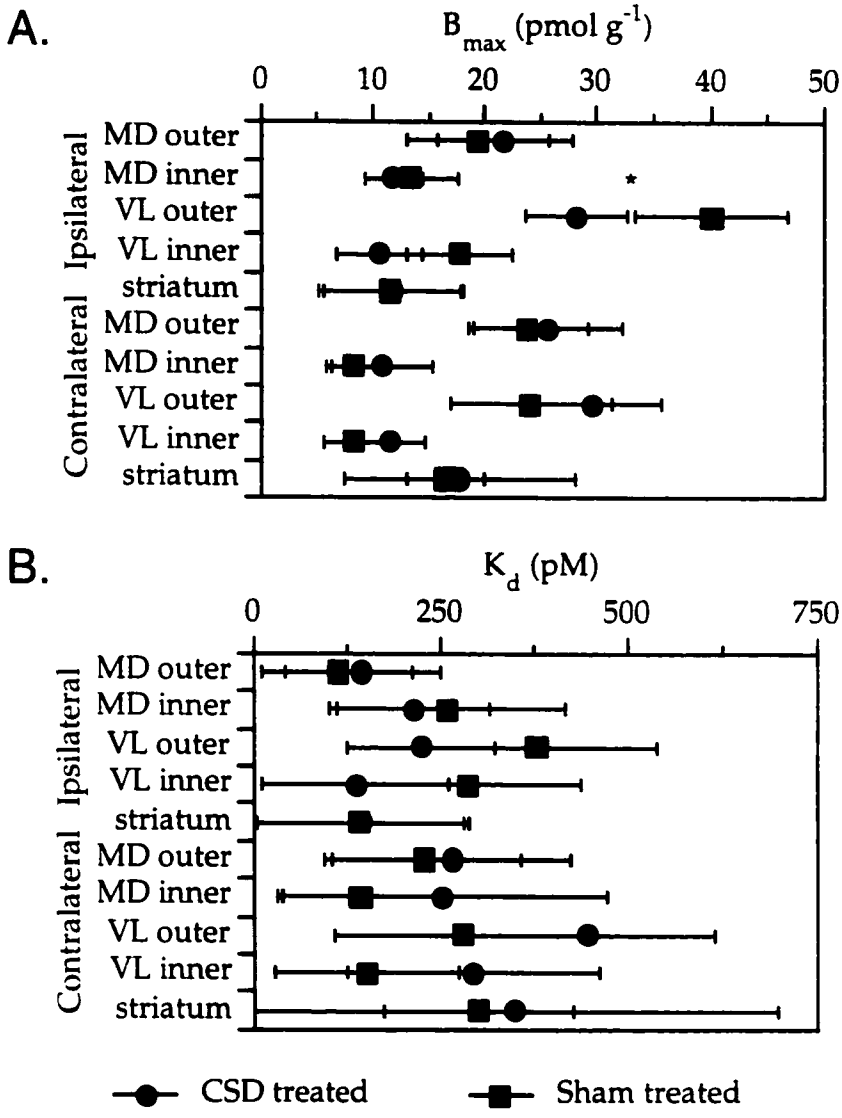

Figure 6-3. Regional estimates and 99% confidence intervals of maximal binding capacity (B_{max}) (**A.**) and binding affinity (K_d) (**B.**) of [^{3}H]nimodipine in vitro binding to brain on day 3 after CSD (n = 6) or sham (n = 6) treatment. * No overlapping at 99% confidence interval. CSD, cortical spreading depression; DM outer, dorsal medial outer cortex; DM inner, dorsal medial inner cortex; VL outer, ventral lateral outer cortex; VL inner, ventral lateral inner cortex.

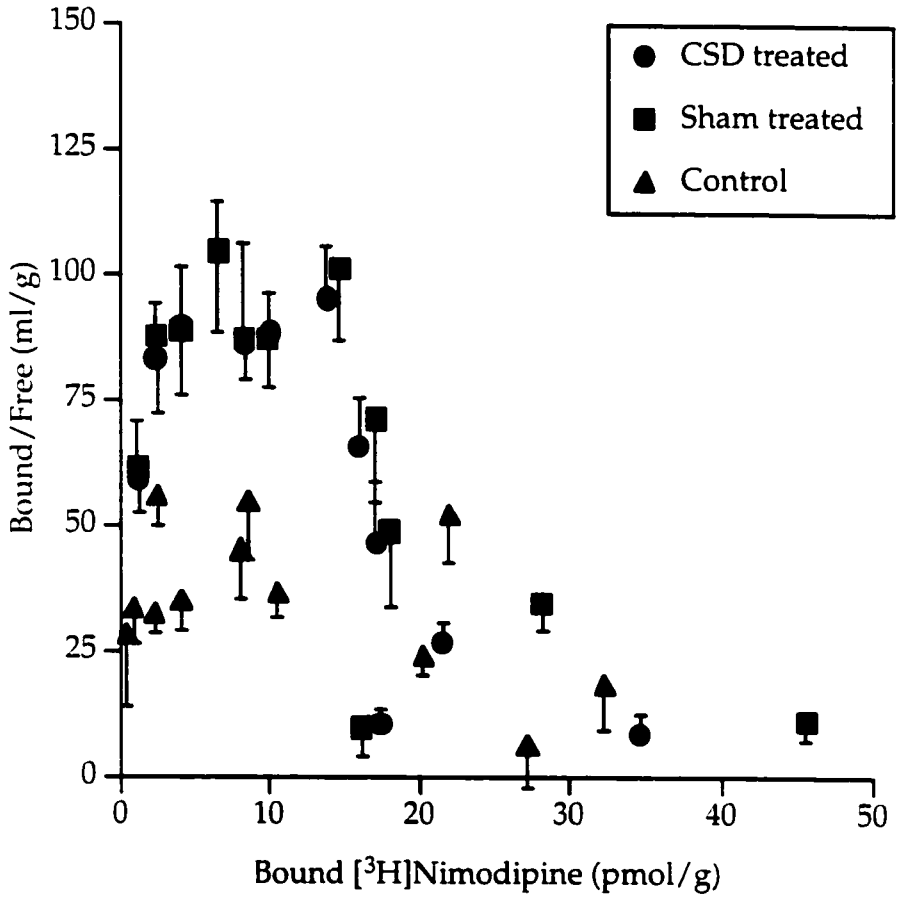

Figure 6-4. Scatchard plots of specific [^{3}H]nimodipine in vitro binding in ipsilateral ventrolateral outer cortex (VL outer). Data are from CSD, sham and control groups. Mean ± SD are shown for each point CSD, cortical spreading depression; SD. standard deviation.

[^{3}H]Dizocilpine binding

[^{3}H]Dizocilpine binding was measured at 13 different free ligand concentrations ranging from 0.18 ± 0.02 to 160.92 ± 5.18 nM. Non-specific binding to the tissue sections as a percentage of total binding was 31.5 ± 0.1% at a free ligand concentration of 0.18 nM and increased linearly to 81.5 ± 0.1% at a free ligand concentration of 160.92 nM. Figure 6-5 shows average images of [^{3}H]dizocilpine specific binding from the two studies groups with an average free ligand concentration of 12.38 ± 0.38 nM. Nonlinear regression using a model of one saturable binding site [Bound = B_{max} * Free/(K_d + Free)] was highly significant for all regions ($F > 194$; $r^2 > 0.945$ $p < 0.00001$). Addition of a second saturable binding site did not improve the fit in any of the VOI studied.

Estimates and 95% confidence interval of B_{max} and K_d for all VOI are shown in Figure 6-6. In the contralateral hemisphere (used as internal control), regional estimated B_{max} ranged from 375 ± 32 pmol g^{-1} (estimate ± standard error of estimate) to 899 ± 56 pmol g^{-1}, whereas K_d ranged from 8.55 ± 31 nM to 33.73 ± 8.61 nM. These values were consistent with reported values obtained using autoradiography (Sakurai et al., 1991). All 95% confidence intervals for the estimated B_{max} and K_d between the treated hemisphere and contralateral hemisphere and between the CSD and sham treated groups overlapped. Figure 6-7 shows a Scatchard plot of specific [^{3}H]nimodipine binding in the ipsilateral ventrolateral outer cortex in the CSD, sham and

control groups. In the site of CSD or sham treatment, no visible anomaly was identified in any incubation concentrations. Average specific images incubated at a free ligand concentration of 12.38 ± 0.38 pM is shown in Figure 6-8.

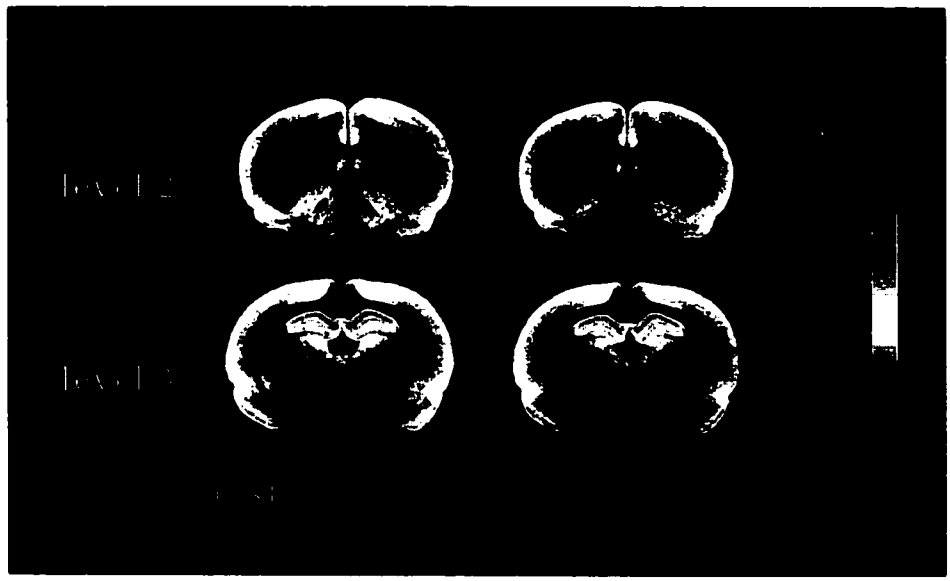

Figure 6-5. Average specific [^{3}H]dizocilpine in vitro binding autoradiographs from 2 coronal levels studied. The CSD or sham treated hemisphere is on the left side of the figures. Free ligand concentration was 12.38 ± 0.38 pM. Calibrated colour scale is shown, as are the number of rats used to obtain each image. CSD, cortical spreading depression.

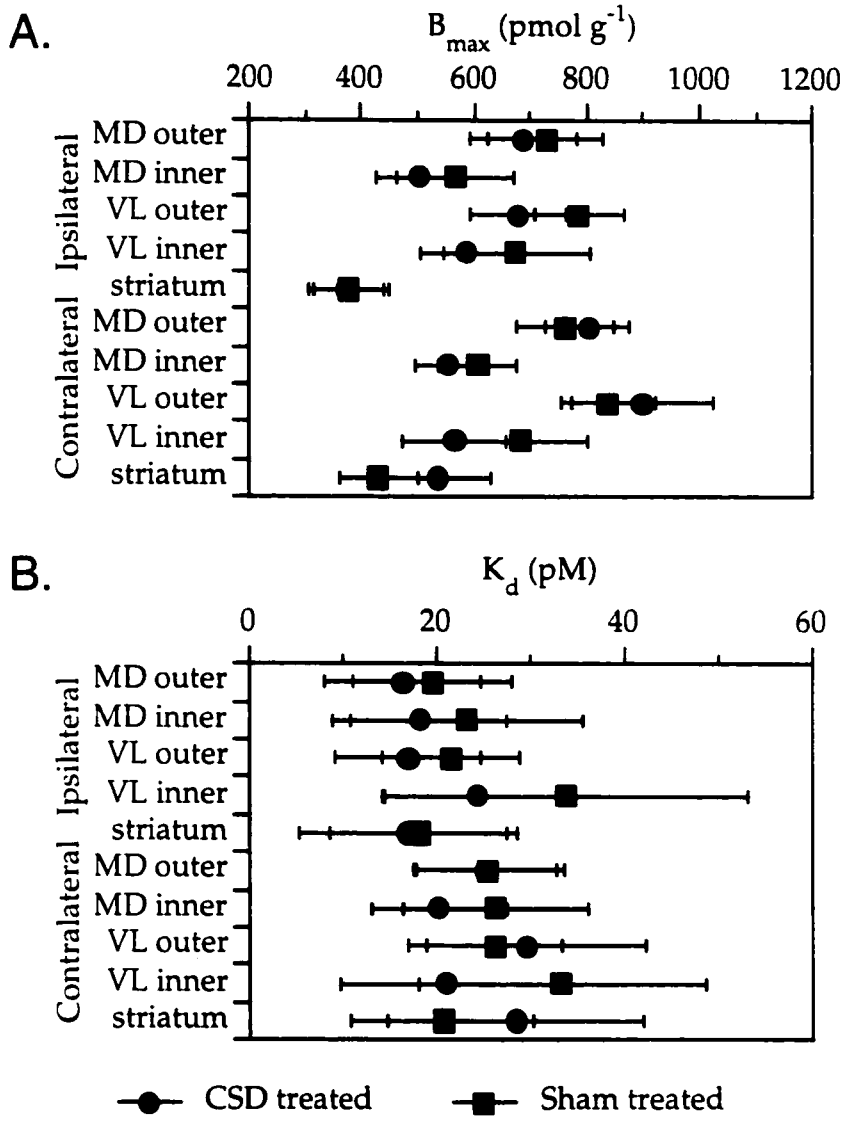

Figure 6-6. Regional estimates and 95% confidence intervals of maximal binding capacity (B_{max}) (**A.**) and binding affinity (K_d) (**B.**) of [^{3}H]dizocilpine in vitro binding to brain on day 3 after CSD (n = 6) or sham (n = 6) treatment. CSD, cortical spreading depression; DM outer, dorsal medial outer cortex; DM inner, dorsal medial inner cortex; VL outer, ventral lateral outer cortex; VL inner, ventral lateral inner cortex.

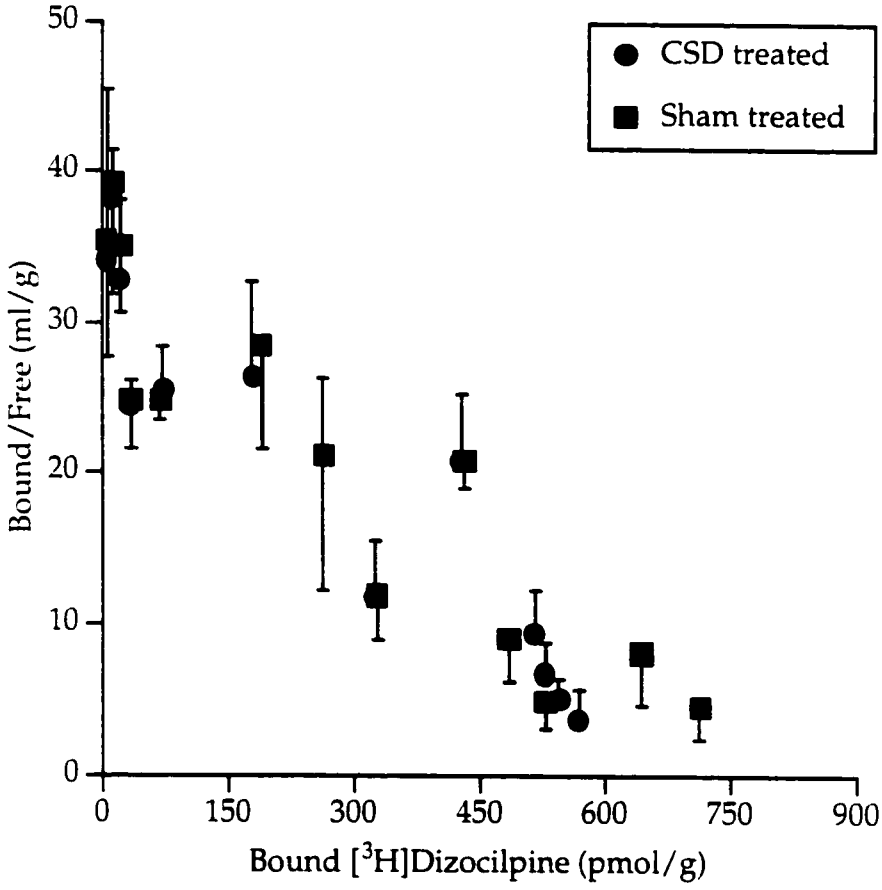

Figure 6-7. Scatchard plots of specific [^{3}H]dizocilpine in vitro binding in ipsilateral ventrolateral outer cortex (VL outer). Data are from CSD, sham and control groups. Mean ± SD are shown for each point. CSD, cortical spreading depression; SD. standard deviation.

Figure 6-8. Average specific [^{3}H]dizocilpine in vitro binding autoradiographs at the level of CSD induction. CSD is induced with 0.5 M KCl at the left occipital cortex on intact dura. Sham studies received 0.5 M NaCl at the same location. No anomaly is seen at the site of CSD or sham treatment. Free ligand concentration was 12.38 ± 0.38 pM. Calibrated colour scale is shown, as are the number of rats used to obtain each image. CSD, cortical spreading depression.

Discussion

In vitro binding kinetics of [^{3}H]nimodipine, an L-type VSCC antagonist, and [^{3}H]dizocilpine, a non-competitive NMDA receptor channels blocker, was measured on day 3 after recurrent CSD preconditioning. The data showed an increase in the total [^{3}H]nimodipine binding capacity (B_{max}) in the ipsilateral neocortex in the sham treated studies. This increases were absent in the recurrent CSD treated ipsilateral cortex. The [^{3}H]nimodipine binding capacity in the contralateral cortex is consistent with published in vitro and in vivo results (Hogan et al., 1991; Hogan et al., 1995). The binding affinity (K_d) did not appear to be affected and was similar with reported findings (Hogan et al., 1991; Hogan et al., 1995). [^{3}H]Dizocilpine binding capacity and affinity were similar to those previously reported (Bowery et al., 1988; Wallace et al., 1992)

and the ligand distribution was symmetric. No difference was found in either ligand binding capacity or affinity between CSD treated and sham treated studies.

The increase in [^{3}H]nimodipine binding capacity in the sham treated cortex is unexpected. Previous reports (Matsushima et al., 1998) and our data agree that there is some local tissue loss at the site of CSD treatment, worse in the KCl treated animals (Matsushima et al., 1998). The platinum electrode planted in the frontal cortex can only be identified as a narrow needle track. The effects of these injuries are usually localized as seen in infarct volume measurement and in vivo ligand distribution studies (e.g. Figure 5-4). There has been no clear definition of what these injuries entail. Earlier studies of in vitro [^{3}H]nimodipine binding at 4 hours of focal ischemic ischemia detected no change in [^{3}H]nimodipine binding capacity or affinity (Hogan et al., 1995). However, L-type VSCC appeared to be regulated by ischemic stimulation. In vitro binding of [^{3}H]PN200-110 to the crude synaptosomal membranes of the cortex was shown to increase after 10 minutes of global ischemia and to return to near control levels after 2 hours of reperfusion (Hoehner et al., 1992). In vitro [^{3}H]PN200-110 binding to tissue sections also suggests that mild ischemia, produced by ipsilateral occlusion of the common carotid for 1 hour in the rat, was sufficient to increase the binding capacity of [^{3}H]PN200-110 in the hippocampus but not in the cortex (Magnoni et al., 1988). The increase lasts up to 96 hours after the ischemic event. It is noteworthy that the ipsilateral occlusion of the common carotid is such a mild stimulus that it

does not even lead to ipsilateral tissue depolarization, and it has minimum short term effect on the tissue function. Immunocytochemistry has indicated that ischemic stimulation induces upregulation of α1C subunit of L-type VSCC, but not α1D subunit of L-type VSCC, α1A subunit of P/Q-type, and α1B subunit of N-type in reactive astrocytes (Westenbroek et al., 1998). During severe cerebral ischemia, immediate upregulation or downregulation of VSCC seems unlikely due to the restrictions on energy metabolism, as indicated by in vitro binding studies carried out on tissue after 4 hours of focal ischemia (Hogan et al., 1995). However, VSCC may be subject to 50% internalization after 2 hours of KCl depolarization in cell lines (Liu et al., 1994).

Our [^{3}H]nimodipine in vitro binding data are consistent with previously published reports, indicating higher binding capacities in the outer cortex than the inner cortex and the striatum (Hogan et al., 1995). Immunocytochemistry studies (Hell et al., 1993) have shown that L-type VSCC is unevenly distributed in the dendrites and the soma. L-type VSCC containing α1C isomer is located in dendrites that are more distal whereas L-type VSCC containing α1D isomer is located in dendrites that are more proximal and in soma in clusters.

[^{3}H]Dizocilpine in vitro binding showed no alteration in the NMDA binding capacity and affinity between the CSD treated and sham treated studies on day 3 after 2 hours of recurrent CSD treatment. No difference was

found within the group compared with the contralateral regions either. These findings are consistent with a previous report that [^{3}H]dizocilpine in vitro binding was unaffected by ischemic preconditioning (Kato et al., 1992a). Our data also agree with the report that NMDA receptors are quite stable after 3 hours of focal ischemia (Wallace et al., 1992), and the response of [^{3}H]dizocilpine in vitro binding to glutamate was unaffected after an extended period of focal ischemia (Dewar et al., 1989). Nonetheless, a binding study on the cortical membranes obtained from young and old mice indicate [^{3}H]dizocilpine binding capacity is developmentally controlled (Gordon et al., 1995; Saransaari and Oja, 1995).

Similarly, whereas [^{3}H]dizocilpine in vitro binding studies reveal more of the receptor binding capacity and affinity, in vivo binding indicates immediate functional state of the NMDA receptor channels, indicating the presence of glutamate and glutamate induced membrane depolarization (Schwartz and Wasterlain, 1993; Wallace et al., 1992). Comparison of in vitro binding data also indicates that the topography of [^{3}H]dizocilpine in vitro binding coincides with the distribution of NMDA receptor (Bettler and Mulle, 1995; Petralia et al., 1994a). On the other hand, the [^{3}H]dizocilpine in vivo distribution is localized in the centre of the ischemic tissue (Wallace et al., 1992), indicating the region suffering from focal ischemic injury, and the outer layer of the cortex during recurrent CSD treatment.

In summary, the increased binding capacity of [^{3}H]nimodipine in the sham treated ipsilateral cortex may reflect the small yet noticeable injury

effect produced by sham treatment. Recurrent CSD however might be able to attenuate this effect and prevent the upregulation of VSCC. On the other hand, neither CSD nor sham treatment produces a significant effect on [^{3}H]dizocilpine binding in the ipsilateral hemisphere.

CHAPTER 7. CSD PRECONDITIONING INDUCES DELAYED REDUCTION OF CEREBRAL GLUCOSE UTILIZATION

A lower metabolic rate correlates with increased tolerance against cerebral ischemic insult (Folbergrova et al., 1992; Sokoloff, 1981). Reduced energy consumption should impart increased tolerance against substrate deprivation associated with cerebral ischemia. Therefore it is of interest to investigate whether increased ischemic tolerance is associated with lower regional glucose utilization. Moreover, due to the tight coupling between extracellular glutamate and energy metabolism, the level of regional CGU should reflect the level of synaptic activity (Mason et al., 1995; Sibson et al., 1998a). Using the [^{14}C]deoxyglucose method, regional CGU in the cortex and striatum was studied in rats undergoing 2 hours of recurrent CSD or sham treatment. The data indicated that CSD treatment reduced the levels of regional CGU on day 3 and day 7 after CSD preconditioning.

Methods

Experimental animals and surgical anesthesia were identical to those employed in Chapter 3. Body temperature (rectal) was maintained at 36.5 - 37.5°C in all studies. CSD was induced from the left occipital cortex with 0.5 M KCl as described in Chapter 3. The posterior electrode was not used. Rats were allowed to breathe spontaneously during CSD preconditioning and subsequent [^{14}C]deoxyglucose studies.

Cortical spreading depression and regional CGU measurement

CSD was induced from the left occipital cortex with 0.5 M KCl as described in Chapter 3. Regional CGU was measured at various time intervals after CSD or sham preconditioning using [^{14}C]deoxyglucose method as described (Sokoloff et al., 1977) (Appendix 4). Briefly, femoral vessels were catheterized to deliver radioisotope or to monitor mean arterial blood pressure, arterial blood gases and blood glucose. [^{14}C]Deoxyglucose (50 μCi/kg; specific activity 53.9 mCi mmol^{-1}; Amersham International Plc, Little Chalfont, England, UK) was injected as an intravenous bolus. Timed arterial blood samples were collected during the following 45 minutes. The blood samples were immediately centrifuged to separate plasma from the blood cells and the plasma [^{14}C]deoxyglucose concentration measured using liquid scintillation counting with appropriate quench correction. The rats were decapitated at 45 minutes of [^{14}C]deoxyglucose injection and the brains were rapidly removed and frozen. Seven rats were assigned to CSD or sham treatment group at 3 time intervals on day 1, 3 and 7 after CSD or sham treatment. A total of 42 rats were studied.

Autoradiography

The brains were warmed to -20°C and 20 μm cryostat sections were obtained every 140 μm. Sections from the [^{14}C]deoxyglucose studies were apposed to either Kodak SB-5 or BioMax Mr film (Picker International, Brampton, Ontario, Canada) for 7 to 10 days. Commercial ^{14}C microstandards

(Amersham, Oakville, Ontario, Canada) were used to calibrate the autoradiographs of ^{14}C distribution.

Image analysis

Autoradiographic images at five coronal levels in the brain were digitized using the MCID system. At each coronal level ^{14}C activity was averaged over 3 aligned and registered images. The resulting set of five images from each study were then spatially registered to a set of images from a selected [^{14}C]deoxyglucose study, using multiple anatomically defined fiducial markers (35 - 45) as described above. The spatially registered images were used for all further calculations. A standard ROI template was designed to sample tissue [^{14}C]deoxyglucose content in each study (Figure 7-1). Regional CGU was calculated within each ROI using the measured tissue [^{14}C]deoxyglucose content and the profile of blood [^{14}C]deoxyglucose concentration as described (Sokoloff et al., 1977).

To guide the identification of groups of ROI with similar levels of regional CGU, a K-means cluster analysis (Systat, SPSS Inc., Chicago, Illinois, USA) was performed on the average of the logarithm of the ratio of ipsilateral over contralateral hemisphere glucose utilization values for all ROI over all study groups on two variables representing the CSD and sham treated groups. The resulting ROI clusters were further subdivided to separate cortical and striatal regions into VOI, resulting in four final VOI (Figure 7-1). Regional CGU values were averaged within the resulting fixed set of VOI, weighted for

the size of each component ROI. The ratio of ipsilateral regional CGU over that of the contralateral hemispheric VOI was calculated.

Statistical analysis

All results are expressed as mean ± SD. The physiological data were analyzed using the t-test. Regional CGU data were analyzed with two-way (Time and Treatment) repeated measures analysis of variance (Systat, SPSS Inc., Chicago, Illinois, USA). Between-group difference was analyzed with adjusted degrees of freedom and mean square error followed by Bonferroni adjustment for multiple comparisons, whereas within-group post hoc comparison used Tukey's HSD test with Huynh-Feldt adjustment to the degree of freedom and mean square error (Howell, 1992).

Results

Physiological variables

Physiological variables did not differ between any CSD and sham treated groups, except that P_aO_2 during the [^{14}C]deoxyglucose studies was 96 ± 17 mmHg (n = 21) in the CSD treated group and 87 ± 5 mmHg (n = 21) in the sham treated group ($p < 0.05$). This difference originated from studies done on day 7 when P_aO_2 during the [^{14}C]deoxyglucose studies was 95 ± 5 mmHg (n = 7) in the CSD treated group and 88 ± 7 mmHg (n = 7) in the sham treated group ($p < 0.05$). The difference was not physiologically significant. Physiological variables were then averaged over both the CSD and sham groups and summarized in Table 7-1. The rectal temperature was 37.0± 0.3°C

(n = 42) during preconditioning and 37.1 ± 0.3°C (n = 42) during the regional CGU studies.

Table 7-1. Physiological variables during [^{14}C]deoxyglucose studies

Parameters	CSD treated (n = 21)	Sham treated (n = 21)
MABP (mm Hg)	116 ± 17	119 ± 19
pH	7.45 ± 0.03	7.46 ± 0.03
P_aCO_2 (mm Hg)	51 ± 4	52 ± 6
P_aO_2 (mm Hg)	96 ± 17*	87 ± 5
Blood glucose (mM)	5.53 ± 1.01	5.96 ± 1.15

Values are means ± SD. MABP, mean arterial blood pressure; MCA, middle cerebral artery; P_aCO_2, arterial partial pressure of carbon dioxide; P_aO_2, arterial partial pressure of oxygen. Spontaneous breathing under inhalational anesthesia during preconditioning, spontaneous breathing air during [^{14}C]deoxyglucose studies. Different from sham treated group: *P < 0.05.

Cortical spreading depression waves

Recurrent CSD waves during 2 hour of KCl application on the dura were recorded as a transient negative or biphasic DC potential shift. The average rate of CSD waves during preconditioning averaged over all CSD treated studies was 5.2 ± 1.5 h^{-1} (n = 21) with an amplitude of 6.3 ± 2.6 mV (n = 21) and a duration of 86.4 ± 13.1 second (n =21). In the sham group, no CSD waves were recorded.

Cerebral glucose utilization

The within cluster sum of squares declined most rapidly to 3 clusters (CSD, $F_{(1,19)} = 80.65$, $p = 0$; sham, $F_{(1,19)} = 22.42$, $p < 0.0005$) (Figure 7-1). Cortex 1 encompass the majority of the neocortex, whereas cortex 2 included mainly the parasagittal and the entorhinal cortex. Cortex 3 was strictly limited to the site of CSD or sham treatment and was excluded from further analysis (Figure 7-1). Two-way repeated measures analysis of variance on time (intervals after CSD or sham treatment) and treatment (CSD or sham) over six VOI (Ipsilateral: cortex 1, cortex 2 and striatum; Contralateral: cortex 1, cortex 2 and striatum) indicated that, between groups, regional CGU was significantly lowered in the CSD treated animals ($p = 0.027$). The effect of time was not significant. There was no significant interaction between time and treatment. Within subjects, there was significant variability across the VOI in the ratio of CGU ($p < 0.0001$); the degree of the variability was dependent on neither treatment, nor time. There was no interaction between the effect VOI with time and treatment. Within the contralateral hemisphere regional CGU did not differ within the cortical VOI. Pooled over all study groups the average CGU was 60 ± 8 μmol $100g^{-1}$ min^{-1} ($n = 42$) in the cortex and 63 ± 10 μmol $100g^{-1}$ min^{-1} ($n = 42$) in the striatum.

The average regional CGU images from day 7 after CSD or sham treatment are shown in Figure 7-2. The ratios of regional CGU in each VOI were calculated as the ipsilateral CGU / contralateral CGU and are summarized in Figure 7-3. Two-way repeated measures analysis of variance

on time (intervals after CSD or sham treatment) and treatment (CSD or sham) over three VOI (cortex 1, cortex 2 and striatum) indicated that, between groups, the ratio of regional CGU was significantly lowered in the CSD treated animals ($p < 0.02$). The effect of time was not significant. There was no significant interaction between time and treatment. The treatment effect was identified in cortex 1 ($p = 0.01$) and cortex 2 ($p = 0.02$), but not in striatum. Within subjects, there was significant variability across the VOI in the ratio of CGU ($p < 0.0001$); the degree of the variability was dependent on the treatment (CSD or sham) ($p = 0.001$), but not time. There was no interaction between the effect of VOI with time and treatment.

The ratio of regional CGU between CSD and sham treatment was also compared at individual time intervals studied (Figure 7-3). In cortex 1 the ratio at 24 hours did not significantly differ between CSD treated group (0.95 ± 0.08, $n = 7$), compared with the sham treated group (1.02 ± 0.04, $n = 7$). At 72 hours, the averaged ratio for the CSD treated group was 0.89 ± 0.10 ($n = 7$), compared with 0.98 ± 0.07 ($n = 7$) in the sham treated group ($p < 0.05$). On day 7 the ratio was reduced to 0.89 ± 0.07 ($n = 7$) in the CSD treated group compared with 0.99 ± 0.07 ($n = 7$) in the sham treated group in cortex 1 ($p < 0.001$) (Figure 7-3). In cortex 2, a similar trend was seen but the differences were not significant. In striatum no difference were identified.

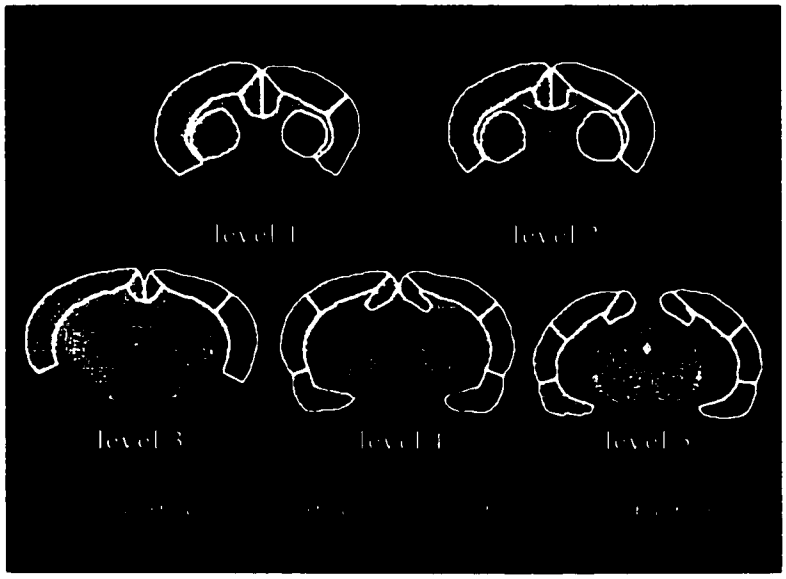

Figure 7-1. The region of interest (ROI) and volume of interest (VOI) template used to sample in vivo [^{14}C]deoxyglucose images after CSD or sham treatment. Five coronal levels in the rat brain are shown. The levels correspond to coronal sections from Bregma in mm at 1.20 (level 1), 0.20 (level 2), -3.30 (level 3), -5.60 (level 4), -6.30 (level 5). The ROI template is on the right side of the sections with lines to define ROI. The ROI groupings used to define the 4 VOI are on the left side of the sections and are labeled at the bottom of the figure..

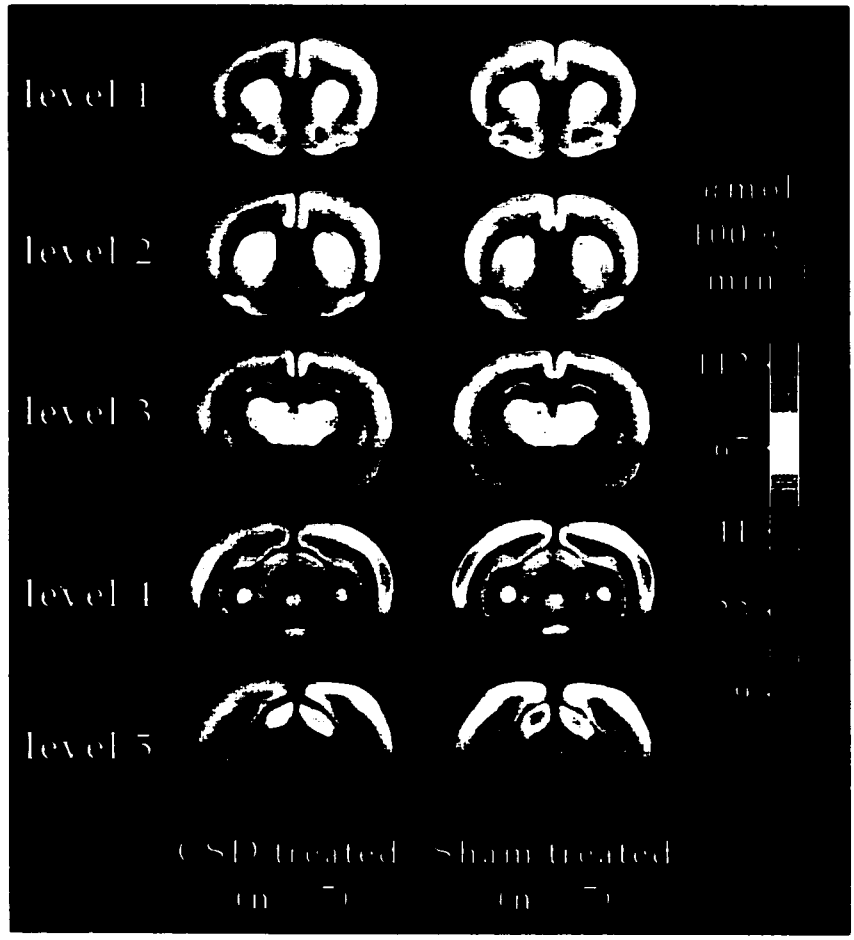

Figure 7-2. Average autoradiographic images of regional CGU on day 7 after CSD or sham treatments. The levels correspond to coronal sections from Bregma in mm at 1.20 (level 1), 0.20 (level 2), -3.30 (level 3), -5.60 (level 4), -6.30 (level 5). The treated hemisphere is on the left side of the sections. Calibrated colour scale is shown, as are the number of rats used to obtain each image. CGU, cerebral glucose utilization; CSD, cortical spreading depression

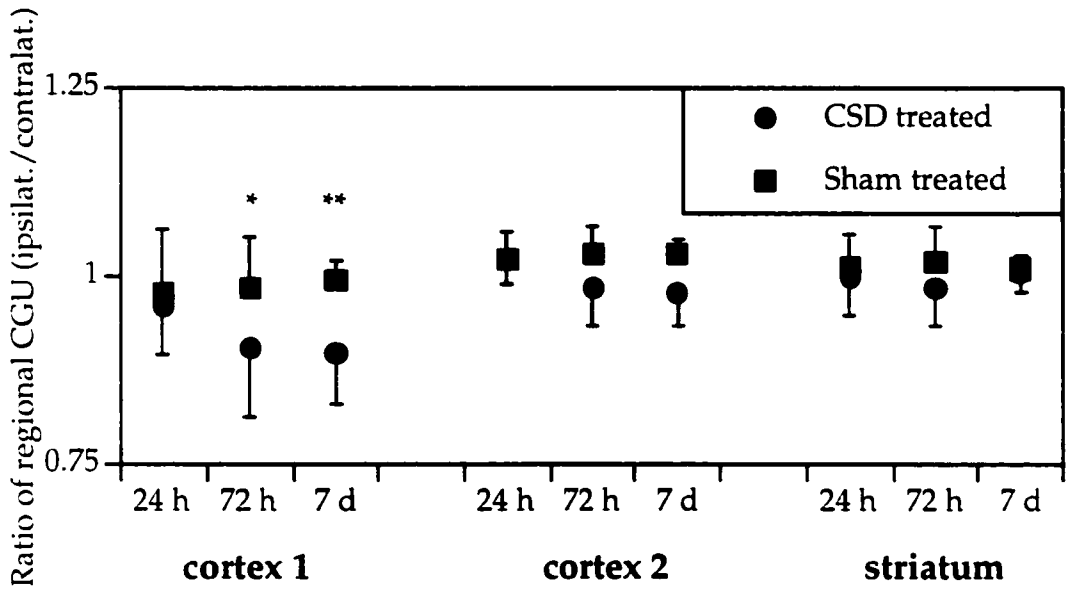

Figure 7-3. Ratio of regional CGU (Ipsilateral/Contralateral hemisphere) within volumes of interest (VOI) on day 1, 3 and 7 after CSD (n = 7) or sham (n = 7) treatment. All values are mean ± SD. Different between the CSD and sham treated groups: * $p < 0.05$, ** $p < 0.01$. CSD, cortical spreading depression; SD, standard deviation; d, days; h, hours.

Discussion

The regional CGU data indicated that after recurrent CSD preconditioning, there is a moderate decrease in metabolic activity in the neocortex. The reduction did not appear until day 3 and persisted on day 7 after the preconditioning. The striatum was not affected. The attenuation was less remarkable than that shown by others (Kawahara et al., 1994a; b). These investigators have indicated that CSD elicited on the neocortex produced delayed neural protection against the selective vulnerability in the hippocampus. However, our data indicate that regional CGU in the striatum and hippocampus is unlikely to be affected by CSD preconditioning.

Furthermore, the temporal profile of the regional CGU data indicated on day 1 after recurrent CSD preconditioning, ipsilateral regional CGU remained near the normal levels. On day 3 and 7 ipsilateral regional CGU was significantly lower in the CSD preconditioned cortex. In contrast, the reported findings showed that on day 7, the regional CGU returned to normal levels (Kawahara et al., 1994a; b). Nonetheless, our regional CGU data seem to agree with the suggestion that CSD treatment induces a lower level of energy consumption. A lower metabolic rate is certainly of benefit under ischemic conditions (Folbergrova et al., 1992). However, it does not seem to play a major role, since CSD-induced ischemic tolerance appears at 24 hours after the preconditioning (Barone et al., 1998; Kitagawa et al., 1990; Taga et al., 1997). Together with improved CBF response during an ischemic insult and other molecular changes, it is arguable that CSD induces a complex cellular functional modification that may underlie the induced ischemic tolerance.

During CSD regional CGU is markedly increased in most areas of the neocortex and reduced in many subcortical structures (Shinohara et al., 1979). During recovery, regional CGU remains elevated, but the increased metabolic activity runs in columns perpendicular through the cortex. Although increase neuronal firing and glial depolarization during CSD are non-functional, increases in glucose utilization still seem to be physiological (Magistretti and Pellerin, 1997; Magistretti et al., 1999). The hyperemia associated with CSD seem to be mediated, at least partially, by increased synaptic glutamate and activation of glutamate receptors (Fabricius et al., 1995;

Fabricius and Lauritzen, 1994). The increased glucose phosphorylation may not result only from increased synaptic glutamate, since a significant portion of lactate produced by CSD is not metabolized, but instead escapes to the venous blood (Cruz et al., 1999). Hypoperfusion immediately after CSD (Duckrow, 1991; Fabricius et al., 1995; Lauritzen et al., 1982) seems to uncouple CBF from regional CGU, which may indicate a different functional state of the cortex after CSD (Shinohara et al., 1979). Our regional CGU data indicated that regional CGU returns to normal (Lauritzen and Diemer, 1986) during a period when full cortical response to hypercapnia is not established (Florence et al., 1994; Lauritzen, 1984). Moreover, the regional CGU data from day 3 and day 7 after CSD preconditioning indicated that regional CGU undergoes a delayed reduction with stable cortical perfusion, even though the potential regional CBF response to ischemia may differ (Caggiano and Kraig, 1998).

Lower regional CGU in CSD preconditioned cortex is unlikely the result of degeneration caused by tissue depolarization during CSD treatment (Osuga et al., 1997) and associated glutamate release (Fabricius et al., 1993; Nedergaard and Hansen, 1988; Obrenovitch and Zilkha, 1995). However, measurements of glucose utilization have characterized the changes in metabolic rate during and after cerebral ischemia. There are two conditions that lead to lower regional CGU after ischemic induced neural toxicity: lower regional CGU due to acute or delayed neuronal cell death or, secondarily, due to loss of projection input (Beck et al., 1995). There are also intensely enhanced regional CGU before the delayed ischemic tissue injury, possibly

due to delayed neurotoxicity (Kataoka et al., 1989; Yao et al., 1995), and after the delayed decreases in regional CGU, due to enhanced microglial activity (Komatsumoto et al., 1989; Tanaka et al., 1985).

In summary, CSD preconditioning induced a delayed and mild reduction in regional CGU. The reduction is not the result of tissue degeneration but rather a reduction in tissue CGU levels. Since the onset of this reduction occurs later than the appearance of induced ischemic tolerance, it may not constitute the major protective mechanism of the CSD-induced ischemic tolerance. The onset of this reduction is also later than the downregulation of EAAT2 and 1 after CSD treatment, further suggesting that lower regional CGU plays a less important role in CSD-induced ischemic tolerance. Nonetheless a 10% reduction in energy consumption may provide some protection.

CHAPTER 8. CORTICAL SPREADING DEPRESSION DOWNREGULATES THE HIGH AFFINITY GLUTAMATE TRANSPORTER EAAT1 AND EAAT2 FROM RAT CORTICAL PLASMA MEMBRANES

Glutamate mediated synaptic transmission is terminated by electrogenic uptake via a family of high affinity excitatory amino acid transporters (EAAT) located on the astrocytic and neuronal plasma membranes (Rothstein, 1996; Rothstein et al., 1994). During cerebral ischemia extracellular glutamate rises due to increased vesicular release from the presynaptic terminal and reversed uptake through EAAT (Szatkowski and Attwell, 1994). However, glutamatergic vesicle cycling is ATP-dependent and only those fully primed and docked vesicles are capable of immediate Ca^{2+}-dependent release (Coorssen et al., 1998). Thus the presynaptic terminal may not be the main source of extracellular glutamate during cerebral ischemia (Rutledge and Kimelberg, 1996; Seki et al., 1999; Szatkowski and Attwell, 1994).

In the forebrain, three subtypes of EAAT have been identified. EAAT1 and EAAT2, also known as GLAST and GLT-1 respectively, are predominantly astrocytic, while EAAT3 is mainly present within neurons (Conti et al., 1998; Mennerick and Zorumski, 1994; Rothstein et al., 1996). Knockout studies have indicated that EAAT1 and EAAT2, but not the neuronal EAAT3, are responsible for the majority of glutamate clearance in the cerebral cortex (Rothstein et al., 1996). Moreover, the abundance of

EAAT1 and EAAT2, but not EAAT3, seems to be subject to relatively fast regulation (Ginsberg et al., 1995; Raghavendra Rao et al., 1998; Rothstein, 1996). Downregulation of both EAAT1 and EAAT2 has been observed in crude homogenates following regional deafferentation within the rat cerebral cortex (Ginsberg et al., 1995) and traumatic cortical injury induced by controlled impact (Raghavendra Rao et al., 1998).

Direct measurement of extracellular glutamate concentration demonstrated that CSD preconditioning significantly decreased glutamate exposure in ischemic cerebral cortex (Douen et al., 2000). Reduced exposure to glutamate during cerebral ischemia would be consistent with the hypothesis that attenuated glutamate-mediated neurotoxcity is involved in CSD-induced ischemic tolerance. Since EAAT reverse uptake during cerebral ischemia (Rutledge and Kimelberg, 1996; Seki et al., 1999; Szatkowski and Attwell, 1994), the modulation of plasma membrane glutamate transporters may underlie the observed reduction in glutamate exposure during cerebral ischemia in animals preconditioned with CSD. The immunoprotein analysis was undertaken to assess the effect of CSD on the abundance of EAAT2, EAAT1 and EAAT3 proteins in plasma membrane extracted from rat cerebral cortex, using the same paradigm shown to induce ischemic tolerance. We observed a significant decrease in EAAT1 and EAAT2, but not EAAT3, immunoreactivity in a plasma membrane fraction extracted from the cerebral cortex of CSD treated cortex, indicating CSD preconditioning downregulated EAAT2 and EAAT1 from plasma membrane. We subsequently explored the

time course for EAAT2 downregulation after CSD and observed a delayed, transient decrease in EAAT2 from the plasma membrane fraction that was evident on day 1 after CSD and more pronounced on day 3. This downregulation persisted for at least 7 days before returning to baseline levels.

Material and Methods

Experimental animals and surgical anesthesia were identical to those employed in Chapter 3. CSD was induced from the left occipital cortex with 0.5 M KCl as described in Chapter 3. The posterior electrode was not used. Rats were allowed to breathe spontaneously during CSD preconditioning. Body temperature (rectal) was maintained at 36.5 - 37.5°C in all in vivo studies. Immunoprotein analysis of EAAT was performed on day 0, day 1, day 3, day 7 and day 21, after CSD preconditioning (n = 3 at each time intervals). Rats from day 3 following sham treatment (n = 3) were used as controls.

Reagents

Phenylmethanesulfonyl fluoride (PMSF), Tris-HCl, sodium dodecyl sulfate (SDS), urea and dithiothreitol were purchased from Sigma (St. Louis, Missouri, USA). TEMED, Tween 20, acrylamide, bisacrylamide, ethylene diamine tetraamine (EDTA), glycine, nitrocellulose paper and protein assay kit were purchased from Biorad (Hercules, California, USA). Enhanced chemoluminescence kit was purchased from Amersham (Buckinghamshire,

England, UK). All other bench chemicals were purchased from Sigma and were analytical grade. Monoclonal antibodies to the Na^+,K^+-ATPase α1 subunit, polyclonal antibodies to EAAT2 and polyclonal antibodies to glial fibrillary acidic protein were purchased from Affinity Bioreagents (Golden, Connecticut, USA). Polyclonal antibodies to EAAT1 and EAAT3 were supplied by Dr. J. D. Rostwin. Secondary antibodies were purchased from Transduction Laboratories (Lexington, Kentucky, USA).

Cell membrane fractionation

Extraction of a plasma membrane enriched fraction from cerebral cortex was achieved through modification of subcellular fraction techniques previously established in fatty tissue (Douen et al., 1988) and skeletal muscles (Douen et al., 1991), in which differential centrifugation and discontinuous sucrose density gradient centrifugation were used. At predetermined time intervals after CSD or sham treatment the rats were decapitated and the brains were rapidly removed and placed in ice cold saline. All remaining procedures were conducted at 4°C. Visible pial vessels were removed; ipsilateral and contralateral cortices were dissected from subcortical structures. Cortices were homogenized at 500 rpm in 10 mL of 10 mM $NaHCO_3$ - 0.1 m M PMSF buffer at pH 7.0 with 10 strokes of a Teflon pestle in a Wheaton glass homogenizer. The homogenizer was rinsed with 10 mM $NaHCO_3$ - 0.1 m M PMSF buffer, and these washings combined with the homogenized sample to yield a final volume of up to 20 mL. After removing an aliquot of 1 mL for

subsequent analysis, the crude homogenate was spun at 30,000 g for 30 minutes to yield a pellet and a supernatant. The pellet was resuspended in 10 mL of 10 mM $NaHCO_3$ - 0.1 mM PMSF buffer. The suspension was then layered onto 5.5 mL of ice cold 35% sucrose solution (35 g sucrose in 100 mL 10 mM $NaHCO_3$ - 0.1 mM PMSF buffer) in 12 mL Beckman ultracentrifuge tubes. Samples were centrifuged at 150,000 g for 2 hours in a Beckman titanium SW 41 swing bucket rotor. The membrane fraction at the interface was harvested, washed and resuspended in 10 mL of 10 mM NaHCO3 - 0.1 mM PMSF buffer and precipitated by centrifugation at 200,000 g for 1 hour. The precipitated membranes were resuspended in 10 mM $NaHCO_3$ - 0.1 mM PMSF buffer and stored at -80°C. The supernatant was spun at 200,000 g for 2 hours to yield a non-plasma membrane fraction. Protein was determined by Bradford's coomassie blue method (Bradford, 1976) using Biorad's protein determination kits.

Detection of plasma membrane

Immunoprotein analysis using monoclonal antibody to the plasma specific Na^+,K^+-ATPase $\alpha 1$ subunit was used to identify the presence of plasma membrane as previously reported (Marette et al., 1992).

Immunoprotein analysis

Equivalent amounts of membrane protein (0.05, 0.1, or 0.2 µg per sample) were subjected to SDS polyacrylamide gel electrophoresis on 10% polyacrylamide gels according to Laemmli (Laemmli, 1970). The membrane

protein was then transferred to nitrocellulose filter membrane for 2 hours. The nitrocellulose membrane was incubated for 1 hour at room temperature with phosphate buffered saline containing 0.1 % tween-20 at pH 7.2 and then blocked for 3 hours with phosphate buffered saline containing 0.1% tween-20 and 5% skimmed milk. Nitrocellulose membranes were incubated overnight with primary antibody at 4°C followed by 4 washes with phosphate buffered saline containing 0.1% tween-20 and then incubated with secondary antibody for 3 hours at room temperature. After 2 washes with phosphate buffered saline the nitrocellulose membrane was exposed to the enhanced chemoluminescence solutions for 1 minute, and apposed to Hyperfilm (Amersham International Plc, England, UK) for 1, 5, 15 and 30 seconds. Immunoblot analysis for each sample was conducted in duplicate or triplicate.

Lane analysis

A semi-quantitative analysis was performed using the MCID system. The Hyperfilm immunoreactive bands, visualized with the enhanced chemoluminescence, were digitized and the band intensities calculated as the product of the increased average relative optical density and the area of the band measured. The ratio of band intensities from samples obtained from the ipsilateral (received CSD or sham treatment) over the contralateral (no treatment) cortex was calculated.

Statistical analysis

All results are expressed as mean ± SD. The physiological data were analyzed using the two-sample t-test. Lane analysis data were analyzed with the two-sample t-test or one-way analysis of variance followed by post hoc comparison using Tukey's HSD (Systat, SPSS Inc., Chicago, Illinois, USA).

Results

Physiological variables

Physiological variables did not differ between any CSD and sham treated groups. All physiological variables were then averaged over both the CSD and sham treated groups and are summarized in Table 8-1. The rectal temperature was 36.9 ± 0.3°C (n = 18) during preconditioning.

Table 8-1. Physiological variables for immunoprotein analysis of EAAT

Parameters	Preconditioning
MABP (mm Hg)	90 ± 8
pH	7.39 ± 0.03
P_aCO_2 (mm Hg)	51 ± 4
P_aO_2 (mm Hg)	208 ± 32
Blood glucose (mM)	6.33 ± 0.61

Values are means ± SD; n = 18. MABP, mean arterial blood pressure; P_aCO_2, arterial partial pressure of carbon dioxide; P_aO_2, arterial partial pressure of oxygen. Spontaneous breathing under inhalational anesthesia during preconditioning.

Cortical spreading depression waves

Recurrent CSD waves during 2 hours of KCl application on the dura were recorded as a transient negative or biphasic DC potential shift. The average rate of CSD during preconditioning average over all CSD treated studies was 5.7 ± 1.1 h^{-1} (n = 15) with an amplitude of 8.8 ± 3.8 mV (n = 15) and a duration of 84.2 ± 9.6 second (n = 15). No CSD was recorded in sham treated studies.

Characterization of plasma membrane enriched fraction

Identification of plasma membrane enriched fractions by immunodetection of the plasma membrane specific Na^+,K^+-ATPase α1 subunit has been found to be at least three times more sensitive than biochemical techniques (Marette et al., 1992). Na^+,K^+-ATPase α1 subunit monoclonal antibodies readily detected the 110 KD band of this protein in the 35% sucrose fraction compared to minimally detectable levels in the crude homogenate (Figure 8-1), confirming the ability of the fractionation technique to isolate a plasma membrane enriched fraction.

There was no significant difference in the ratio of ipsilateral / contralateral cortex Na^+,K^+-ATPase α1 subunit levels in plasma membrane prepared from CSD treated (0.70 ± 0.25, n = 3) versus sham treated (0.81 ± 0.23, n = 3) animals, indicating that CSD did not alter the enrichment of the plasma membrane fractions. Quantification of this enrichment yielded values in excess of 40-fold. However, these values may be inflated as in some blots

Na^+,K^+-ATPase α1 subunit was undetectable in the crude homogenate compared with a robust response in the 35% sucrose fraction.

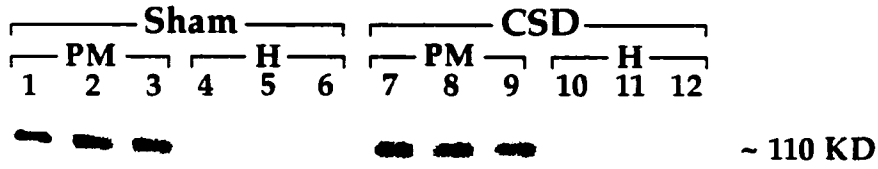

Figure 8-1. Comparison of the distribution of the plasma membrane specific Na^+,K^+-ATPase α1 subunit in plasma membrane enriched fraction and crude homogenate from two selected studies representing CSD or sham treated groups on day 3 after treatment. Membranes (2.5 μg) were prepared from ipsilateral cortex on day 3 after CSD or sham treatment. Immunoassay was performed in triplicate using antibodies to Na^+,K^+-ATPase α1 subunit. CSD, cortical spreading depression; PM, plasma membranes enriched fraction; H, crude homogenate.

Immunoprotein blot analysis of EAAT

The presence of EAAT2 in the membrane fractions prepared on day 7 after CSD was first studied, using the same paradigm previously shown to impart neuroprotection against focal ischemia (Matsushima et al., 1998). On day 3 after CSD treatment there was marked reduction in EAAT2 levels in the plasma membrane enriched fraction from the ipsilateral (CSD treated) cortex compared with the contralateral (not treated) cortex (Figure 8-2). However, a concomitant decrease in EAAT2 from crude homogenate extracts corresponding to the CSD treated cortex was not observed (Figure 8-2). There was no difference in the EAAT2 in the plasma membrane enriched fractions prepared from the ipsilateral and contralateral cortex of the sham animal and

the contralateral (not treated) cortex of the CSD treated animal (Figure 8-2). These observations were corroborated by the semi-quantitative lane analysis (Figure 8-3). In the plasma membrane enriched fraction, ipsilateral / contralateral ratio of EAAT2 was 0.17 ± 0.10 (n = 3) for CSD treated animals, compared with 1.05 ± 0.18 (n = 3) for sham treated animals. The difference represents a greater than 80% reduction in detectable EAAT2 signal in the plasma membrane enriched fraction from CSD treated cortex ($p = 0.004$). By comparison, the ipsilateral / contralateral ratio of EAAT2 levels in the crude homogenate for CSD and sham treatment were 0.97 ± 0.47 (n = 3) and 1.10 ± 0.01 (n = 3), respectively. Subsequently the temporal profile for CSD mediated downregulation of EAAT2 in plasma membrane enriched fraction was determined (Figure 8-4). Downregulation of EAAT2 in plasma membrane enriched fraction was not observed until 24 hours after CSD and persisted for a week with the maximal effect occurring on day 3. CSD did not decrease EAAT2 content within the crude homogenate fractions at any time.

Similarly, on day 3 after CSD treatment there was also a significant reduction in EAAT1 levels in plasma membrane enriched fraction from the ipsilateral (CSD treated) cortex compared with the contralateral (not treated) cortex (Figure 8-2). A significant decrease in EAAT1 from crude homogenate was not observed. These observations were confirmed by the semi-quantitative lane analysis (Figure 8-3). In the plasma membrane enriched fraction, ipsilateral / contralateral ratio of EAAT1 was 0.58 ± 0.07 (n = 3) for CSD and 1.10 ± 0.09 (n = 3) for sham treated animals. The difference

represents a 45% reduction in detectable EAAT1 signal in the plasma membrane enriched fraction of the CSD treated cortex ($p = 0.001$). In contrast, the ipsilateral / contralateral ratio of EAAT1 levels in the crude homogenate for CSD and sham treatment were 1.16 ± 0.58 ($n = 3$) and 0.97 ± 0.13 ($n = 3$), respectively.

However, on day 3 after CSD treatment, no reduction of EAAT3 was observed in either the plasma membrane or crude homogenate fractions (Figure 8-2). The ipsilateral / contralateral ratio of EAAT3 in the plasma membrane enriched fraction for CSD and sham treated animals were 1.02 ± 0.17 ($n = 3$) and 1.10 ± 0.45 ($n = 3$) respectively (Figure 8-3). The ipsilateral / contralateral ratio of EAAT3 levels in the crude homogenate for CSD and sham treatment were 0.87 ± 0.32 ($n = 3$) and 1.05 ± 0.09 ($n = 3$), respectively.

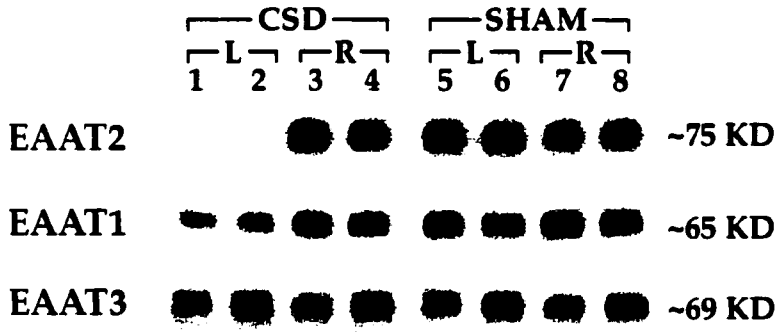

Figure 8-2. Immunoblots of EAAT2, EAAT1 and EAAT3 glutamate transporters in plasma membrane enriched fractions from two selected studies representing CSD or sham treated groups on day 3 after treatment. Membranes (1 μg) were immunoassayed in triplicate or duplicates using antibodies against the EAAT2, EAAT1 and EAAT3 proteins. CSD, cortical spreading depression; EAAT, excitatory amino acid transporter; L, left cortex (ipsilateral); PM, plasma membrane enriched fraction; R, right cortex (contralateral).

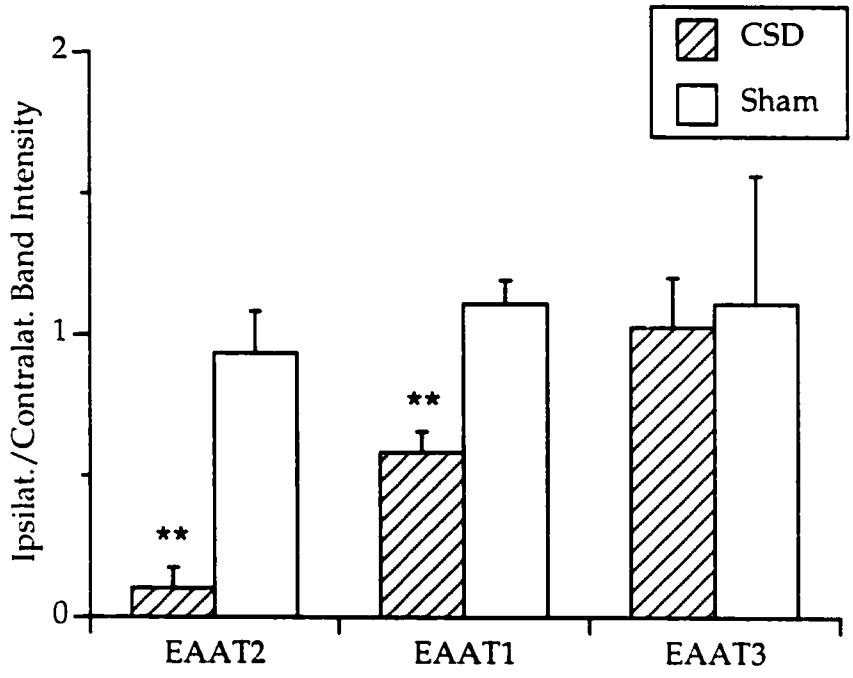

Figure 8-3. Semi-quantitative lane analysis of the ratio of the ipsilateral / contralateral cortex band intensities of EAAT2, EAAT1 and EAAT3 antibody binding in the plasma membrane enriched fractions. Autoradiographs were digitized and the intensities of each lane were analyzed. Data indicate mean ± SD (n = 3 in each group). CSD, cortical spreading depression; EAAT, excitatory amino acid transporter.

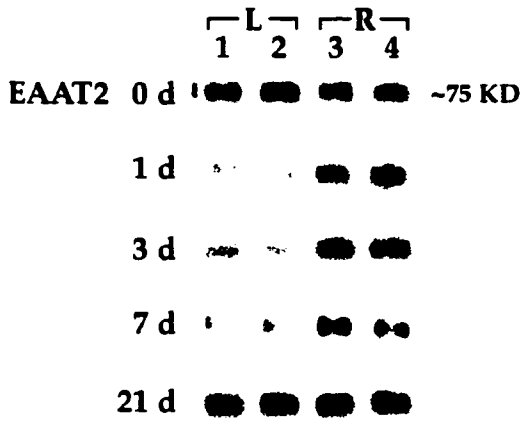

Figure 8-4. Time course for the downregulation of EAAT2 from plasma membrane enriched and homogenate fractions from selected studies. Membranes (1 μg) were immunoassayed in duplicate. L, left cortex (ipsilateral); R, right cortex (contralateral). Blots labeled with 1 d, 3 d, 7 d and 21 d represent the time elapsed after CSD treatment. Studies conducted immediately following 2 hours of CSD treatment is labeled as 0 d.

Discussion

CSD had no immediate effect on the presence of EAAT2 within plasma membrane. However, the immunoprotein analysis data indicated that on day 3 after CSD preconditioning, there was a significant downregulation of the astrocytic EAAT2 and, to a lesser degree, EAAT1 in the plasma membranes. Temporal data demonstrated that this downregulation appeared before day 1 and returned to normal levels before day 21 for EAAT2. However, EAAT3, the neuronal glutamate transporter, was not changed. These observations corroborate well with the observation that CSD preconditioning attenuates glutamate exposure in focal ischemic tissue

(Douen et al., 2000). The observed downregulation also appears to agree with the report that EAAT are developmentally and functionally regulated (Ginsberg et al., 1995; Raghavendra Rao et al., 1998; Rothstein, 1996; Rothstein et al., 1996). EAAT mediates most of the functional glutamate uptake (Rothstein, 1996; Rothstein et al., 1996; Rothstein et al., 1994), which couples the glutamine synthase activity with the phosphorylation of intracellular glucose (Magistretti et al., 1999). It is therefore hypothesized that downregulation of EAAT represents a molecular response to the large-scale reversal of glutamate uptake by EAAT during recurrent CSD treatment and is responsible to the lower regional CGU in the CSD preconditioned neocortex.

In contrast, CSD did not alter the plasma membrane protein Na^+,K^+-ATPase (Figure 8-1), suggesting that the effect of CSD on downregulation of plasma membrane EAAT2 is a specific response. This delayed, transient effect of CSD on plasma membrane EAAT2 coincide with the delayed neuroprotection (Kawahara et al., 1995; Matsushima et al., 1996; Matsushima et al., 1998). In addition, the observed transient downregulation of the astrocytic EAAT (Figure 8-2) is consistent with the observation that controlled cortical impact-induced traumatic brain injury transiently down regulates both astrocytic glutamate transporters (Raghavendra Rao et al., 1998). In that study, uncharacterized plasma membrane fraction was obtained from crude cortical homogenate. The membrane fraction represents neither the total crude homogenate nor purified plasma membranes. However it more than likely contains plasma membranes in addition to other membrane

components. Nevertheless, these researchers showed that although EAAT2 and EAAT1 were not immediately affected by traumatic brain injury, within 6 hours following cortical injury there was significant downregulation of these transporters, which persisted for at least 3 days and recovered by day seven. These authors speculated that downregulation of glial EAAT could decrease glutamate clearance and promote excitotoxicity. However, CSD-mediated downregulation of EAAT2 is concordant with the time frame reported for CSD-induced neuroprotection (Kawahara et al., 1995; Matsushima et al., 1996). Since both CSD-induced neuroprotection and downregulation of EAAT2 occur at the same time, it seems unlikely that EAAT2 downregulation would promote excitotoxicity. However, if reversal of EAAT contributes to excessive extracellular glutamate release during ischemia as reported (Nicholls and Attwell, 1990; Szatkowski and Attwell, 1994), downregulation of EAAT following CSD preconditioning would decrease the number of transporters present in the plasma membranes. The downregulation would presumably mean less EAAT available for efflux of glutamate during ischemia. Thus, downregulation of glutamate transporters may be one mechanism by which CSD preconditioning promotes neuroprotection.

Under normal conditions one would expect that reduction of EAAT from the plasma membrane would reduce glutamate clearance and promote excitotoxicity. This notion led some investigators to speculate that transient downregulation of EAAT following traumatic brain injury leads to glutamate induced susceptibility to excitotoxicity (Raghavendra Rao et al., 1998),

although these researchers did not measure intracerebral glutamate levels. Nonetheless, this may be a reasonable assumption, since trauma has previously been reported to induce waves of spreading depression (Hossmann, 1996). Hence downregulation of glial EAAT following cortical impact injury may be a CSD-induced phenomenon rather than a direct consequence of trauma. Controlled cortical impact injury produces localized tissue injury, likely mediated by excitotoxicity (Raghavendra Rao et al., 1998). Whether it induces ischemic tolerance is unknown. The resulting increase in extracellular glutamate may serve to activate synaptic glutamate receptors (Cochilla and Alford, 1999; Conn and Pin, 1997), as well as glutamate receptors on presynaptic and astrocytic membranes. The suggestion is supported by the findings that CSD preconditioning attenuates tissue depolarization, which may result from less glutamate activation during subsequent ischemic insult. It is further supported by the findings that, after CSD preconditioning, the regional CGU is reduced in the neocortex on day 3 and day 7.

Other mechanisms may participate in CSD-induced synaptic glutamate control. It has been previously suggested that a tonic rise in synaptic glutamate levels, potentiated through the blockade of glutamate transporters using L-trans-2,4-pyrrolidine dicarboxylic acid (transPDC), leads to a reduction in presynaptic glutamate release via activation of metabotropic glutamate receptors (Maki et al., 1994). Others have shown that excitatory postsynaptic potentials can be manipulated by agonists or antagonists of specific presynaptic mGluR, suggesting a role of mGluR as autoreceptors controlling

glutamate release (Ikeda, 1996). The NMDA receptor has also been identified in the presynaptic membrane suggesting presynaptic release can be modulated directly through Ca^{2+} influx through NMDA receptor channels (Cochilla and Alford, 1999; Schwartz and Alford, 1998). In addition, whereas astrocytes clearly lack AMPA and kainate receptors, both NMDA and mGluR receptors have been located on the astrocyte membranes (Barres, 1991). Hence, it is possible that downregulation of plasma membrane EAAT induced by CSD treatment represents a reduction in glutamate uptake under normal conditions and a reduction in the reversal of glutamate uptake during cerebral ischemia.

In contrast to the reduction in plasma membrane EAAT1 and EAAT2 following CSD pretreatment, these proteins remained unaltered in the crude homogenate fractions. This specific downregulation may indicate that the total cellular levels of EAAT2 and EAAT1 are unaffected. Without morphological information, the mechanism of the specific downregulation can be only speculated on. Since the total protein of EAAT2, EAAT1 and EAAT3 in the crude homogenate did not change, it is rather unlikely that increased degradation or impaired synthesis led to the specific downregulation. It seems reasonable to explore the possibility of subcellular redistribution from plasma membranes to an intracellular compartment. Thus, the observed decrease in EAAT2 and EAAT1 in the intracellular membrane fraction needs to be further studied.

In summary, the immunoprotein analysis data show that CSD induces a delayed and transient downregulation of EAAT2 and EAAT1 but not EAAT3 in the plasma membrane. This specific downregulation was maximum on day 3 after CSD preconditioning, coinciding with the neuroprotective effect of CSD (Kawahara et al., 1995; Matsushima et al., 1996). Since glutamate clearance through EAAT is the coupling mechanism between synaptic activity and glucose utilization, a concurrent downregulation of astrocytic EAAT and reduction of regional CGU in the neocortex is expected.

Although chronic downregulation of EAAT has been demonstrated to be associated with decreased glutamate clearance and neurotoxicity, the mechanisms underlying the downregulation are different. Thus, biological effects mitigated through an acute transient decrease in astrocytic EAAT would be different from those of chronic depletion of this transporter. Membrane depolarization and ionic perturbation occurring during cerebral ischemia trigger presynaptic glutamate release and reversal of glutamate flux through EAAT. Reduction of EAAT present in the plasma membranes could potentially decrease the reversed uptake of glutamate during cerebral ischemia. These data support the hypothesis that downregulation of EAAT induced by CSD preconditioning contributes to the state of increased ischemic tolerance.

CHAPTER 9. GENERAL DISCUSSION

Ischemic tolerance induced by CSD is a well-established phenomenon in both focal and global ischemic models (Kawahara et al., 1995; Kobayashi et al., 1995; Matsushima et al., 1996; Taga et al., 1997; Yanamoto et al., 1998). CSD induced ischemic tolerance was first confirmed in our laboratory in a focal ischemic model produced with the intraluminal occlusion of the MCA. Recurrent CSD cause tissue depolarization (Osuga and Hakim, 1996; Osuga et al., 1997) that increases extracellular glutamate (Lauritzen, 1992; Marrannes et al., 1988; Nedergaard et al., 1995). Consequently, the activation of glutamate receptors may lead to a series of signaling events that alter tissue response to subsequent ischemic insults. Consistent with these reports, [^{3}H]dizocilpine in vivo distribution, an indicator of glutamate-induced NMDA receptor activation, was identified in cortex both after a single CSD and during 1 hour of recurrent CSD (Schwartz and Wasterlain, 1993; Wallace et al., 1992).

To understand underlying physiological events that constitute ischemic tolerance, we hypothesized that prior CSD preconditioning attenuated ischemic excitotoxicity, which is initiated by energy failure and mediated by the excessive increases in extracellular glutamate. To address this hypothesis, we studied the regional CBF in CSD preconditioned tissue using [^{14}C]IAP autoradiography at 3 hours of focal ischemia. Cerebral [^{3}H]nimodipine in vivo distribution was used to study the state of tissue depolarization and infer VSCC activation (Hakim and Hogan, 1991; Hogan et

al., 1991; Hogan and Hakim, 1992; Takizawa et al., 1994). Cerebral [^{3}H]dizocilpine in vivo distribution was used to indicate the opening of NMDA receptor Ca^{2+} channels and to infer intra-ischemic glutamate release (Schwartz and Wasterlain, 1993; Wallace et al., 1992). [^{3}H]Nimodipine and [^{3}H]dizocilpine in vitro binding was performed to test whether the binding kinetics of VSCC and NMDA receptors were altered by CSD preconditioning, since the alteration of VSCC and NMDA receptor would be reflected in the response of in vivo activation during ischemic injury.

Our data demonstrated that in the regions outside of the ischemic core, including the periinfarct and non-ischemic cortex, CBF was significantly higher in the CSD preconditioned cortex than that in the sham treated cortex. Cortical [^{3}H]nimodipine in vivo distribution was attenuated in the ischemic core in the CSD preconditioned cortex. In the identical region in the [^{14}C]IAP studies, regional CBF was found to be increased. Cortical [^{3}H]dizocilpine in vivo distribution was not significantly altered but the data suggested a trend in which [^{3}H]dizocilpine distribution was decreased in a region outside the ischemic core in the CSD preconditioned cortex, but higher in the ischemic core. The total binding capacity for [^{3}H]nimodipine was increased in the sham treated cortex whereas this increase was absent in the CSD preconditioned cortex. [^{3}H]Dizocilpine in vitro binding capacity and affinity were unaltered by CSD preconditioning. Furthermore, we measured regional CGU after CSD treatment. The ratio of regional CGU decreased on day 3 and 7 after CSD treatment, indicating that preconditioning reduced the rate of glucose

metabolism. Moreover, we semi-quantified astrocytic and neuronal EAAT with immunoblotting following CSD preconditioning. We found a transient downregulation of astrocytic EAAT1 and EAAT2, but not neuronal EAAT3. These findings corroborate well with the observation that regional CGU in the majority of neocortex were reduced.

These results were discussed individually in detail in their respective chapters. To summarize these results, more discussion is presented to illustrate the multiplicity and complexity of the CSD-induced ischemic tolerance. Although these individual observations may contribute to the CSD-induced ischemic tolerance, the mechanisms are inseparable. Since CSD preconditioning induces activation of glutamate receptors, which are associated with some of the mechanisms, the role of increased extracellular glutamate induced by CSD depolarization in triggering a wide range of signal cascades warrants further investigation.

CSD-induced ischemic protection involves multiple mechanisms

The multiplicity of the CSD-induced ischemic tolerance includes attenuated tissue depolarization in the ischemic core, as well as improved regional blood flow in the periinfarct and non-ischemic region. [^{3}H]Nimodipine in vivo distribution was attenuated in the ischemic core. As an indicator of tissue depolarization, persistent increases in regional [^{3}H]nimodipine in vivo distribution maps impending ischemic injury by identifying regions of tissue depolarization and increased VSCC activation. Therefore, attenuation of [^{3}H]nimodipine in vivo distribution suggests

reduced tissue depolarization and reduced threat of tissue injury. In vitro [^{3}H]nimodipine binding indicated that this attenuation is unlikely to be the result of significant changes in the VSCC binding characteristics.

The significance of [^{3}H]dizocilpine in vivo distribution data can be speculated in terms of the effect of CSD preconditioning. Two regions of interest were identified with the difference template approach. In a region corresponding to the periinfarct region there was a tendency of decreased [^{3}H]dizocilpine accumulation, whereas in the ischemic core there was a tendency of more [^{3}H]dizocilpine accumulation. We speculate that these patterns of [^{3}H]dizocilpine accumulation may indicate a trend of decreased extracellular glutamate in the periinfarct region. The trend of an increase in the ischemic core is not clear (Chapter 5). [^{3}H]Dizocilpine in vitro binding indicated that CSD preconditioning altered neither the NMDA binding capacity nor affinity, suggesting that downregulaiton of NMDA receptor was not a mechanism of neuroprotection. The [^{3}H]dizocilpine in vitro binding data further supported the notion that the trend of lower [^{3}H]dizocilpine in vivo distribution may suggest less accumulation of glutamate in the periinfarct region.

Regional CBF measurement at 3 hours of ischemic insult indicated that the cerebral perfusion was better maintained in the periinfarct and non-ischemic region. Increased neuronal NOS activity may play a key role in the improvement of cerebral perfusion after CSD preconditioning (Caggiano and Kraig, 1998), even though other mechanisms are possible (Chedotal et al.,

1994; Markowitz and Moskowitz, 1986; Moskowitz, 1984). Increased NO synthesis may be mediated by the opening of NMDA Ca^{2+} channels in neurons (Zhang and Snyder, 1995) and by mGluR activation in astrocytes (Agullo and Garcia, 1992). NO synthesis is triggered mainly in tissue surrounding the ischemic core since NO production requires energy (Zhang and Snyder, 1995). Although it has been believed that uncontrolled release of NO could exacerbate the ischemic injury through free radical production while providing limited relief in ischemia, recent evidence showed that the role of NO in ischemic injury depends on the location of its production. It has been demonstrated that in the periinfarct region the turnover of citrulline was high, indicating increased NO production, whereas the production of 3-nitrotyrosine was restricted in the ischemic core, indicating increased production of the free radical peroxynitrite (Eliasson et al., 1999). The observation that higher CBF appears in the periinfarct and the non-ischemic cortex is consistent with the understanding NO turnover is increased in the periinfarct region but not in the ischemic core (Eliasson et al., 1999). These observations strongly support the idea that in the CSD preconditioned cortex increased neuronal NOS expression in the astrocytes provides protection against the ischemic insult.

We observed about 10% reduction in regional CGU in the CSD preconditioned cortex on day 3 and 7 after CSD, but not on day 1, suggesting that the onset of lower CGU after CSD preconditioning is more delayed than the appearance of ischemic protection (Kato et al., 1991; Taga et al., 1997). The

lag between the appearance of CSD-induced neuroprotection and the attenuation of regional CGU may indicate that attenuation of regional CGU is not essential to CSD-induced neuroprotection, although a reduced metabolic rate may be of considerable benefit.

Coinciding with the first appearance of CSD-induced ischemic tolerance, EAAT2 downregulation started on day 1 after CSD, persisted through day 3 and 7, and returned to the control levels on day 21. Though EAAT bind and transport extracellular glutamate intracellularly, the transporters can be reversed under ischemic conditions when extracellular K^+ is increased and energy metabolism is restricted (Kimelberg et al., 1995; Obrenovitch et al., 1996; Rutledge and Kimelberg, 1996; Seki et al., 1999). Thus, reduction in the astrocytic EAAT may reduce the number of sites available for glutamate leakage through EAAT, attenuating the increases in extracellular glutamate and the acute ischemic tissue injury (Choi, 1988a; Choi, 1988b; Choi et al., 1988; Rothman, 1985). However the reversal of EAAT is restricted by extracellular pH (Billups and Attwell, 1996). As the extracellular pH decreases the leakage of intracellular astrocytic glutamate through EAAT eventually ceases (Billups and Attwell, 1996). Furthermore, EAAT function in two discrete steps. Glutamate binds EAAT within 10 milliseconds whereas the transmembrane transportation takes 5 - 10 times longer (Bergles et al., 1997). Thus, for instant clearance of glutamate in the synaptic cleft, a relatively large pool of EAAT is necessary. Severe shortage of EAAT1 and EAAT2 lead to increased extracellular glutamate levels,

neurodegeneration characteristic of excitotoxicity, and a progressive functional deficit (Rothstein et al., 1996). Chronic downregulation of EAAT is associated with many neural degenerative diseases (Robinson and Dowd, 1997).

The multiple protective mechanisms are linked

The complexity of CSD-induced ischemic tolerance is illustrated by the close correlation of the protective mechanisms studied. Improved regional CBF in the periinfarct region may result from the activation of neuronal NOS which is dependent on the Ca^{2+} influx associated with the activation of NMDA receptors and VSCC (Zhang and Snyder, 1995). The activation of calmodulin by increased intracellular Ca^{2+} is required in the activation of NO synthesis (Zhang and Snyder, 1995). However, it is noteworthy that the regional CBF was higher in the ischemic core where [^{3}H]nimodipine in vivo distribution was found to be significantly attenuated. This attenuation of [^{3}H]nimodipine in vivo distribution in the ischemic core may therefore result from improved blood flow (Chapter 5), in addition to lower excitotoxicity (Chapter 8) and lower metabolic rate in CSD preconditioned cortex (Chapter 7) (Folbergrova et al., 1992).

Alternatively, it is also conceivable that increased regional CBF was the result of improved viability of the brain tissue, suggesting that the production of free radical peroxynitrite was reduced in favour of increased NO turnover by CSD preconditioning in the ischemic core (Eliasson et al., 1999). The brain tissue must be able to prevent the formation of peroxynitrite for the beneficial

effect of NO to take place (Eliasson et al., 1999). Increased ischemic tolerance may be associated with the increased capability to handle NO. Thus, the improved CBF in the ischemic core would be a sign of tissue viability due to other factors, such as improved energy metabolism and reduced excitotoxic injury, as indicated by the attenuated [^{3}H]nimodipine in vivo distribution. On the other hand, the ability to prevent peroxynitrite formation was damaged and the benefits of increased presence of NO was lost in the sham treated brain (Eliasson et al., 1999).

Downregulation of EAAT may lead to the attenuation of the increases in extracellular glutamate. Attenuated ischemic tissue depolarization observed at 3 hours of focal ischemia in the CSD preconditioned rats may represent the effect of less glutamate exposure, as suggested by the downregulation of EAAT1 and EAAT2 (Szatkowski and Attwell, 1994), and increased tolerance against substrate deprivation, as suggested by reduced regional CGU. However, increases in extracellular glutamate have a limit even in the most severely ischemic region, since the reversal of EAAT is inhibited at extracellular pH 6.8 (Billups and Attwell, 1996). It has been estimated that regions with CBF lower than 12 mL $100g^{-1}$ min^{-1} have a corresponding pH 6.6 or less (Hakim, 1987). Though the pH was not measured in our studies, it can be inferred from our measured CBF values that considerable extracellular acidosis must be present (Hakim, 1987; Osuga and Hogan, 1997) (Chapter 5). In fact, in our studies, the regional CBF in the ischemic core in the sham preconditioned studies 23 ± 25 mL $100g^{-1}$ min^{-1} (n =

6), indicating some studies had very low regional CBF in the core. NO in the core may be predominantly converted into peroxynitrite. In CSD preconditioned studies, the value is 56 ± 23 mL $100g^{-1}$ min^{-1}.

A reduction in the rate of glucose metabolism, as indicated by lower regional CGU, may indicate the preconditioned tissue is geared to be more tolerant to energy shortage. CSD preconditioning downregulated astrocytic EAAT, but not the neuronal type, consistent with the suggestion that lower glucose utilization may be the result of reduced EAAT activities. This downregulation may also suggest that reversed glutamate uptake during ischemia by astrocytes may become attenuated in preconditioned cortex, thus reducing glutamate exposure upon ischemic insult (Szatkowski and Attwell, 1994). Decreases in regional CGU are more likely the result of EAAT downregulation, although they may contribute to the reduction in infarct volume and the attenuation of [^{3}H]nimodipine in vivo distribution at 3 hours of focal ischemia. However, it is noted that the onset of the reduction in regional CGU is later than the downregulation of EAAT, suggesting regional CGU may decrease independent of EAAT downregulation. Though the degree of EAAT downregulation seemed considerably larger than the degrees of regional CGU reduction, it should be noted that it is very unlikely that the true degree of EAAT downregulation can be quantitatively represented by immunoblotting at current settings due to the nature of the methodology.

EAAT coupling is not essential for basal level neuronal energy metabolism (Pellerin and Magistretti, 1994). However the coupling is on when activity levels are higher due to increased glutamate release from the synaptic terminal (Magistretti et al., 1999). Higher extracellular glutamate increases excitotoxicity as well as increases energy consumption. Thus, the downregulation of EAAT could be viewed as a coupling mechanism to reduce both excitotoxicity and associated energy metabolism, both of which may have considerable effects on the tissue tolerance against depolarization and ischemic injury.

The ischemic core is smaller in the CSD preconditioned cortex

The term periinfarct has been used interexchangably with penumbra (Dirnagl et al., 1999). However, the cerebral ischemic penumbra is pathophysiologically well defined. It is the region that is viable but not functional (Hakim, 1998). In terms of regional CBF, the penumbra maintains a level of perfusion at 12 - 18 mL $100g^{-1}$ min^{-1}. Regional CGU remains above 17 μmol $100g^{-1}$ min^{-1}. There is considerable acidosis with the tissue pH lowered to 6.6. Extracellular K^+ is elevated but manageable at 4 - 10 mM (Hakim, 1987). The penumbra undergoes dynamic changes after the onset of an ischemic event, which determines the outcome of the ischemic tissue injury (Dirnagl et al., 1999).

In our studies, two regions of great interest were identified with the difference image approach. The sqareroot CBF difference image identified a region outside the ischemic core, where regional CBF was higher at 147 ± 27

mL $100g^{-1}$ min^{-1} in CSD preconditioned cortex compared with 73 ± 41 mL $100g^{-1}$ min^{-1}. Though this region does not qualify as the ischemic penumbra, the difference in the regional perfusion due to CSD preconditioning may indicate the consequence of increased NOS expression (Eliasson et al., 1999), which can be activated by periinfarct depolarizations.

The [^{3}H]nimodipine V_d difference image however identified a region typically viewed as the ischemic core (Matsushima et al., 1998). In this region, the regional CBF in CSD preconditioned studies is 56 ± 23 mL $100g^{-1}$ min^{-1} suggesting an expansion of the penumbra in CSD preconditioned studies. By contrast in the sham the regional CBF is 23 ± 25 mL $100g^{-1}$ min^{-1} (n = 6). Though the average seems to be above the criteria for the penumbra, the standard deviation indicates that some studies had a core where regional CBF was considerably lower than the cut off level of the ischemic penumbra (Hakim, 1987). The large variability is innate to the focal ischemic model. Nonetheless, the ischemic core was arguably smaller (Chapter 5). In addition to improved regional CBF, the attenuated [^{3}H]nimodipine in vivo distribution suggested that there was considerably less tissue depolarization, thus less tissue injury. Furthermore, though the difference was not statistically significant, the trend in [^{3}H]dizocilpine in vivo distribution outside the ischemic core indicates a tendency of less NMDA receptor activation, another sign of attenuated excitotoxicity due to decreases in extracellular glutamate.

Though the glucose metabolism data and EAAT data cannot be used to identify the ischemic penumbra, a smaller ischemic core may result from those effects. Downregulation of EAAT in the penumbra may indicate a region suffering less excitotoxicity but sufficiently activated to promote NOS activity. In the ischemic core, the attenuated leakage of glutamate may reduce excitotoxicity and tissue depolarization. Thus, tissue possesses enhanced capability to deal with the increased NO production to convert it to improve tissue survival in the ischemic core. Outside the ischemic core, the lower regional CGU may provide little benefits. However, in the core region, 10% reduction in substrate use may be considerable.

Possible role of glutamate in CSD-induced ischemic tolerance

Many molecular changes after CSD treatment are downstream of glutamate receptor activation (Fabricius et al., 1993; Herdegen et al., 1993; Kokaia et al., 1993; Levine and Black, 1997). Increased extracellular glutamate during CSD, predominantly due to increased release from synaptic terminal and reversed EAAT action (Billups and Attwell, 1996; Kimelberg et al., 1995; Munoz-Martinez, 1970; Rutledge and Kimelberg, 1996), may serve as a signal that leads to multiple messenger responses. Ketamine, an NMDA antagonist, given during KCl-induced CSD was found to block CSD-induced ischemic tolerance (Taga et al., 1997). Activation of metabotropic glutamate receptors has been shown to attenuate N-type VSCC activation through increased G-protein β/γ subunits binding with these presynaptic membrane channels (Ikeda, 1996). The observation that [^{3}H]dizocilpine in vivo distribution is

increased during 1 hour of recurrent CSD is consistent with the hypothesized role of glutamate in the induction of ischemic tolerance.

A consistent effect of CSD preconditioning has been the induction of reactive gliosis (Belayev et al., 1996; Bonthius and Steward, 1993; Caggiano and Kraig, 1998), which is blocked by NMDA receptor antagonist, dizocilpine (Bonthius and Steward, 1993). This process has been reported to be mediated by increases in extracellular glutamate (Herrera and Cuello, 1992; Herrera and Robertson, 1990; Levine and Black, 1997). Thus induction of neuronal NOS by CSD (Caggiano and Kraig, 1998) could also be blocked by dizocilpine, although it has not been experimentally confirmed. CSD preconditioning has been reported to increase the transcription and translation of several neural growth factors (Kariko et al., 1998; Kawahara et al., 1997; Kokaia et al., 1993; Matsushima et al., 1998). These neural growth factors in turn modify the cellular functions by modulation of signal cascades and new protein synthesis (Lessmann, 1998). CSD preconditioning has also been reported to induce increased transcription and translation of immediate early genes (Herdegen et al., 1993; Herrera et al., 1993). Immediate early genes predominantly function as transcription factors that bring about the transcription and translation of other molecules (Akins et al., 1996).

CONCLUSIONS

To understand the mechanisms of CSD-induced neuroprotection, we hypothesized that prior CSD preconditioning attenuates ischemia-induced excitotoxic injury. Since energy failure initiates excitotoxic glutamate releases and excitotoxicity further exacerbates energy failure, we approached the hypothesis by investigating the effect of prior CSD treatment on the regional CBF during acute focal cerebral ischemia. Our data demonstrated that the regional CBF was significantly higher in the periinfarct region and the ischemic core during 3 hours of focal cerebral ischemia. These results indicated that the CSD preconditioned cortex was more resistant to energy failure associated with cerebral ischemia. We further tested the hypothesis by studying the changes in postsynaptic L-type VSCC and NMDA receptor Ca^{2+} channels after CSD treatment. Our data indicated that membrane depolarization was attenuated by CSD preconditioning in the ischemic core and we thus inferred the attenuation of L-type VSCC activation in the ischemic core. [^{3}H]Dizocilpine in vivo distribution showed a trend of less NMDA receptor activation outside the ischemic core, suggesting possible attenuation of increased extracellular glutamate. [^{3}H]Nimodipine and [^{3}H]dizocilpine in vitro binding indicated the binding characteristics of VSCC and NMDA receptor were unaltered by CSD preconditioning, showing that a change in density of these postsynaptic Ca^{2+} channels was not a mechanism of CSD-induced neuroprotection. Our regional CGU measurement showed that

it decreased on day 3 and day 7 after CSD treatment, suggesting energy use was decreased by CSD preconditioning. Immunoprotein analysis of glutamate transporter indicated that the astrocytic EAAT1 and EAAT2, but not neuronal EAAT3, downregulated on day 3 after CSD, suggesting that glutamate leakage through these transporters during ischemic insult may be reduced. Thus, our studies demonstrated that CSD preconditioning may attenuate excitotoxicity by increasing regional CBF and decreasing excitotoxicity as indicated by the decreased Ca^{2+} channel activation. Our observation of the reduction of regional CGU and the downregulation of astrocytic EAAT support the modulation of the excitatory synapses as a mechanism of CSD-induced neuroprotection.

APPENDICES

1. Measurement of regional cerebral blood flow

The equation for calculating blood flow using measurable tracer is described by Kety in 1951 (Kety, 1951). Based on the Fick principle,

$$\frac{dM}{dt} = F(C_a - C_v) \tag{1-1}$$

where M is quantity of the tracer taken up by the tissue, t is time, F is blood flow per unit mass of tissue, C_a is the arterial tracer concentration, C_v is the venous tracer concentration. At equilibrium on a single pass,

$$C_v = \frac{M}{\lambda}, \tag{1-2}$$

where λ is the radiotracer partition coefficient between blood and tissue, the Fick principle can be expressed as

$$\frac{dM}{dt} + \frac{F}{\lambda} M = FC_a . \tag{1-3}$$

Integration of the equation (1-3) obtains Kety's equation,

$$M(t) = Fe^{-\frac{F}{\lambda}t} \int_0^t C_a(s) e^{\frac{F}{\lambda}s} ds, \tag{1-4}$$

where M(t) is the concentration of the tracer in the tissue at time t, $C_a(s)$ is the arterial concentration at time s after the induction of a radiotracer.

When the tracer is H_2 gas, a platinum electrode is inserted into the tissue and polarized to a positive voltage with respect to a stable reference electrode (Farrar, 1987). The following oxidation reaction proceeds,

$$H_2 \rightarrow 2H^+ + 2e^- . \tag{1-5}$$

When the polarizing voltage is sufficiently high, the molecular H_2 concentration is reduced to zero at the electrode surface. This creates a concentration gradient between the bulk tissue and the electrode surface. The tissue H_2 concentration can be described as

$$C = \frac{IL}{nFD}, \tag{1-6}$$

where C is the tissue H_2 concentration, I is the current density per unit area per unit time, n is the number of electrons transferred by the molecule of hydrogen, F is Faraday's number, D is the diffusion coefficient for H_2 in the tissue, L is the thickness of the diffusion layer. Then Kety's equation becomes

$$I(t) = Fe^{-\frac{F}{\lambda}t}\int_0^t C_a(s)e^{\frac{F}{\lambda}s}ds. \tag{1-7}$$

When I_a is constant and positive during saturation, the equation reduces to

$$I(t) = \lambda I_a[1 - e^{-\frac{F}{\lambda}t}]. \tag{1-8}$$

When I_a is constant and zero during desaturation.

$$I(t) = I_a(0)e^{-\frac{F}{\lambda}t}. \tag{1-9}$$

Since λ for H_2 gas is 1 (Farrar, 1987), the above equation becomes

$$I(t) = I_a(0)e^{-Ft}. \tag{1-10}$$

Take natural logarithm on both sides

$$In[I(t)] = In[I_a(0)] - Ft, \tag{1-11}$$

$$F = \frac{In[I_a(0) - In[I(t)]}{t}. \tag{1-12}$$

When the tracer is [^{14}C]iodoantipyrine delivered with a ramp infusion over 1 minute, C_a is measured with frequent arterial samples and remove the brain at 1 minute, Kety's equation remains

$$M(t) = Fe^{-\frac{F}{\lambda}t}\int_0^t C_a(s)e^{\frac{F}{\lambda}s}ds. \tag{1-13}$$

Assume a linear ramp arterial input with a slope of α, the solutions for M versus F is

$$M(t) = F\alpha\left(\frac{F}{\lambda}\right)^{-2}\left[\frac{F}{\lambda}(t-t_0) - \left(1 - e^{-\frac{F}{\lambda}(t-t_0)}\right)\right]. \tag{1-14}$$

The equation can be solved iteratively.

[^{14}C]Iodoantipyrine is chosen as the radiotracer because it freely diffuses across blood brain barrier so the CBF values only reflect the tissue perfusion

but not the limitation of the blood brain barrier (Sakurada et al., 1978). The brain/blood equilibrium partition coefficient for [^{14}C]iodoantipyrine is 0.8 ml/g. This coefficient is independent of the hematocrit (Sakurada et al., 1978). Patlak et al showed that a ramp arterial input function, coupled with a relatively short experimental duration, tends to minimize errors in blood flow produced by uncertainty in the partition coefficient λ (Ginsberg, 1987; Patlak et al., 1984).

2. Infarct volume measurement

The edema ratio is calculated as:

$$ER = \frac{T_I}{T_C}, \tag{2-1}$$

where ER is the edema ratio, T_I is total ipsilateral volume, T_C is total contralateral volume (Hiramatsu et al., 1993).

Assuming ischemic injury induces edematous reaction in both injured tissue and unaffected tissue, the infarct volume can be calculated as:

$$IV = V_C - V_I / ER, \tag{2-2}$$

where IV is infarct volume, V_C is contralateral volume of the target structure, V_I is the volume of the non-ischemic region of the target studies in the ischemic hemisphere.

3. Notes on ligand binding kinetics

Receptor-ligand binding can be expressed as:

$$F + R \leftrightarrow B, \tag{3-1}$$

where F is free ligand; R is free receptor; B is ligand-receptor complex (bound). According to the law of mass interaction, binding of ligand with receptor is proportional to the concentration of free ligand and free receptor; and the dissociation of the ligand-receptor complex is proportional to the concentration of the ligand-receptor complex, i.e.:

$$V_{on} = k_{on} FR, \tag{3-2}$$

and

$$V_{off} = k_{off} B, \tag{3-3}$$

where V_{on} is association velocity, V_{off} is dissociation velocity, k_{on} is binding constant, k_{off} = dissociation constant.

At equilibrium, the velocity of binding equals the velocity of dissociation, i.e.:

$$V_{on} = V_{off}, \; FRk_{on} = Bk_{off}. \tag{3-4}$$

Define

$$K = \frac{k_{off}}{k_{on}} = \frac{FR}{B}, \tag{3-5}$$

and the degree of binding, X, is defined by the moles of bound ligand per mole of receptor,

$$X = \frac{B}{R+B}, \; X = \frac{B}{B_{max}}. \tag{3-6}$$

Replace B by 3-5 gives

$$X = \frac{F}{K+F} \text{ and } \frac{B}{B_{max}} = \frac{F}{K+F}. \tag{3-7}$$

At low F, $B/B_{max} \rightarrow 0$; at high F, $B/B_{max} \rightarrow 1$; when half of the receptors are occupied, K=F. Rearrange 3-7, the Scatchard plot is obtained:

$$\frac{B}{F} = \frac{B}{K} + \frac{B_{max}}{K}. \tag{3-8}$$

Because the logarithm of the ligand activity is proportional to the chemical potential of the ligand, we can plot B/B_{max} against log F to get titration curve.

Sometimes there is more than one binding site on the receptor. In a sequential binding model the stepwise reaction can be expressed as:

$$F + R \leftrightarrow B_1,\ B_1 + R \leftrightarrow B_2. \tag{3-9}$$

$$K_1 = \frac{FR}{B_1},\ K_2 = \frac{FR}{B_2}. \tag{3-10}$$

or in overall reaction:

$$F + R \leftrightarrow B_1,\ 2F + R \leftrightarrow B_2. \tag{3-11}$$

$$\beta_1 = \frac{FR}{B_1},\ \beta_2 = \frac{F^2R}{B_2},\ \beta_2 = K_1K_2. \tag{3-12}$$

The moles of bound ligand per mole of receptor in all forms gives the degree of binding:

$$X = \frac{B}{B_{max}} = \frac{B_1 + 2B_2}{R + B_1 + B_2}. \tag{3-13}$$

In terms of the stepwise reaction, we obtain

$$X = \frac{K_1F + 2K_1K_2F}{1 + K_1F + K_2F}. \tag{3-14}$$

Likewise in terms of overall reaction, we obtain

$$X = \frac{\beta_1F + 2\beta_2F^2}{1 + K_1F + K_2F^2}. \tag{3-15}$$

The principle of ligand binding can also be applied to ligand purity assay. From the derivation of Michaelis-Menten equation,

$$K = \frac{k_{off}}{k_{on}} = \frac{FR}{B}, \tag{3-16}$$

Since $B_{max} = R + B;\ L = F + B,$

$$K = \frac{(B_{max} - B)(L - B)}{B} = \frac{B_{max}L - B_{max}B - BL + B^2}{B}, \tag{3-17}$$

$$KB = B_{max}L - B_{max}B - BL + B^2, \tag{3-18}$$

$$B^2 - (B_{max} + L + K)B + B_{max}L = 0. \tag{3-19}$$

$$\underset{B_{max}\to\infty}{LimB} = \frac{B_{max} \pm B_{max} + 2L}{2}. \tag{3-20}$$

Take the meaningful terms,

$$\underset{B_{max}\to\infty}{LimB} = \frac{2L}{2} = L. \tag{3-21}$$

4. Theoretical basis of [^{14}C]deoxyglucose methodology

The [^{14}C]deoxyglucose method was used to map local metabolism levels in this study. The [^{14}C]deoxyglucose method for the measurement of regional CGU was derived by analysis of a model based on the biochemical properties of [^{14}C]deoxyglucose in central nervous tissue (Sokoloff et al., 1989; Sokoloff et al., 1977). [^{14}C]deoxyglucose is transported bidirectionally between blood and brain by the same carrier that transports glucose across the blood-brain barrier. In the cerebral tissues, it is phosphorylated by hexokinase to 2-deoxyglucose-6-phosphate (DG-6-P). Deoxyglucose and glucose are competitive substrates for both blood-brain transport and hexokinase-catalyzed phosphorylation. Unlike glucose-6-phosphate, DG-6-P cannot be converted to fructose-6-phosphate, and it is also not a substrate for glucose-6-phosphate dehydrogenase. Other break down processes are slow, and the metabolites (DG-6-P) are relatively stable. The biochemical processing of [^{14}C]deoxyglucose is therefore stopped at this stage; DG-6-P is trapped in the cerebral tissue (Sokoloff et al., 1989).

If the DG-6-P accumulation time is kept short enough to allow the assumption of negligible loss of [^{14}C]DG-6-P from the neurons, then the quantity of [^{14}C]DG-6-P accumulated in cerebral tissue at any given time following the introduction of [^{14}C]deoxyglucose into the circulation is equal to the integral of the rate of [^{14}C]deoxyglucose phosphorylation by hexokinase in that tissue during the accumulation time. This integral is in turn, related to the amount of glucose that has been phosphorylated over the same interval, depending on the time course of the relative concentrations of [^{14}C]deoxyglucose and glucose in the precursor pools and the Michaelis-Menten kinetic constants for hexokinase with respect to both [^{14}C]deoxyglucose and glucose. With glucose consumption in a steady state, the amount of glucose phosphorylation during the interval of time equals the steady-state flux of glucose through the hexokinase-catalyzed step times the

duration of the interval, and the net rate of flux of glucose through this step equals the rate of glucose utilization (Sokoloff et al., 1989).

An operational equation is derived from the model, requiring the following assumptions:

1. Plasma glucose and the rate of cross-membrane glucose transportation remain constant throughout the experimental period;

2. Tissue compartment is homogeneous, within which the concentrations of [^{14}C]deoxyglucose and glucose are uniform and exchange directly with the plasma; and

3. Molecular concentrations of free [^{14}C]deoxyglucose are essentially equal to zero.

General equation for measurement of reaction rates with tracers (Sokoloff et al., 1989):

$$\text{Rate of Reaction} = \frac{\text{Labeled Product Formed in Interval of Time, 0 to T}}{\left[\begin{array}{c}\text{Isotope Effect} \\ \text{CorrectionFactor}\end{array}\right]\left[\begin{array}{c}\text{Integrated Specific Activity} \\ \text{of Precoursor}\end{array}\right]} \qquad (4\text{-}1)$$

Operational equation of [^{14}C]deoxyglucose method:

Labeled Product Formed in Interval of Time, 0 to T

Total ^{14}C in Tissue at Time, T — ^{14}C in Precursor Remaining in Tissue at Time, T

$$Ri = \frac{C_i^*(T) - K_1^* e^{-(k_2^* + k_3^*)T} \int_0^T C_p e^{(k_2^* + k_3^*)t} dt}{\left[\frac{\lambda \cdot V_m^* \cdot K_m}{\phi \cdot V_m \cdot K_m^*}\right]\left[\int_0^T \left(\frac{C_p^*}{C_p}\right) dt - e^{-(k_2^* + k_3^*)T} \int_0^T \left(\frac{C_p^*}{C_p}\right) e^{(k_2^* + k_3^*)t} dt\right]}$$

Isotope Effect Correction Factor — Integrated Plasma Specific Activity — Correction for Lag in Tissue Equlibration with Plasma

Labeled Product Formed in Interval of Time, 0 to T (4-2)

This operational equation can be solved by measuring the following variables: 1) The entire history of the arterial plasma [^{14}C]deoxyglucose concentration, C_p^*, from zero time to the time of decapitation, T; 2) The steady-state arterial plasma glucose concentration, C_p, over the same interval; and 3) The concentration of ^{14}C in the tissue, $C_i^*(T)$, which is determined densitometrically from the autoradiographs (Sokoloff et al., 1989; Sokoloff et al., 1977).

Because the operational equation of the method was derived on the basis of the assumption that arterial plasma glucose concentration remains constant during the experimental period, the original method is applicable only to experiments in which this assumption is satisfied (Savaki et al., 1980; Sokoloff et al., 1989). If the plasma glucose level is unstable, it is required that a modified operational equation be used (Savaki et al., 1980; Sokoloff et al., 1989).

REFERENCES

Agullo L, Garcia A (1992) Different receptors mediate stimulation of nitric oxide-dependent cyclic GMP formation in neurons and astrocytes in culture. *Biochem Biophys Res Commun*, 182:1362-1368.

Akgoren N, Fabricius M, Lauritzen M (1994) Importance of nitric oxide for local increases of blood flow in rat cerebellar cortex during electrical stimulation. *Proc Natl Acad Sci U S A*, 91:5903-5907.

Akins PT, Liu PK, Hsu CY (1996) Immediate early gene expression in response to cerebral ischemia. Friend or foe? *Stroke*, 27:1682-1687.

Alagarsamy S, Marino MJ, Rouse ST, Gereau RWt, Heinemann SF, Conn PJ (1999) Activation of NMDA receptors reverses desensitization of mGluR5 in native and recombinant systems. *Nat Neurosci*, 2:234-240.

Ambrosini A, Bresciani L, Fracchia S, Brunello N, Racagni G (1995) Metabotropic glutamate receptors negatively coupled to adenylate cyclase inhibit N-methyl-D-aspartate receptor activity and prevent neurotoxicity in mesencephalic neurons in vitro. *Mol Pharmacol*, 47:1057-1064.

Andine P, Jacobson I, Hagberg H (1992) Enhanced calcium uptake by CA1 pyramidal cell dendrites in the postischemic phase despite subnormal evoked field potentials: excitatory amino acid receptor dependency and relationship to neuronal damage. *J Cereb Blood Flow Metab*, 12:773-783.

Arakawa S, Nakamura S, Kawashima N, Nishiike S, Fujii Y (1997) Antidromic burst activity of locus coeruleus neurons during cortical spreading depression. *Neuroscience*, 78:1147-1158.

Araki T, Kato H, Shuto K, Oshima Y, Itoyama Y (1998) Postischemic changes of [^{3}H]nimodipine and [^{3}H]ryanodine binding in the gerbil striatum and hippocampus. *Eur J Neurol*, 5:195-201.

Asai S, Iribe Y, Kohno T, Ishikawa K (1996) Real time monitoring of biphasic glutamate release using dialysis electrode in rat acute brain ischemia. *Neuroreport*, 7:1092-1096.

Back T, Kohno K, Hossmann KA (1994) Cortical negative DC deflections following middle cerebral artery occlusion and KCl-induced spreading depression: effect on blood flow, tissue oxygenation, and electroencephalogram. *J Cereb Blood Flow Metab*, 14:12-19.

Baker AJ, Zornow MH, Scheller MS, Yaksh TL, Skilling SR, Smullin DH, Larson AA, Kuczenski R (1991) Changes in extracellular concentrations of glutamate, aspartate, glycine, dopamine, serotonin, and dopamine metabolites after transient global ischemia in the rabbit brain. *J Neurochem*, 57:1370-1379.

Baron JC, Rougemont D, Soussaline F, Bustany P, Crouzel C, Bousser MG, Comar D (1984) Local interrelationships of cerebral oxygen consumption and glucose utilization in normal subjects and in ischemic stroke patients: a positron tomography study. *J Cereb Blood Flow Metab*, 4:140-149.

Barone FC, White RF, Spera PA, Ellison J, Currie RW, Wang X, Feuerstein GZ (1998) Ischemic preconditioning and brain tolerance: temporal histological and functional outcomes, protein synthesis requirement, and interleukin-1 receptor antagonist and early gene expression. *Stroke*, 29:1937-1950; discussion 1950-1931.

Barres BA (1991) New roles for glia. *J Neurosci*, 11:3685-3694.

Basarsky TA, Duffy SN, Andrew RD, MacVicar BA (1998) Imaging spreading depression and associated intracellular calcium waves in brain slices. *J Neurosci*, 18:7189-7199.

Battaglia G, Bruno V, Ngomba RT, Di Grezia R, Copani A, Nicoletti F (1998) Selective activation of group-II metabotropic glutamate receptors is protective against excitotoxic neuronal death. *Eur J Pharmacol*, 356:271-274.

Bean BP (1984) Nitrendipine block of cardiac calcium channels: high-affinity binding to the inactivated state. *Proc Natl Acad Sci U S A*, 81:6388-6392.

Beck T, Goller HJ, Wree A (1995) Chronic depression of glucose metabolism in postischemic rat brains. *Stroke*, 26:1107-1113.

Belayev L, Ginsberg MD, Alonso OF, Singer JT, Zhao W, Busto R (1996) Bilateral ischemic tolerance of rat hippocampus induced by prior unilateral transient focal ischemia: relationship to c-fos mRNA expression. *Neuroreport*, 8:55-59.

Bergles DE, Dzubay JA, Jahr CE (1997) Glutamate transporter currents in bergmann glial cells follow the time course of extrasynaptic glutamate. *Proc Natl Acad Sci U S A*, 94:14821-14825.

Bergles DE, Jahr CE (1997) Synaptic activation of glutamate transporters in hippocampal astrocytes. *Neuron*, 19:1297-1308.

Berridge MJ (1993) Cell signalling. A tale of two messengers. *Nature*, 365:388-389.

Bettler B, Mulle C (1995) Neurotransmitter receptors. II. AMPA and kainate receptors. *Neuropharmacology*, 34:123-139.

Betz WJ, Angleson JK (1998) The synaptic vesicle cycle. *Annu Rev Physiol*, 60:347-363.

Billups B, Attwell D (1996) Modulation of non-vesicular glutamate release by pH. *Nature*, 379:171-174.

Birrell GJ, Gordon MP, Marcoux FW (1993) (1S,3R)-1-aminocyclopentane-1,3-dicarboxylic acid attenuates N-methyl-D-aspartate-induced neuronal cell death in cortical cultures via a reduction in delayed Ca^{2+} accumulation. *Neuropharmacology*, 32:1351-1358.

Bittar PG, Charnay Y, Pellerin L, Bouras C, Magistretti PJ (1996) Selective distribution of lactate dehydrogenase isoenzymes in neurons and astrocytes of human brain. *J Cereb Blood Flow Metab*, 16:1079-1089.

Bonhaus DW, McNamara JO (1988) N-methyl-D-aspartate receptor regulation of uncompetitive antagonist binding in rat brain membranes: kinetic analysis. *Mol Pharmacol*, 34:250-255.

Bonthius DJ, Steward O (1993) Induction of cortical spreading depression with potassium chloride upregulates levels of messenger RNA for glial fibrillary acidic protein in cortex and hippocampus: inhibition by MK-801. *Brain Res*, 618:83-94.

Bookstein FL (1990) Distortion correction. In: *Three-Dimentional NeuroImaging* (Tiga, AW eds), New York, Raven Press, pp 235-249.

Bouvier M, Szatkowski M, Amato A, Attwell D (1992) The glial cell glutamate uptake carrier countertransports pH-changing anions. *Nature*, 360:471-474.

Bowery NG, Wong EH, Hudson AL (1988) Quantitative autoradiography of [^{3}H]-MK-801 binding sites in mammalian brain. *Br J Pharmacol*, 93:944-954.

Bradford MM (1976) A rapid and sensitive method for the quantitation of microgram quantities of protein utilizing the principle of protein-dye binding. *Anal Biochem*, 72:248-254.

Branston NM (1995) Neurogenic control of the cerebral circulation. *Cerebrovasc Brain Metab Rev*, 7:338-349.

Bruno V, Copani A, Battaglia G, Raffaele R, Shinozaki H, Nicoletti F (1994) Protective effect of the metabotropic glutamate receptor agonist, DCG- IV, against excitotoxic neuronal death. *Eur J Pharmacol*, 256:109-112.

Buchan A, Li H, Pulsinelli WA (1991a) The N-methyl-D-aspartate antagonist, MK-801, fails to protect against neuronal damage caused by transient, severe forebrain ischemia in adult rats. *J Neurosci*, 11:1049-1056.

Buchan A, Pulsinelli WA (1990) Hypothermia but not the N-methyl-D-aspartate antagonist, MK-801, attenuates neuronal damage in gerbils subjected to transient global ischemia. *J Neurosci*, 10:311-316.

Buchan AM, Lesiuk H, Barnes KA, Li H, Huang ZG, Smith KE, Xue D (1993) AMPA antagonists: do they hold more promise for clinical stroke trials than NMDA antagonists? *Stroke*, 24:I148-152.

Buchan AM, Li H, Cho S, Pulsinelli WA (1991b) Blockade of the AMPA receptor prevents CA1 hippocampal injury following severe but transient forebrain ischemia in adult rats. *Neurosci Lett*, 132:255-258.

Buchan AM, Xue D, Huang ZG, Smith KH, Lesiuk H (1991c) Delayed AMPA receptor blockade reduces cerebral infarction induced by focal ischemia. *Neuroreport*, 2:473-476.

Caggiano AO, Breder CD, Kraig RP (1996) Long-term elevation of cyclooxygenase-2, but not lipoxygenase, in regions synaptically distant from spreading depression. *J Comp Neurol*, 376:447-462.

Caggiano AO, Kraig RP (1998) Neuronal nitric oxide synthase expression is induced in neocortical astrocytes after spreading depression. *J Cereb Blood Flow Metab*, 18:75-87.

Carriedo SG, Yin HZ, Sensi SL, Weiss JH (1998) Rapid Ca^{2+} entry through Ca^{2+}-permeable AMPA/Kainate channels triggers marked intracellular Ca^{2+} rises and consequent oxygen radical production. *J Neurosci*, 18:7727-7738.

Chaudhry IA, Nitahara K, Nagashima H, Vizi ES (1995) Neurochemical evidence that $[Ca^{2+}]_o$ antagonizes the effect of neomycin on acetylcholine release from mouse hemidiaphragm preparation: an attempt to assess the margin to safety. *Acta Anaesthesiol Scand*, 39:494-497.

Chedotal A, Umbriaco D, Descarries L, Hartman BK, Hamel E (1994) Light and electron microscopic immunocytochemical analysis of the neurovascular relationships of choline acetyltransferase and vasoactive intestinal polypeptide nerve terminals in the rat cerebral cortex. *J Comp Neurol*, 343:57-71.

Chen J, Graham SH, Zhu RL, Simon RP (1996) Stress proteins and tolerance to focal cerebral ischemia. *J Cereb Blood Flow Metab*, 16:566-577.

Chen T, Kato H, Liu XH, Araki T, Itoyama Y, Kogure K (1994) Ischemic tolerance can be induced repeatedly in the gerbil hippocampal neurons. *Neurosci Lett*, 177:159-161.

Chittajallu R, Braithwaite SP, Clarke VR, Henley JM (1999) Kainate receptors: subunits, synaptic localization and function. *Trends Pharmacol Sci*, 20:26-35.

Choi DW (1987) Ionic dependence of glutamate neurotoxicity. *J Neurosci*, 7:369-379.

Choi DW (1988a) Calcium-mediated neurotoxicity: relationship to specific channel types and role in ischemic damage. *Trends Neurosci*, 11:465-469.

Choi DW (1988b) Glutamate neurotoxicity and diseases of the nervous system. *Neuron*, 1:623-634.

Choi DW, Koh JY, Peters S (1988) Pharmacology of glutamate neurotoxicity in cortical cell culture: attenuation by NMDA antagonists. *J Neurosci*, 8:185-196.

Cochilla AJ, Alford S (1999) NMDA receptor-mediated control of presynaptic calcium and neurotransmitter release. *J Neurosci*, 19:193-205.

Colonna DM, Meng W, Deal DD, Busija DW (1994) Nitric oxide promotes arteriolar dilation during cortical spreading depression in rabbits. *Stroke*, 25:2463-2470.

Colonna DM, Meng W, Deal DD, Gowda M, Busija DW (1997) Neuronal NO promotes cerebral cortical hyperemia during cortical spreading depression in rabbits. *Am J Physiol*, 272:H1315-1322.

Conn PJ, Pin JP (1997) Pharmacology and functions of metabotropic glutamate receptors. *Annu Rev Pharmacol Toxicol*, 37:205-237.

Conti F, DeBiasi S, Minelli A, Rothstein JD, Melone M (1998) EAAC1, a high-affinity glutamate transporter, is localized to astrocytes and GABAergic neurons besides pyramidal cells in the rat cerebral cortex. *Cereb Cortex*, 8:108-116.

Coorssen JR, Blank PS, Tahara M, Zimmerberg J (1998) Biochemical and functional studies of cortical vesicle fusion: the SNARE complex and Ca^{2+} sensitivity. *J Cell Biol*, 143:1845-1857.

Corbett D, Crooks P (1997) Ischemic preconditioning: a long term survival study using behavioural and histological endpoints. *Brain Res*, 760:129-136.

Craig PJ, McAinsh AD, McCormack AL, Smith W, Beattie RE, Priestley JV, Yip JL, Averill S, Longbottom ER, Volsen SG (1998) Distribution of the voltage-dependent calcium channel alpha(1A) subunit throughout the mature rat brain and its relationship to neurotransmitter pathways. *Journal of Comparative Neurology*, 397:251-267.

Cruz NF, Adachi K, Dienel GA (1999) Rapid efflux of lactate from cerebral cortex during K^+-induced spreading cortical depression. *J Cereb Blood Flow Metab*, 19:380-392.

De Waard M, Liu H, Walker D, Scott VE, Gurnett CA, Campbell KP (1997) Direct binding of G-protein beta-gamma complex to voltage-dependent calcium channels. *Nature*, 385:446-450.

De Waard M, Pragnell M, Campbell KP (1994) Ca^{2+} channel regulation by a conserved beta subunit domain. *Neuron*, 13:495-503.

Dewar D, Wallace MC, Kurumaji A, McCulloch J (1989) Alterations in the N-methyl-D-aspartate receptor complex following focal cerebral ischemia. *J Cereb Blood Flow Metab*, 9:709-712.

Dietrich WD, Feng ZC, Leistra H, Watson BD, Rosenthal M (1994) Photothrombotic infarction triggers multiple episodes of cortical spreading depression in distant brain regions. *J Cereb Blood Flow Metab*, 14:20-28.

Dirnagl U, Iadecola C, Moskowitz MA (1999) Pathobiology of ischaemic stroke: an integrated view. *Trends Neurosci*, 22:391-397.

Dirnagl U, Niwa K, Lindauer U, Villringer A (1994) Coupling of cerebral blood flow to neuronal activation: role of adenosine and nitric oxide. *Am J Physiol*, 267:H296-301.

Dolphin AC (1995) The G.L. Brown Prize Lecture. Voltage-dependent calcium channels and their modulation by neurotransmitters and G proteins. *Exp Physiol*, 80:1-36.

Douen AG, Akiyama K, Hogan MJ, Wang F, Dong L, Chow AK , Hakim A (2000) Preconditioning with Cortical Spreading Depression Decreases Intraischemic Cerebral Glutamate Levels and Down-Regulates Excitatory Amino Acid Transporters EAAT1 and EAAT2 from Rat Cerebal Cortex Plasma Membranes. *J Neurochem*, 75:812-818.

Douen AG, Burdett E, Ramlal T, Rastogi S, Vranic M, Klip A (1991) Characterization of glucose transporter-enriched membranes from rat skeletal muscle: assessment of endothelial cell contamination and presence of sarcoplasmic reticulum and transverse tubules. *Endocrinology*, 128:611-616.

Douen AG, Kacem R, Jones MN (1988) Direct interaction of phenylarsine oxide with hexose transporters in isolated rat adipocytes. *Biochim Biophys Acta*, 944:444-450.

Duckrow RB (1991) Regional cerebral blood flow during spreading cortical depression in conscious rats. *J Cereb Blood Flow Metab*, 11:150-154.

Dunlap K, Luebke JI, Turner TJ (1995) Exocytotic Ca^{2+} channels in mammalian central neurons. *Trends Neurosci*, 18:89-98.

Eliasson MJ, Huang Z, Ferrante RJ, Sasamata M, Molliver ME, Snyder SH, Moskowitz MA (1999) Neuronal nitric oxide synthase activation and peroxynitrite formation in ischemic stroke linked to neural damage. *J Neurosci*, 19:5910-5918.

Elliott EM, Malouf AT, Catterall WA (1995) Role of calcium channel subtypes in calcium transients in hippocampal CA3 neurons. *J Neurosci*, 15:6433-6444.

Els T, Rother J, Beaulieu C, de Crespigny A, Moseley M (1997) Hyperglycemia delays terminal depolarization and enhances repolarization after peri-infarct spreading depression as measured by serial diffusion MR mapping. *J Cereb Blood Flow Metab*, 17:591-595.

Fabricius M, Akgoren N, Dirnagl U, Lauritzen M (1997) Laminar analysis of cerebral blood flow in cortex of rats by laser- Doppler flowmetry: a pilot study. *J Cereb Blood Flow Metab*, 17:1326-1336.

Fabricius M, Akgoren N, Lauritzen M (1995) Arginine-nitric oxide pathway and cerebrovascular regulation in cortical spreading depression. *Am J Physiol*, 269:H23-29.

Fabricius M, Jensen LH, Lauritzen M (1993) Microdialysis of interstitial amino acids during spreading depression and anoxic depolarization in rat neocortex. *Brain Res*, 612:61-69.

Fabricius M, Lauritzen M (1994) Examination of the role of nitric oxide for the hypercapnic rise of cerebral blood flow in rats. *Am J Physiol*, 266:H1457-1464.

Faraci FM, Heistad DD (1992) Endothelium-derived relaxing factor inhibits constrictor responses of large cerebral arteries to serotonin. *J Cereb Blood Flow Metab*, 12:500-506.

Farrar JK (1987) Hydrogen clearance technique. In: *Cerebral Blood Flow - Physiologic and Clinical Aspects* (Wood, JH eds), New York, McGraw-Hill Book Company, pp 275-287.

Florence G, Bonvento G, Charbonne R, Seylaz J (1994) Spreading depression reversibly impairs autoregulation of cortical blood flow. *Am J Physiol*, 266:R1136-1140.

Folbergrova J, Memezawa H, Smith ML, Siesjo BK (1992) Focal and perifocal changes in tissue energy state during middle cerebral artery occlusion in normo- and hyperglycemic rats. *J Cereb Blood Flow Metab*, 12:25-33.

Foster AC, Wong EH (1987) The novel anticonvulsant MK-801 binds to the activated state of the N- methyl-D-aspartate receptor in rat brain. *Br J Pharmacol*, 91:403-409.

Fox PT, Raichle ME (1986) Focal physiological uncoupling of cerebral blood flow and oxidative metabolism during somatosensory stimulation in human subjects. *Proc Natl Acad Sci U S A*, 83:1140-1144.

Furuta A, Rothstein JD, Martin LJ (1997) Glutamate transporter protein subtypes are expressed differentially during rat CNS development. *J Neurosci*, 17:8363-8375.

Gallin WJ, Greenberg ME (1995) Calcium regulation of gene expression in neurons: the mode of entry matters. *Curr Opin Neurobiol*, 5:367-374.

Garcia DE, Li B, Garcia-Ferreiro RE, Hernandez-Ochoa EO, Yan K, Gautam N, Catterall WA, Mackie K, Hille B (1998) G-protein beta-subunit specificity in the fast membrane-delimited inhibition of Ca^{2+} channels. *J Neurosc*, 18:9163-9170.

Gardner-Medwin AR, Nicholson C (1983) Changes of extracellular potassium activity induced by electric current through brain tissue in the rat. *J Physiol (Lond)*, 335:375-392.

Gault LM, Lin CW, LaManna JC, Lust WD (1994) Changes in energy metabolites, cGMP and intracellular pH during cortical spreading depression. *Brain Res*, 641:176-180.

Giaume C, Venance L (1998) Intercellular calcium signaling and gap junctional communication in astrocytes. *Glia*, 24:50-64.

Ginsberg MD (1987) Autoradiographic measurement of local cerebral blood flow. In: *Cerebral Blood Flow - Physiologic and Clinical Aspects* (Wood, JH eds), New York, McGraw-Hill Book Company, pp 299-308.

Ginsberg SD, Martin LJ, Rothstein JD (1995) Regional deafferentation down-regulates subtypes of glutamate transporter proteins. *J Neurochem*, 65:2800-2803.

Gjedde A, Hansen AJ, Quistorff B (1981) Blood-brain glucose transfer in spreading depression. *J Neurochem*, 37:807-812.

Glossmann H, Ferry DR (1985) Assay for calcium channels. *Methods Enzymol*, 109:513-550.

Goadsby PJ, Kaube H, Hoskin KL (1992) Nitric oxide synthesis couples cerebral blood flow and metabolism. *Brain Res*, 595:167-170.

Gordon B, Tseng YL, Jaeger R, Petrovic A, Tovar K (1995) The development of MK-801, kainate, AMPA, and muscimol binding sites in cat visual cortex. *Vis Neurosci*, 12:241-252.

Grafstein B (1956) Mechanism of spreading cortical depression. *J Neurophysiol*, 19:154-171.

Hakim AM (1987) The cerebral ischemic penumbra. *Can J Neurol Sci*, 14:557-559.

Hakim AM (1998) Ischemic penumbra: the therapeutic window. *Neurology*, 51:S44-46.

Hakim AM, Hogan MJ (1991) In vivo binding of nimodipine in the brain: I. The effect of focal cerebral ischemia. *J Cereb Blood Flow Metab*, 11:762-770.

Hansen AJ, Olsen CE (1980) Brain extracellular space during spreading depression and ischemia. *Acta Physiol Scand*, 108:355-365.

He M, Bodi I, Mikala G, Schwartz A (1997) Motif III S5 of L-type calcium channels is involved in the dihydropyridine binding site. A combined radioligand binding and electrophysiological study. *J Biol Chem*, 272:2629-2633.

Hell JW, Westenbroek RE, Warner C, Ahlijanian MK, Prystay W, Gilbert MM, Snutch TP, Catterall WA (1993) Identification and differential subcellular localization of the neuronal class C and class D L-type calcium channel alpha 1 subunits. *J Cell Biol*, 123:949-962.

Herbette LG, Mason PE, Sweeney KR, Trumbore MW, Mason RP (1994) Favorable amphiphilicity of nimodipine facilitates its interactions with brain membranes. *Neuropharmacology*, 33:241-249.

Herdegen T, Sandkuhler J, Gass P, Kiessling M, Bravo R, Zimmermann M (1993) JUN, FOS, KROX, and CREB transcription factor proteins in the rat cortex: basal expression and induction by spreading depression and epileptic seizures. *J Comp Neurol*, 333:271-288.

Herrera DG, Cuello AC (1992) MK-801 affects the potassium-induced increase of glial fibrillary acidic protein immunoreactivity in rat brain. *Brain Res*, 598:286-293.

Herrera DG, Maysinger D, Almazan G, Funnel R, Cuello AC (1998) Analysis of c-Fos and glial fibrillary acidic protein (GFAP) expression following topical application of potassium chloride (KCl) to the brain surface. *Brain Res*, 784:71-81.

Herrera DG, Maysinger D, Gadient R, Boeckh C, Otten U, Cuello AC (1993) Spreading depression induces c-fos-like immunoreactivity and NGF mRNA in the rat cerebral cortex. *Brain Res*, 602:99-103.

Herrera DG, Robertson HA (1990) Application of potassium chloride to the brain surface induces the c- fos proto-oncogene: reversal by MK-801. *Brain Res*, 510:166-170.

Heurteaux C, Lauritzen I, Widmann C, Lazdunski M (1995) Essential role of adenosine, adenosine A1 receptors, and ATP-sensitive K^+ channels in cerebral ischemic preconditioning. *Proc Natl Acad Sci U S A*, 92:4666-4670.

Higashida H, Mitarai G, Watanabe S (1974) A comparative study of membrane potential changes in neurons and neuroglial cells during spreading depression in the rabbit. *Brain Res*, 65:411-425.

Hiramatsu K, Kassell NF, Goto Y, Soleau S, Lee KS (1993) A reproducible model of reversible, focal, neocortical ischemia in Sprague-Dawley rat. *Acta Neurochir*, 120:66-71.

Hockerman GH, Peterson BZ, Sharp E, Tanada TN, Scheuer T, Catterall WA (1997) Construction of a high-affinity receptor site for dihydropyridine agonists and antagonists by single amino acid substitutions in a non-L- type Ca^{2+} channel. *Proc Natl Acad Sci U S A*, 94:14906-14911.

Hoehner PJ, Blanck TJ, Roy R, Rosenthal RE, Fiskum G (1992) Alteration of voltage-dependent calcium channels in canine brain during global ischemia and reperfusion. *J Cereb Blood Flow Metab*, 12:418-424.

Hoffman CJ, Clark FJ, Ochs S (1973) Intracortical impedance changes during spreading depression. *J Neurobiol*, 4:471-486.

Hogan MJ, Gjedde A, Hakim AM (1991) In vivo binding of nimodipine in the brain: II. Binding kinetics in focal cerebral ischemia. *J Cereb Blood Flow Metab*, 11:771-778.

Hogan MJ, Hakim AM (1992) Reversibility of nimodipine binding to brain in transient cerebral ischemia. *J Neurochem*, 59:1745-1752.

Hogan MJ, Takizawa S, Hakim AM (1995) In vitro binding of [^{3}H]nimodipine and [^{3}H]CGS-19755 to rat brain in focal cerebral ischemia. *Exp Neurol*, 134:56-63.

Hossmann KA (1996) Periinfarct depolarizations. *Cerebrovasc Brain Metab Rev*, 8:195-208.

Howell DC (1992) Repeated-measures designs. In: *Statistical Methods for Psychology, 3rd ed.* (Howell, DC eds), Belmont, California, Duxbury Press, pp 430-483.

Huang Z, Huang PL, Ma J, Meng W, Ayata C, Fishman MC, Moskowitz MA (1996) Enlarged infarcts in endothelial nitric oxide synthase knockout mice are attenuated by nitro-L-arginine. *J Cereb Blood Flow Metab*, 16:981-987.

Huang Z, Huang PL, Panahian N, Dalkara T, Fishman MC, Moskowitz MA (1994) Effects of cerebral ischemia in mice deficient in neuronal nitric oxide synthase. *Science*, 265:1883-1885.

Hucker HB, Hutt JE, White SD, Arison BH, Zacchei AG (1983) Disposition and metabolism of (+)-5-methyl-10,11-dihydro-5H- dibenzo[a,d] cyclohepten-5,10-imine in rats, dogs, and monkeys. *Drug Metab Dispos*, 11:54-58.

Iadecola C, Pelligrino DA, Moskowitz MA, Lassen NA (1994) Nitric oxide synthase inhibition and cerebrovascular regulation. *J Cereb Blood Flow Metab*, 14:175-192.

Iadecola C, Xu X (1994) Nitro-L-arginine attenuates hypercapnic cerebrovasodilation without affecting cerebral metabolism. *Am J Physiol*, 266:R518-525.

Iadecola C, Zhang F (1994) Nitric oxide-dependent and -independent components of cerebrovasodilation elicited by hypercapnia. *Am J Physiol*, 266:R546-552.

Ikeda M, Nakazawa T, Abe K, Kaneko T, Yamatsu K (1989) Extracellular accumulation of glutamate in the hippocampus induced by ischemia is not calcium dependent--in vitro and in vivo evidence. *Neurosci Lett*, 96:202-206.

Ikeda SR (1996) Voltage-dependent modulation of N-type calcium channels by G-protein beta gamma subunits. *Nature*, 380:255-258.

Jones LP, Wei SK, Yue DT (1998) Mechanism of auxiliary subunit modulation of neuronal alpha1E calcium channels. *Journal of General Physiology*, 112:125-143.

Judd MG, Nagaraja TN, Brookes N (1996) Potassium-induced stimulation of glutamate uptake in mouse cerebral astrocytes: the role of intracellular pH. *J Neurochem*, 66:169-176.

Kariko K, Harris VA, Rangel Y, Duvall ME, Welsh FA (1998) Effect of cortical spreading depression on the levels of mRNA coding for putative neuroprotective proteins in rat brain. *J Cereb Blood Flow Metab*, 18:1308-1315.

Kataoka K, Hayakawa T, Yamada K, Mushiroi T, Kuroda R, Mogami H (1989) Neuronal network disturbance after focal ischemia in rats. *Stroke*, 20:1226-1235.

Katayama Y, Kawamata T, Tamura T, Hovda DA, Becker DP, Tsubokawa T (1991) Calcium-dependent glutamate release concomitant with massive potassium flux during cerebral ischemia in vivo. *Brain Res*, 558:136-140.

Kato H, Araki T, Kogure K (1992a) Preserved neurotransmitter receptor binding following ischemia in preconditioned gerbil brain. *Brain Res Bull*, 29:395-400.

Kato H, Araki T, Murase K, Kogure K (1992b) Induction of tolerance to ischemia: alterations in second-messenger systems in the gerbil hippocampus. *Brain Res Bull*, 29:559-565.

Kato H, Kogure K, Araki T, Itoyama Y (1994) Astroglial and microglial reactions in the gerbil hippocampus with induced ischemic tolerance. *Brain Res*, 664:69-76.

Kato H, Liu Y, Araki T, Kogure K (1991) Temporal profile of the effects of pretreatment with brief cerebral ischemia on the neuronal damage following secondary ischemic insult in the gerbil: cumulative damage and protective effects. *Brain Res*, 553:238-242.

Kato H, Liu Y, Araki T, Kogure K (1992c) MK-801, but not anisomycin, inhibits the induction of tolerance to ischemia in the gerbil hippocampus. *Neurosci Lett*, 139:118-121.

Kauppinen RA, Nicholls DG (1986) Synaptosomal bioenergetics. The role of glycolysis, pyruvate oxidation and responses to hypoglycaemia. *Eur J Biochem*, 158:159-165.

Kawahara N, Croll SD, Wiegand SJ, Klatzo I (1997) Cortical spreading depression induces long-term alterations of BDNF levels in cortex and hippocampus distinct from lesion effects: implications for ischemic tolerance. *Neurosci Res*, 29:37-47.

Kawahara N, Reutzler CA, Klatzo I (1994a) A delayed effect of spreading depression on brain tissue associated with protection against ischemic neuronal damage. *Brain Pathology*, 4:509.

Kawahara N, Reutzler CA, Klatzo I (1994b) Factors modulating ischemic neuronal death and survival. *Brain Pathology*, 4:308.

Kawahara N, Ruetzler CA, Klatzo I (1995) Protective effect of spreading depression against neuronal damage following cardiac arrest cerebral ischaemia. *Neurol Res*, 17:9-16.

Kety SS (1951) The theory and applications of the exchange of inert gas at the lungs and tissues. *Pharmacol Rev*, 3:1-41.

Kimelberg HK, Rutledge E, Goderie S, Charniga C (1995) Astrocytic swelling due to hypotonic or high K^+ medium causes inhibition of glutamate and aspartate uptake and increases their release. *J Cereb Blood Flow Metab*, 15:409-416.

Kirino T, Tsujita Y, Tamura A (1991) Induced tolerance to ischemia in gerbil hippocampal neurons. *J Cereb Blood Flow Metab*, 11:299-307.

Kitagawa K, Matsumoto M, Tagaya M, Hata R, Ueda H, Niinobe M, Handa N, Fukunaga R, Kimura K, Mikoshiba K, et al. (1990) 'Ischemic tolerance' phenomenon found in the brain. *Brain Res*, 528:21-24.

Kobayashi S, Harris VA, Welsh FA (1995) Spreading depression induces tolerance of cortical neurons to ischemia in rat brain. *J Cereb Blood Flow Metab*, 15:721-727.

Koh JY, Palmer E, Cotman CW (1991) Activation of the metabotropic glutamate receptor attenuates N-methyl-D- aspartate neurotoxicity in cortical cultures. *Proc Natl Acad Sci U S A*, 88:9431-9435.

Kokaia Z, Gido G, Ringstedt T, Bengzon J, Kokaia M, Siesjo BK, Persson H, Lindvall O (1993) Rapid increase of BDNF mRNA levels in cortical neurons following spreading

depression: regulation by glutamatergic mechanisms independent of seizure activity. *Brain Res Mol Brain Res*, 19:277-286.

Komatsumoto S, Greenberg JH, Hickey WF, Reivich M (1989) Local cerebral glucose utilization in chronic middle cerebral artery occlusion in the cat. *J Cereb Blood Flow Metab*, 9:535-547.

Krivanek J (1970) Effects of spreading cortical depression on the incorporation of [^{14}C]leucine into proteins of rat brain. *J Neurochem*, 17:531-538.

Laemmli UK (1970) Cleavage of structural proteins during the assembly of the head of bacteriophage T4. *Nature*, 227:680-685.

Largo C, Cuevas P, Somjen GG, Martin del Rio R, Herreras O (1996) The effect of depressing glial function in rat brain in situ on ion homeostasis, synaptic transmission, and neuron survival. *J Neurosci*, 16:1219-1229.

Lauritzen M (1984) Long-lasting reduction of cortical blood flow of the brain after spreading depression with preserved autoregulation and impaired CO2 response. *J Cereb Blood Flow Metab*, 4:546-554.

Lauritzen M (1992) Spreading depression and migraine. *Pathol Biol (Paris)*, 40:332-337.

Lauritzen M, Diemer NH (1986) Uncoupling of cerebral blood flow and metabolism after single episode of cortical spreading depression in the rat brain. *Brain Res*, 370:405-408.

Lauritzen M, Hansen AJ (1992) The effect of glutamate receptor blockade on anoxic depolarization and cortical spreading depression. *J Cereb Blood Flow Metab*, 12:223-229.

Lauritzen M, Jorgensen MB, Diemer NH, Gjedde A, Hansen AJ (1982) Persistent oligemia of rat cerebral cortex in the wake of spreading depression. *Ann Neurol*, 12:469-474.

Leao AAP (1944) Spreading depression of activity in the cerebral cortex. *J Neurophysiol*, 7:199-210.

Leao AAP (1986) Spreading depression. *Funct Neurol*, 1:363-366.

Leao AAP, Morison RS (1945) Propagation of spreading depression. *J Neurophysiol*, 8:33-46.

Lehmenkuhler A, Speckmann EJ, Caspers H (1976) Cortical spreading depression in relation to potassium activity, oxygen tension, local flow and carbon dioxide tension. pp. 311-5. *In: Kessler M, et al, ed Ion and enzyme electrodes in biology and medicine Baltimore, University Park Press,*.

Lessmann V (1998) Neurotrophin-dependent modulation of glutamatergic synaptic transmission in the mammalian CNS. *Gen Pharmacol*, 31:667-674.

Levine ES, Black IB (1997) Trophic factors, synaptic plasticity, and memory. *Ann New York Acad Sci*, 835:12-19.

Lewin GR, Barde YA (1996) Physiology of the neurotrophins. *Ann Rev Neurosci*, 19:289-317.

Li H, Buchan AM (1993) Treatment with an AMPA antagonist 12 hours following severe normothermic forebrain ischemia prevents CA1 neuronal injury. *J Cereb Blood Flow Metab*, 13:933-939.

Li JY, Ueda H, Seiyama A, Nakano M, Matsumoto M, Yanagihara T (1997) A near-infrared spectroscopic study of cerebral ischemia and ischemic tolerance in gerbils. *Stroke*, 28:1451-1456; discussion 1456-1457.

Lin TN, He YY, Wu G, Khan M, Hsu CY (1993) Effect of brain edema on infarct volume in a focal cerebral ischemia model in rats. *Stroke*, 24:117-121.

Liu J, Bangalore R, Rutledge A, Triggle DJ (1994) Modulation of L-type Ca^{2+} channels in clonal rat pituitary cells by membrane depolarization. *Mol Pharmacol*, 45:1198-1206.

Lomeli H, Mosbacher J, Melcher T, Hoger T, Geiger JR, Kuner T, Monyer H, Higuchi M, Bach A, Seeburg PH (1994) Control of kinetic properties of AMPA receptor channels by nuclear RNA editing. *Science*, 266:1709-1713.

Luebke JI, Dunlap K, Turner TJ (1993) Multiple calcium channel types control glutamatergic synaptic transmission in the hippocampus. *Neuron*, 11:895-902.

Magistretti PJ, Pellerin L (1997) Metabolic coupling during activation. A cellular view. *Adv Exp Med Biol*, 413:161-166.

Magistretti PJ, Pellerin L, Rothman DL, Shulman RG (1999) Energy on demand. *Science*, 283:496-497.

Magnoni MS, Govoni S, Battaini F, Trabucchi M (1988) L-type calcium channels are modified in rat hippocampus by short-term experimental ischemia. *J Cereb Blood Flow Metab*, 8:96-99.

Maki R, Robinson MB, Dichter MA (1994) The glutamate uptake inhibitor L-trans-pyrrolidine-2,4-dicarboxylate depresses excitatory synaptic transmission via a presynaptic mechanism in cultured hippocampal neurons. *J Neurosci*, 14:6754-6762.

Marette A, Burdett E, Douen A, Vranic M, Klip A (1992) Insulin induces the translocation of GLUT4 from a unique intracellular organelle to transverse tubules in rat skeletal muscle. *Diabetes*, 41:1562-1569.

Markowitz S, Moskowitz MA (1986) Vascular head pain: a neurobiologist's approach. *Funct Neurol*, 1:351-356.

Marrannes R, Willems R, De Prins E, Wauquier A (1988) Evidence for a role of the N-methyl-D-aspartate (NMDA) receptor in cortical spreading depression in the rat. *Brain Res*, 457:226-240.

Mason GF, Gruetter R, Rothman DL, Behar KL, Shulman RG, Novotny EJ (1995) Simultaneous determination of the rates of the TCA cycle, glucose utilization, alpha-ketoglutarate/glutamate exchange, and glutamine synthesis in human brain by NMR. *J Cereb Blood Flow Metab*, 15:12-25.

Matsushima K, Hakim AM (1995) Transient forebrain ischemia protects against subsequent focal cerebral ischemia without changing cerebral perfusion. *Stroke*, 26:1047-1052.

Matsushima K, Hogan MJ, Hakim AM (1996) Cortical spreading depression protects against subsequent focal cerebral ischemia in rats. *J Cereb Blood Flow Metab*, 16:221-226.

Matsushima K, Schmidt-Kastner R, Hogan MJ, Hakim AM (1998) Cortical spreading depression activates trophic factor expression in neurons and astrocytes and protects against subsequent focal brain ischemia. *Brain Res*, 807:47-60.

Mayevsky A, Weiss HR (1991) Cerebral blood flow and oxygen consumption in cortical spreading depression. *J Cereb Blood Flow Metab*, 11:829-836.

McBain CJ, DiChiara TJ, Kauer JA (1994) Activation of metabotropic glutamate receptors differentially affects two classes of hippocampal interneurons and potentiates excitatory synaptic transmission. *J Neurosci*, 14:4433-4445.

McBain CJ, Mayer ML (1994) N-methyl-D-aspartic acid receptor structure and function. *Physiol Rev*, 74:723-760.

McLachlan RS (1992) Suppression of spreading depression of Leao in neocortex by an N-methyl-D-aspartate receptor antagonist. *Can J Neurol Sci*, 19:487-491.

Mennerick S, Zorumski CF (1994) Glial contributions to excitatory neurotransmission in cultured hippocampal cells. *Nature*, 368:59-62.

Michaels RL, Rothman SM (1990) Glutamate neurotoxicity in vitro: antagonist pharmacology and intracellular calcium concentrations. *J Neurosci*, 10:283-292.

Mies G (1993) Inhibition of protein synthesis during repetitive cortical spreading depression. *J Neurochem*, 60:360-363.

Mies G, Iijima T, Hossmann KA (1993a) Correlation between peri-infarct DC shifts and ischaemic neuronal damage in rat. *Neuroreport*, 4:709-711.

Mies G, Kohno K, Hossmann KA (1993b) MK-801, a glutamate antagonist, lowers flow threshold for inhibition of protein synthesis after middle cerebral artery occlusion of rat. *Neurosci Lett*, 155:65-68.

Mies G, Paschen W (1984) Regional changes of blood flow, glucose, and ATP content determined on brain sections during a single passage of spreading depression in rat brain cortex. *Exp Neurol*, 84:249-258.

Miettinen S, Fusco FR, Yrjanheikki J, Keinanen R, Hirvonen T, Roivainen R, Narhi M, Hokfelt T, Koistinaho J (1997) Spreading depression and focal brain ischemia induce cyclooxygenase-2 in cortical neurons through N-methyl-D-aspartic acid-receptors and phospholipase A2. *Proc Natl Acad Sci U S A*, 94:6500-6505.

Miller RJ (1998) Presynaptic receptors. *Ann Rev Pharmacol Toxicol*, 38:201-227.

Mitani A, Namba S, Ikemune K, Yanase H, Arai T, Kataoka K (1998) Postischemic enhancements of N-methyl-D-aspartic acid (NMDA) and non-NMDA receptor-mediated responses in hippocampal CA1 pyramidal neurons. *J Cereb Blood Flow Metab*, 18:1088-1098.

Moncada S (1992) Nitric oxide gas: mediator, modulator, and pathophysiologic entity. *J Lab Clin Med*, 120:187-191.

Moskowitz MA (1984) The neurobiology of vascular head pain. *Ann Neurol*, 16:157-168.

Mraovitch S, Calando Y, Goadsby PJ, Seylaz J (1992) Subcortical cerebral blood flow and metabolic changes elicited by cortical spreading depression in rat. *Cephalalgia*, 12:137-141; discussion 127.

Munoz-Martinez EJ (1970) Facilitation of cortical cell activity during spreading depression. *J Neurobiol*, 2:47-60.

Nakagomi T, Kirino T, Kanemitsu H, Tsujita Y, Tamura A (1993) Early recovery of protein synthesis following ischemia in hippocampal neurons with induced tolerance in the gerbil. *Acta Neuropathol*, 86:10-15.

Nakanishi S (1994) Metabotropic glutamate receptors: synaptic transmission, modulation, and plasticity. *Neuron*, 13:1031-1037.

Nakata N, Kato H, Liu Y, Kogure K (1992) Effects of pretreatment with sublethal ischemia on the extracellular glutamate concentrations during secondary ischemia in the gerbil hippocampus evaluated with intracerebral microdialysis. *Neurosci Lett*, 138:86-88.

Nedergaard M, Cooper AJ, Goldman SA (1995) Gap junctions are required for the propagation of spreading depression. *J Neurobiol*, 28:433-444.

Nedergaard M, Hansen AJ (1988) Spreading depression is not associated with neuronal injury in the normal brain. *Brain Res*, 449:395-398.

Nedergaard M, Hansen AJ (1993) Characterization of cortical depolarizations evoked in focal cerebral ischemia. *J Cereb Blood Flow Metab*, 13:568-574.

Nellgard B, Wieloch T (1992) NMDA-receptor blockers but not NBQX, an AMPA-receptor antagonist, inhibit spreading depression in the rat brain. *Acta Physiol Scand*, 146:497-503.

Nicholls D, Attwell D (1990) The release and uptake of excitatory amino acids. *Trends Pharmacol Sci*, 11:462-468.

Nicotera P, Leist M, Manzo L (1999) Neuronal cell death: a demise with different shapes. *Trends Pharmacol Sci*, 20:46-51.

Obrenovitch TP (1996) Origins of glutamate release in ischaemia. *Acta Neurochir Suppl*, 66:50-55.

Obrenovitch TP, Zilkha E (1995) High extracellular potassium, and not extracellular glutamate, is required for the propagation of spreading depression. *J Neurophysiol*, 73:2107-2114.

Obrenovitch TP, Zilkha E, Urenjak J (1996) Evidence against high extracellular glutamate promoting the elicitation of spreading depression by potassium. *J Cereb Blood Flow Metab*, 16:923-931.

Ochs S, Hunt K (1960) Apical dendrites and propagation of spreading depression in cerebral cortex. *J Neurophysiol*, 23:432-444.

Ohta S, Furuta S, Matsubara I, Kohno K, Kumon Y, Sakaki S (1996) Calcium movement in ischemia-tolerant hippocampal CA1 neurons after transient forebrain ischemia in gerbils. *J Cereb Blood Flow Metab*, 16:915-922.

Olney JW (1986) Inciting excitotoxic cytocide among central neurons. *Adv Exp Med Biol*, 203:631-645.

Osuga H, Hakim AM (1996) Relationship between extracellular glutamate concentration and voltage- sensitive calcium channel function in focal cerebral ischemia in the rat. *J Cereb Blood Flow Metab*, 16:629-636.

Osuga S, Hakim AM, Osuga H, Hogan MJ (1997) In vivo uptake of [^{3}H]nimodipine into brain during cortical spreading depression. *J Cereb Blood Flow Metab*, 17:586-590.

Osuga S, Hogan MJ (1997) In vivo uptake of [^{3}H]nimodipine in focal cerebral ischemia: modulation by hyperglycemia. *J Cereb Blood Flow Metab*, 17:1057-1065.

Ozyurt E, Graham DI, Woodruff GN, McCulloch J (1988) Protective effect of the glutamate antagonist, MK-801 in focal cerebral ischemia in the cat. *J Cereb Blood Flow Metab*, 8:138-143.

Page KM, Canti C, Stephens GJ, Berrow NS, Dolphin AC (1998) Identification of the amino terminus of neuronal Ca^{2+} channel alpha1 subunits alpha1B and alpha1E as an essential determinant of G-protein modulation. *J Neurosci*, 18:4815-4824.

Pardridge WM (1991) Advances in cell biology of blood-brain barrier transport. *Semin Cell Biol*, 2:419-426.

Paschen W (1996) Glutamate excitotoxicity in transient global cerebral ischemia. *Acta Neurobiol Exp*, 56:313-322.

Paschen W, Schmitt J, Uto A (1996) RNA editing of glutamate receptor subunits GluR2, GluR5 and GluR6 in transient cerebral ischemia in the rat. *J Cereb Blood Flow Metab*, 16:548-556.

Patlak CS, Blasberg RG, Fenstermacher JD (1983) Graphical evaluation of blood-to-brain transfer constants from multiple- time uptake data. *J Cereb Blood Flow Metab*, 3:1-7.

Patlak CS, Blasberg RG, Fenstermacher JD (1984) An evaluation of errors in the determination of blood flow by the indicator fractionation and tissue equilibration (Kety) methods. *J Cereb Blood Flow Metab*, 4:47-60.

Paxinos G, Watson C (1986) *The rat brain in stereotaxic coordinates* (2nd edn). Sydney, Australia: Academic Press.

Pellerin L, Magistretti PJ (1994) Glutamate uptake into astrocytes stimulates aerobic glycolysis: a mechanism coupling neuronal activity to glucose utilization. *Proc Natl Acad Sci U S A*, 91:10625-10629.

Pellerin L, Magistretti PJ (1997) Glutamate uptake stimulates Na^+,K^+-ATPase activity in astrocytes via activation of a distinct subunit highly sensitive to ouabain. *J Neurochem*, 69:2132-2137.

Pellerin L, Stolz M, Sorg O, Martin JL, Deschepper CF, Magistretti PJ (1997) Regulation of energy metabolism by neurotransmitters in astrocytes in primary culture and in an immortalized cell line. *Glia*, 21:74-83.

Petralia RS, Wang YX, Wenthold RJ (1994a) Histological and ultrastructural localization of the kainate receptor subunits, KA2 and GluR6/7, in the rat nervous system using selective antipeptide antibodies. *J Comp Neurol*, 349:85-110.

Petralia RS, Yokotani N, Wenthold RJ (1994b) Light and electron microscope distribution of the NMDA receptor subunit NMDAR1 in the rat nervous system using a selective anti-peptide antibody. *J Neurosci*, 14:667-696.

Piper RD, Lambert GA, Duckworth JW (1991) Cortical blood flow changes during spreading depression in cats. *Am J Physiol*, 261:H96-102.

Pragnell M, De Waard M, Mori Y, Tanabe T, Snutch TP, Campbell KP (1994) Calcium channel beta-subunit binds to a conserved motif in the I-II cytoplasmic linker of the alpha 1-subunit. *Nature*, 368:67-70.

Pulsinelli WA, Levy DE, Duffy TE (1982) Regional cerebral blood flow and glucose metabolism following transient forebrain ischemia. *Ann Neurol*, 11:499-502.

Qin N, Olcese R, Stefani E, Birnbaumer L (1998) Modulation of human neuronal alpha 1E-type calcium channel by alpha 2 delta-subunit. *Am J Physiol*, 274:C1324-1331.

Raghavendra Rao VL, Baskaya MK, Dogan A, Rothstein JD, Dempsey RJ (1998) Traumatic brain injury down-regulates glial glutamate transporter (GLT- 1 and GLAST) proteins in rat brain. *J Neurochem*, 70:2020-2027.

Ramos-Franco J, Fill M, Mignery GA (1998) Isoform-specific function of single inositol 1,4,5-trisphosphate receptor channels. *Biophys J*, 75:834-839.

Reid CA, Bekkers JM, Clements JD (1998) N- and P/Q-type Ca^{2+} channels mediate transmitter release with a similar cooperativity at rat hippocampal autapses. *J Neurosci*, 18:2849-2855.

Reid KH, Marrannes R, De Prins E, Wauquier A (1987) Potassium translocation and spreading depression induced by electrical stimulation of the brain. *Exp Neurol*, 97:345-364.

Reshef A, Sperling O, Zoref-Shani E (2000) Opening of K(ATP) channels is mandatory for acquisition of ischemic tolerance by adenosine. *Neuroreport*, 11:463-465.

Richter F, Lehmenkuhler A (1993) Spreading depression can be restricted to distinct depths of the rat cerebral cortex. *Neurosci Lett*, 152:65-68.

Ritchie JM (1992) Voltage-gated ion channels in Schwann cells and glia. *Trends Neurosci*, 15:345-351.

Robinson MB, Dowd LA (1997) Heterogeneity and functional properties of subtypes of sodium-dependent glutamate transporters in the mammalian central nervous system. *Adv Pharmacol*, 37:69-115.

Rosenthal M, Somjen G (1973) Spreading depression, sustained potential shifts, and metabolic activity of cerebral cortex of cats. *J Neurophysiol*, 36:739-749.

Rothman SM (1985) The neurotoxicity of excitatory amino acids is produced by passive chloride influx. *J Neurosci*, 5:1483-1489.

Rothman SM, Olney JW (1995) Excitotoxicity and the NMDA receptor--still lethal after eight years. *Trends Neurosci*, 18:57-58.

Rothstein JD (1996) Excitotoxicity hypothesis. *Neurology*, 47:S19-25; discussion S26.

Rothstein JD, Dykes-Hoberg M, Pardo CA, Bristol LA, Jin L, Kuncl RW, Kanai Y, Hediger MA, Wang Y, Schielke JP, Welty DF (1996) Knockout of glutamate transporters reveals a major role for astroglial transport in excitotoxicity and clearance of glutamate. *Neuron*, 16:675-686.

Rothstein JD, Martin L, Levey AI, Dykes-Hoberg M, Jin L, Wu D, Nash N, Kuncl RW (1994) Localization of neuronal and glial glutamate transporters. *Neuron*, 13:713-725.

Roy CS, Sherrington CS (1890) On the regulation of the blood-supply of the brain. *J Physiol (Lond)*, 11:85 - 108.

Rutledge EM, Kimelberg HK (1996) Release of [^{3}H]-D-aspartate from primary astrocyte cultures in response to raised external potassium. *J Neurosci*, 16:7803-7811.

Sakurada O, Kennedy C, Jehle J, Brown JD, Carbin GL, Sokoloff L (1978) Measurement of local cerebral blood flow with iodo [^{14}C] antipyrine. *Am J Physiol*, 234:H59-66.

Sakurai SY, Cha JH, Penney JB, Young AB (1991) Regional distribution and properties of [^{3}H]MK-801 binding sites determined by quantitative autoradiography in rat brain. *Neuroscience*, 40:533-543.

Salter MW (1998) Src, N-methyl-D-aspartate (NMDA) receptors, and synaptic plasticity. *Biochem Pharmacol*, 56:789-798.

Saransaari P, Oja SS (1995) Dizocilpine binding to cerebral cortical membranes from developing and ageing mice. *Mech Ageing Dev*, 85:171-181.

Savaki HE, Davidsen L, Smith C, Sokoloff L (1980) Measurement of free glucose turnover in brain. *J Neurochem*, 35:495-502.

Schurr A, Miller JJ, Payne RS, Rigor BM (1999) An increase in lactate output by brain tissue serves to meet the energy needs of glutamate-activated neurons. *J Neurosci*, 19:34-39.

Schwartz NE, Alford S (1998) Modulation of pre- and postsynaptic calcium dynamics by ionotropic glutamate receptors at a plastic synapse. *J Neurophysiol*, 79:2191-2203.

Schwartz PH, Wasterlain CG (1991) Cardiac arrest and resuscitation alters the pharmacokinetics of MK-801 in the rat. *Res Commun Chem Pathol Pharmacol*, 73:181-195.

Schwartz PH, Wasterlain CG (1993) Determination of serum and brain concentrations of neuroprotective and non-neuroprotective doses of MK-801. *J Neurol Sci*, 115:26-31.

Seeburg PH (1996) The role of RNA editing in controlling glutamate receptor channel properties. *J Neurochem*, 66:1-5.

Seki Y, Feustel PJ, Keller RW, Jr., Tranmer BI, Kimelberg HK (1999) Inhibition of ischemia-induced glutamate release in rat striatum by dihydrokinate and an anion channel blocker. *Stroke*, 30:433-440.

Shashidharan P, Huntley GW, Murray JM, Buku A, Moran T, Walsh MJ, Morrison JH, Plaitakis A (1997) Immunohistochemical localization of the neuron-specific glutamate transporter EAAC1 (EAAT3) in rat brain and spinal cord revealed by a novel monoclonal antibody. *Brain Res*, 773:139-148.

Sheng ZH, Westenbroek RE, Catterall WA (1998) Physical link and functional coupling of presynaptic calcium channels and the synaptic vesicle docking/fusion machinery. *J Bioenerg Biomembr*, 30:335-345.

Shibata M, Bures J (1974) Optimum topographical conditions for reverberating cortical spreading depression in rats. *J Neurobol*, 5:107-118.

Shimazaki K, Nakamura T, Nakamura K, Oguro K, Masuzawa T, Kudo Y, Kawai N (1998) Reduced calcium elevation in hippocampal CA1 neurons of ischemia-tolerant gerbils. *Neuroreport*, 9:1875-1878.

Shinohara M, Dollinger B, Brown G, Rapoport S, Sokoloff L (1979) Cerebral glucose utilization: local changes during and after recovery from spreading cortical depression. *Science*, 203:188-190.

Shockley RP, LaManna JC (1988) Determination of rat cerebral cortical blood volume changes by capillary mean transit time analysis during hypoxia, hypercapnia and hyperventilation. *Brain Res*, 454:170-178.

Sibson NR, Dhankhar A, Mason GF, Rothman DL, Behar KL, Shulman RG (1998a) Stoichiometric coupling of brain glucose metabolism and glutamatergic neuronal activity. *Proc Natl Acad Sci U S A*, 95:316-321.

Sibson NR, Shen J, Mason GF, Rothman DL, Behar KL, Shulman RG (1998b) Functional energy metabolism: in vivo ^{13}C-NMR spectroscopy evidence for coupling of cerebral glucose consumption and glutamatergic neuronal activity. *Dev Neurosci*, 20:321-330.

Simon RP, Niiro M, Gwinn R (1993) Prior ischemic stress protects against experimental stroke. *Neurosci Lett*, 163:135-137.

Simpson PB, Mehotra S, Langley D, Sheppard CA, Russell JT (1998) Specialized distributions of mitochondria and endoplasmic reticulum proteins define Ca^{2+} wave amplification sites in cultured astrocytes. *J Neurosci Res*, 52:672-683.

Snutch TP, Reiner PB (1992) Ca^{2+} channels: diversity of form and function. *Curr Opin Neurobiol*, 2:247-253.

Sokoloff L (1981) Relationships among local functional activity, energy metabolism, and blood flow in the central nervous system. *Fed Proc*, 40:2311-2316.

Sokoloff L, Kennedy C, Smith CB (1989) The [^{14}C]deoxyglucose method for measurement of local cerebral glucose utilization. In: *Neuromethods, Volume II: Carbonhydrates and energy metabolism.* (Boulton, AA & Baker, GB eds), Clifton, New Jersey, The humana Press Inc., pp 155-193.

Sokoloff L, Reivich M, Kennedy C, Des Rosiers MH, Patlak CS, Pettigrew KD, Sakurada O, Shinohara M (1977) The [^{14}C]deoxyglucose method for the measurement of local cerebral glucose utilization: theory, procedure, and normal values in the conscious and anesthetized albino rat. *J Neurochem*, 28:897-916.

Somjen GG, Aitken PG, Czeh GL, Herreras O, Jing J, Young JN (1992) Mechanism of spreading depression: a review of recent findings and a hypothesis. *Can J Physiol Pharmacol*, 70:S248-254.

Sontheimer H, Black JA, Waxman SG (1996) Voltage-gated Na^+ channels in glia: properties and possible functions. *Trends Neurosci*, 19:325-331.

Sorimachi T, Takeuchi S, Abe H, Tanaka R (1997) Effect of acquired tolerance to ischemia on focal infarction in gerbils. *Neurol Med Chir (Tokyo)*, 37:236-242.

Stamler JS, Jia L, Eu JP, McMahon TJ, Demchenko IT, Bonaventura J, Gernert K, Piantadosi CA (1997) Blood flow regulation by S-nitrosohemoglobin in the physiological oxygen gradient. *Science*, 276:2034-2037.

Sudhof TC (1995) The synaptic vesicle cycle: a cascade of protein-protein interactions. *Nature*, 375:645-653.

Sugaya E, Takato M, Noda Y (1975) Neuronal and glial activity during spreading depression in cerebral cortex of cat. *J Neurophysiol*, 38:822-841.

Swanson LW, Petrovich GD (1998) What is the amygdala? *Trends Neurosci*, 21:323-331.

Swanson RA, Morton MT, Tsao-Wu G, Savalos RA, Davidson C, Sharp FR (1990) A semiautomated method for measuring brain infarct volume. *J Cereb Blood Flow Metab*, 10:290-293.

Szatkowski M, Attwell D (1994) Triggering and execution of neuronal death in brain ischaemia: two phases of glutamate release by different mechanisms. *Trends Neurosci*, 17:359-365.

Taga K, Patel PM, Drummond JC, Cole DJ, Kelly PJ (1997) Transient neuronal depolarization induces tolerance to subsequent forebrain ischemia in rats. *Anesthesiology*, 87:918-925.

Takizawa S, Hogan MJ, Buchan AM, Hakim AM (1994) In vivo binding of [^{3}H]nimodipine in rat brain after transient forebrain ischemia. *J Cereb Blood Flow Metab*, 14:397-405.

Takizawa S, Matsushima K, Fujita H, Nanri K, Ogawa S, Shinohara Y (1995) A selective N-type calcium channel antagonist reduces extracellular glutamate release and infarct volume in focal cerebral ischemia. *J Cereb Blood Flow Metab*, 15:611-618.

Tanaka K, Gotoh F, Gomi S, Takashima S, Mihara B, Shirai T, Nogawa S, Nagata E (1991) Inhibition of nitric oxide synthesis induces a significant reduction in local cerebral blood flow in the rat. *Neurosci Lett*, 127:129-132.

Tanaka K, Greenberg JH, Gonatas NK, Reivich M (1985) Regional flow-metabolism couple following middle cerebral artery occlusion in cats. *J Cereb Blood Flow Metab*, 5:241-252.

Tenneti L, D'Emilia DM, Troy CM, Lipton SA (1998) Role of caspases in N-methyl-D-aspartate-induced apoptosis in cerebrocortical neurons. *J Neurochem*, 71:946-959.

Triggle CR, Tabrizchi R (1993) Changes in vascular smooth muscle function in hypertension. *Chin Med J (Engl)*, 106:250-257.

Triggle DJ (1994) Molecular pharmacology of voltage-gated calcium channels. *Ann N Y Acad Sci*, 747:267-281.

Van den Kerckhoff W, Drewes LR (1985) Transfer of the Ca-antagonists nifedipine and nimodipine across the blood brain barrier and their regional distribution in vivo. *J Cereb Blood Flow Metab*, 5:S459-460.

Vance CL, Begg CM, Lee WL, Haase H, Copeland TD, McEnery MW (1998) Differential expression and association of calcium channel alpha1B and beta subunits during rat brain ontogeny. *J Biol Chem*, 273:14495-14502.

Vezzani A, Serafini R, Stasi MA, Caccia S, Conti I, Tridico RV, Samanin R (1989) Kinetics of MK-801 and its effect on quinolinic acid-induced seizures and neurotoxicity in rats. *J Pharmacol Exp Ther*, 249:278-283.

Vinogradova LV, Koroleva VI, Bures J (1991) Re-entry waves of Leao's spreading depression between neocortex and caudate nucleus. *Brain Res*, 538:161-164.

Wada K, Miyazawa T, Kato H, Nomura N, Yano A, Shima K, Chigasaki H (1997) Intraischemic hypothermia during pretreatment with sublethal ischemia reduces the induction of ischemic tolerance in the gerbil hippocampus. *Acta Neurochir Suppl*, 70:257-259.

Wallace MC, Teasdale GM, McCulloch J (1992) Autoradiographic analysis of ^{3}H-MK-801 (dizocilpine) in vivo uptake and in vitro binding after focal cerebral ischemia in the rat. *J Neurosurg*, 76:127-133.

Watkins JC, Evans RH (1981) Excitatory amino acid transmitters. *Annu Rev Pharmacol Toxicol*, 21:165-204.

Wei XY, Rutledge A, Triggle DJ (1989) Voltage-dependent binding of 1,4-dihydropyridine Ca^{2+} channel antagonists and activators in cultured neonatal rat ventricular myocytes. *Mol Pharmacol*, 35:541-552.

Westenbroek RE, Bausch SB, Lin RC, Franck JE, Noebels JL, Catterall WA (1998) Upregulation of L-type Ca^{2+} channels in reactive astrocytes after brain injury, hypomyelination, and ischemia. *J Neurosci*, 18:2321-2334.

Wheeler DB, Randall A, Tsien RW (1994) Roles of N-type and Q-type Ca^{2+} channels in supporting hippocampal synaptic transmission [see comments]. *Science*, 264:107-111.

Willette RN, Lysko PG, Sauermelch CF (1994) A comparison of (+)SK&F 10047 and MK-801 on cortical spreading depression. *Brain Res*, 648:347-351.

Williams ME, Washburn MS, Hans M, Urrutia A, Brust PF, Prodanovich P, Harpold MM, Stauderman KA (1999) Structure and functional characterization of a novel human low-voltage activated calcium channel. *J Neurochem*, 72:791-799.

Witcher DR, De Waard M, Sakamoto J, Franzini-Armstrong C, Pragnell M, Kahl SD, Campbell KP (1993) Subunit identification and reconstitution of the N-type Ca^{2+} channel complex purified from brain. *Science*, 261:486-489.

Wolf T, Lindauer U, Reuter U, Back T, Villringer A, Einhaupl K, Dirnagl U (1997) Noninvasive near infrared spectroscopy monitoring of regional cerebral blood oxygenation changes during peri-infarct depolarizations in focal cerebral ischemia in the rat. *J Cereb Blood Flow Metab*, 17:950-954.

Wong EH, Kemp JA, Priestley T, Knight AR, Woodruff GN, Iversen LL (1986) The anticonvulsant MK-801 is a potent N-methyl-D-aspartate antagonist. *Proc Natl Acad Sci U S A*, 83:7104-7108.

Yamaguchi K, Yamaguchi F, Miyamoto O, Hatase O, Tokuda M (1999) The reversible change of GluR2 RNA editing in gerbil hippocampus in course of ischemic tolerance. *J Cereb Blood Flow Metab*, 19:370-375.

Yanamoto H, Hashimoto N, Nagata I, Kikuchi H (1998) Infarct tolerance against temporary focal ischemia following spreading depression in rat brain. *Brain Res*, 784:239-249.

Yang J, Tsien RW (1993) Enhancement of N- and L-type calcium channel currents by protein kinase C in frog sympathetic neurons. *Neuron*, 10:127-136.

Yao H, Ginsberg MD, Eveleth DD, LaManna JC, Watson BD, Alonso OF, Loor JY, Foreman JH, Busto R (1995) Local cerebral glucose utilization and cytoskeletal proteolysis as indices of evolving focal ischemic injury in core and penumbra. *J Cereb Blood Flow Metab*, 15:398-408.

Yawo H, Chuhma N (1993) Preferential inhibition of omega-conotoxin-sensitive presynaptic Ca^{2+} channels by adenosine autoreceptors. *Nature*, 365:256-258.

Zamponi GW, Bourinet E, Nelson D, Nargeot J, Snutch TP (1997) Crosstalk between G proteins and protein kinase C mediated by the calcium channel alpha1 subunit. *Nature*, 385:442-446.

Zea Longa E, Weinstein PR, Carlson S, Cummins R (1989) Reversible middle cerebral artery occlusion without craniectomy in rats. *Stroke*, 20:84-91.

Zhang F, Iadecola C (1994) Reduction of focal cerebral ischemic damage by delayed treatment with nitric oxide donors. *J Cereb Blood Flow Metab*, 14:574-580.

Zhang F, Xu S, Iadecola C (1995) Time dependence of effect of nitric oxide synthase inhibition on cerebral ischemic damage. *J Cereb Blood Flow Metab*, 15:595-601.

Zhang J, Snyder SH (1995) Nitric oxide in the nervous system. *Annu Rev Pharmacol Toxicol*, 35:213-233.

Zhang Y, Bendahan A, Zarbiv R, Kavanaugh MP, Kanner BI (1998) Molecular determinant of ion selectivity of a (Na^+ + K^+)-coupled rat brain glutamate transporter. *Proc Natl Acad Sci U S A*, 95:751-755.

Zhang ZG, Chopp M, Maynard KI, Moskowitz MA (1994) Cerebral blood flow changes during cortical spreading depression are not altered by inhibition of nitric oxide synthesis. *J Cereb Blood Flow Metab*, 14:939-943.

Curriculum Vitae

Fuhu Wang

4645 Ogilvie Walk Crescent
Ottawa, Ontario
Canada K1J 1G7
613 749 3808 (H)

Neuroscience Research Institute
University of Ottawa
Ottawa, Ontario
Canada K1N 8M5
Phone: 613 562-5800 ext. 8269 (W)
Fax: 613 562 5403
E-mail: wangf@uottawa.ca

Professional Experience

University of Ottawa
451 Smyth Rd., Ottawa
Ontario, Canada, K1N 5M8

July 1999 - current
Neuroscience Research Institute: Postdoctoral fellow with Dr. David S. Park.

September 1998 – June 1999
Neuroscience Research Institute: Postdoctoral fellow with Dr. Matthew J. Hogan.

September 1993 - August 1999
Department of Anatomy and Neurobiology: Teaching assistant, 1st and 2nd yr. Medical Histology

Demonstrator, Nursing Anatomy

Research assistant to Dr. Alastair M. Buchan and Dr. Matthew J. Hogan

October 1993 - October 1995
National Research Council
Institute of Biological Sciences
M54, Montreal Rd. Campus, Ottawa
Ontario, Canada, K1A 0R6
Cellular Signaling Group: Guest Worker

September 1993 - June 1995

Loeb Institute
Ottawa Civic Hospital
1053 Carling Ave.
Ottawa, Ontario, Canada, K1Y 4E9
Research Assistant to Dr. Alastair M. Buchan

September 1991 - August 1993

Brock University
St. Catharines, Ontario, Canada, L2S 3A1
Department of Biological Sciences: Teaching Assistant (1st yr. Biology; 2nd yr. Zoology; 3rd yr. Biology Laboratory).

Department of Psychology: Research Assistant to Dr. Peter Ramm

December 1990 - August 1991

National Institute of Mental Health, NIH
9000 Rockville Pike, Bethesda
Maryland, USA 20892
Laboratory of Cerebral Metabolism: WHO (World Health Organization) Post doctoral fellow

Supervisors: Dr. Louis Sokoloff, MD, Dr. Charles Kennedy, MD

NIH Postdoctoral fellowship offered but declined due to non-academic reason.

February 1987 - October 1987

Ninewells Hospital
Dundee, Scotland, UK
Department of Anaesthetics: British Council clinical scholarship; Supervisor: Dr. William A. Macrae, BM, ChB, FRCPS

August 1984 - November 1990

Jiangsu Province Hospital
300 Guangzhou Rd.
Nanjing, Jiangsu, China, 210029
Department of Anesthesiology: Resident, Sr. Resident

Education

September 1993 - July 2000

University of Ottawa
451 Smyth Rd., Ottawa
Ontario, Canada, K1N 5M8
Department of Anatomy and Neurobiology: Ph.D.

Thesis: Mechanisms of ischemic tolerance in the rat brain preconditioned with cortical spreading depression.

Thesis supervisors: Dr. Alastair M. Buchan, MD (September 1993 - June 1995), Dr. Matthew J. Hogan, MD, Ph.D. (August 1995 - July 2000)

September 1991 - August 1993

Brock University
St. Catharines, Ontario, Canada, L2S 3A1
Department of Biological Sciences: M.Sc.

Thesis: Effects of intracerebroventricular administration of bombesin on local cerebral glucose utilization in the rat.

Thesis supervisors: Dr. Peter Ramm, Ph.D.

September 1979 - July 1984

Nanjing Medical University
600 Hanzhong Rd.
Nanjing, Jiangsu, China, 210029
Faculty of Medicine: MD, Ranked 6th out of 160; on the Dean's list.

Awards

December 1993 - November 1995

1. University of Ottawa Ph.D. program entrance scholarship with the Department of Anatomy and Neurobiology.

December 1990 - November 1991

2. WHO (World Health Organization) Post doctoral fellowship with Dr. Sokoloff at NIMH, Bethesda, MD, USA.

December 1987 - November 1988

3. British Council clinical scholarship with Department of anaesthetics, Ninewells Hospital, Dundee, Scotland.

Skills

1. Small animal surgery, including stereotaxic brain surgery.
2. Cerebral ischemic models in rats and mice: All published ischemic models.
3. Functional autoradiography: Cerebral glucose metabolism; Cerebral blood flow, Cerebral protein synthesis.
4. In vivo and in vitro ligand binding.
5. Histological techniques and histochemistry.
6. Quantitative imaging.
7. Computer skills: Windows, Macitosh and UNIX operating systems. HTML, LAN network setup.
8. Statistics: Chi-square, T tests, linear and non-linear regression, analyses of variance, nonparametric and distribution free statistics.

Publications

Papers:

1. Wang F, Hogan MJ (2000) Effect of prior cortical spreading depression on cerebral blood flow and [^{3}H]nimodipine distribution during focal ischemia. In preparation.
2. Wang F, Hogan MJ (2000) In vivo [^{3}H]dizocilpine (MK-801) mapping of the brain during cortical spreading depression. In preparation.
3. Wang F, Hogan (2000) Delayed changes in cortical glucose utilization in rats treated with cortical spreading deression. In preparation.
4. Osuga H, Osuga S, **Wang F**, Fetni R, Hogan M J, Slack R S, Hakim A M, Park D S (2000) Cyclin dependent kinases as a therapeutic target for stroke. PNAS, in press.
5. Douen AG, Akiyama K, Hogan MJ, **Wang F**, Dong L, Hakim AM (1999) Preconditioning with cortical spreading depression decreases intra-ischemic cerebral glutamate levels and down regulates EAAT1 and EAAT2 from rat cerebral cortex plasma membranes. J Neurochem, 75:812-818.
6. Chakravarthy BR, Wang J, Tremley R, Atkinson TG, **Wang F**, Li H, Buchan AM (1998) Comparison of the changes in protein kinase C induced by glutamate in primary cortical neurons and by in vivo verebral ischemia. Cellular Signalling 10(4):291-295.
7. Sokoloff L, Kennedy C, Adachi K, **Wang F**, Takahashi S , P Meizer (1992) Effects of inhibition of nitric oxide synthase on resting local cerebral blood flow and on changes induced by hypercapnia or local functional activity. In: Pharmacology of Cerebral Ischemia 1992, J. Krieglstain and H. Oberpichler-Schwenk (Eds.), Wissenaschaftliche Verlagsgesellschaft mbH, Stuttgart. p.371-81.
8. **Wang F**, Zhang G (1992) A clinical investigation of awareness under intravenous general anesthesia. Chinese J Clin Anesthesiol 8(1):12-16.
9. **Wang F**, Zhang G (1989) Awareness during surgical anesthesia (Review). Second national conference of advances in anesthesia (Yixing, Jiangsu, November 1989); Advances in Overseas Medicine (Anesthesia) 10(6):375-379.

Abstracts:

1. **Wang F**, Osuga S, Osuga H, Fetni R, Slack R, Hakim AM, Hogan MJ, Ikeda J-E, Park DS (2000) Cyclin dependent kinases as a therapeautic target for cerebral ischemia. Soc Neurosci Abstr.
2. Douen AG, **Wang F**, Dong L, Hogan MJ (1999) Cortical spreading depression selectively down regulates glial glutamate transporter

isoforms EAAT1 and EAAT2 from rat cerebral cortex plasma membranes. Can J Neurol Sci 26(suppl 1):279.

3. Douen AG, Hogan MJ, **Wang F**, Dong L, Hakim AM, Doumit G (1999) Cortical spreading depression induces a delayed transient down regulation of excitatory amino acid transporter 2 (EAAT2) from rat ceerebral cortex plasma membranes. J Cereb Blood Flow Metab 19(Suppl 1):S706.
4. Douen AG, **Wang F**, Dong L, Hogan MJ (1998) Cortical spreading depression down regulates plasma membrane GLT-1 glutamte transporter in rat cerebral cortex. Stroke 29(1):279.
5. **Wang F**, Hogan MJ (1998) Prior cortical spreading depression decreases [^{3}H]nimodipine uptake in focally ischemic brain. Stroke 29(1):329.
6. **Wang F**, Hogan MJ (1997) In vivo uptake of [^{3}H]MK-801 into rat brain during cortical spreding depression. J Cereb Blood Flow Metab 17(Suppl 1):S546.
7. **Wang F**, Chakravarthy BR, Li H, Durkin JP, Buchan AM (1995) Protein kinase C activity changes in global ischemic rats treated with NBQX and SNX-111. Can J Neurol Sci 22(suppl 1):S45.
8. **Wang F**, Merali Z, Ramm P (1993) Effects of intracerebroventricular bombesin administration on local cerebral glucose utilization in the restrained and unrestrained rat. Soc Neurosci Abstr 19:1151.
9. Adachi K, Kennedy C, **Wang F**, Takahashi S, Melzer P, Sokoloff L (1992) Effects of nitric oxide synthase inhibitors on increases in local cerebral blood flow induced by whisker stroking. J Cereb Blood Flow Metab 13(Suppl 1):S152.
10. **Wang F**, Zhang G (1989) A clinical investigation of awareness under intravenous general anesthesia. First national conference of clinical anesthesia (Beijing, May 1989).

References

Dr. Alastair M. Buchan, MD., FRCPC
Clinical Neuroscience
Foothills Hospital
University of Calgary
Calgary, Alberta, Canada T2N 2T9
Phone: 403 670 1668
Fax: 403 670 1602
Email: Buchan@acs.ucalgary.ca

Dr. Gerald A. Deinel, Ph.D.
Department of Neurology, Box 500
University of Arkansa for Medical Sciences
4301 W Markham St., Little Rock, Arkansas 72205-7199, USA
Phone: 501 686 5007
Fax: 501 686 8689
Email: gdienel@neurology.uams.edu

Dr. Andre Douen, MD, Ph.D., FRCPC
Neuroscience Research Institute
Faculty of Medicine, University of Ottawa
451 Smyth, Ottawa, Ontario, Canada, K1H 8M5
Phone: 613 562 5800 ext. 8206
Fax: 613 562 5403
Email: adouen@uottawa.ca

Dr. Matthew Hogan, MD, Ph.D., FRCPC
Neuroscience Research Institute
Faculty of Medicine, University of Ottawa
451 Smyth, Ottawa, Ontario, Canada, K1H 8M5
Phone: 613 562 5431
Fax: 613 562 5403
Email: mjhogan@uottawa.ca

Dr. Peter Ramm, Ph.D.
Department of Psychology
John Decew School, Brock University
500 Glenridge Ave., St. Catharines, Ontario, Canada L2S 3A1
Phone: 905 688 2040
Email: pramm@spartan.ac.BrockU.CA

Dr. David S. Park, Ph.D.
Neuroscience Research Institute
Faculty of Medicine, University of Ottawa
451 Smyth, Ottawa, Ontario, Canada, K1H 8M5
Phone: 613 562 5800 ext. 8816
Fax: 613 562 5403
Email: dpark@uottawa.ca